FORMABILITY OF ALUMINUM AND STEEL IN DRAWING SQUARE CUPS

by

William T. Cloke, B. Sc. (Hons.)

A Thesis

Submitted to the Faculty of Graduate Studies

in Partial Fulfilment of the Requirements

for the Degree

Master of Engineering

McMaster University

May 1975

FORMABILITY OF ALUMINUM AND STEEL IN DRAWING SQUARE CUPS

TO THE MEMORY OF JOHN G. HAYWARD

Master of Engineering (1975)
Mechanical Engineering

McMaster University
Hamilton, Ontario

TITLE: Formability of Aluminum and Steel in Drawing Square Cups

AUTHOR: William Torrance Cloke, B.Sc. (Hons.)
Queen's University at Kingston

SUPERVISOR: Dr. J. L. Duncan

NUMBER OF PAGES: xii, 151

SCOPE AND CONTENTS:

A series of mechanical formability tests were performed on an aluminum-killed steel and five aluminum alloys. Three of the aluminum alloys exhibited strength levels and strain hardening abilities equal to or better than those of steel, but had very low fracture strains. The other two aluminum alloys had low strength but formed reasonably well, except for negligible strain hardening ability of one of them. All of the aluminum alloys exhibited planar anisotropy detrimental to deep drawability.

Tooling for deep drawing 2" wide square cups was designed and constructed. Tests were performed to find a suitable lubricant for square cupping tests and a combination of a heavy gear lubricant and polyethylene film was selected.

Tests with the square punch and die set confirmed the results of the mechanical tests. The steel produced the deepest cups while height of cups drawn from the high strength aluminum alloys was severely limited by brittle fracture in the corner walls.

Careful blank development proved to be a definite asset in square cup drawing. The best results were obtained with blanks designed to produce flat-topped cups but some application of blanks with extra material at the corners may be useful for materials exhibiting low fracture strains.

ACKNOWLEDGEMENTS

I wish to acknowledge the assistance, guidance and continual encouragement of my supervisor, J. L. Duncan.

Thanks are extended to B. D. McLaughlan of the Aluminum Company of Canada for the supply of materials and experimental data, and to John Hiam of Dofasco and A. S. Kasper and D. G. Adams of Chrysler Corporation for the supply of materials.

The financial support of the National Research Council both personally in the form of a Postgraduate Scholarship, and in the form of research operating funds is gratefully acknowledged.

I also wish to express my thanks to BettyAnne Bedell for typing the manuscript and to Bob Brown, Frank Drieman and Dave Schick for their ready assistance on many occasions.

TABLE OF CONTENTS

LIST OF FIGURES

MATERIAL FLOW PICTURES

LIST OF TABLES

CHAPTER 1

INTRODUCTION

Low carbon sheet steel has for several decades been the most important engineering material in the consumer products industry. Recently, however, more attention is being paid, particularly in the automotive industry, to materials offering greater strength-to-weight ratios. The two main contenders have been high-strength low alloy steels and high-strength wrought aluminum alloys. The purpose of this project is to investigate some aluminum alloys and compare them with a traditional aluminum-killed, low carbon steel.

Aside from its low density (1/3 that of steel) aluminum differs from steel in many other properties. It has a lower melting point and poor resistance to creep at elevated temperatures. On the other hand, at low temperature where steel becomes brittle, aluminum alloys may actually increase in ductility. In most situations aluminum exhibits greater corrosion resistance than steel due to the formation of a protective surface layer of oxide. The modulus of elasticity is one third as large as the modulus of steel. This leads to greater springback in forming, higher stored strain energy (at the same stress level) which may influence fracture propagation and lower resistance to deflection and buckling if yield stress and thickness are equal.

In addition aluminum has high thermal and electrical conductivity, is non-magnetic, is relatively transparent to neutrons, reflects radiant energy from ultraviolet to radio waves, is non-sparking and forms non-toxic compounds.

The main structural difference between the two is that aluminum has a face-centred cubic crystal structure (f.c.c.) and steel at room temperature, a body-centred cubic (b.c.c.). The f.c.c. structure has more available slip systems and is therefore intrinsically more isotropic than b.c.c.. The b.c.c. structure is more open (less close-packed than f.c.c.) and more readily permits the diffusion of interstitial solutes. It is the presence of carbon and nitrogen as interstitial solutes which gives steel many of its mechanical properties.

In conventional steels the important strengthening mechanisms are strain-hardening, grain refinement and the presence of carbon interstitials. In aluminum the high strength alloys depend mainly on substitutional solid solution hardening and precipitation hardening.

The purpose of this project however is not to examine these microscopic properties. Instead, we are interested in the static, room temperature, continuum properties affecting formability.

A variety of mechanical tests were performed in order to measure strain hardening, ductility and plastic anisotropy. Strain hardening is important in determining a material's ability to distribute strain over a large area.

Ductility refers to the ability to deform locally without fracture. Plastic anisotropy is the variation in strength with the direction of the applied stress.

The materials examined here exhibit both high and low strain hardening ability and high and low ductility. In addition, some of the materials exhibited the same strain-hardening ability but different ductilities. The plastic anisotropy in aluminum alloys is less than in steel.

A study of forming properties might also include measurements of strain rate sensitivity, homogeneity and inclusion content. These topics are not, however, treated in depth in this work.

Low carbon sheet steel is a highly developed product and its formability has been extensively studied [1], [2]. On the other hand, while a large literature exists on the texture and earing behaviour of aluminum alloys, less has been done in the realm of general formability. Finch, Wilson and Dorn [3] performed some early work on deep drawing at elevated temperatures. Hecker [4], [5] has determined tensile properties and forming limit curves (spherical punch tests) for several aluminum alloys and concluded that they had poorer formability than steel. Ghosh [6] has studied the localization of strain in the diffuse neck in tensile tests and concluded that aluminum alloys fail quickly due to adverse strain rate sensitivity.

In this project further assessment of the formability of the test materials was obtained in the deep drawing of square

cups. In laboratory testing circular cups are commonly drawn to measure the "drawability" of a material. The restrictive axisymetric nature of this test may mask material differences. In the drawing of square cups three types of deformation occur; stretching over the punch radii, drawing-type deformation in the flange at the corners and bending and straightening at the cup sides. It was felt that the material properties would affect the interaction of these types of deformation.

Finch, Wilson and Dorn [3] used round and square cups in the drawing aluminum alloys at elevated temperature and Thomson, Hobbs and Brammar [7] have used square cups in the assessment of new grades of steel. Textbooks on sheet metal forming [8], [9], [10] generally include a section on the drawing of box-shaped parts but the literature is very limited and most conclusions are rules-of-thumb based on general commercial experience. It was felt therefore, that laboratory study of the straining processes involved in the drawing of square cups might be a valuable contribution.

CHAPTER 2

MECHANICAL PROPERTIES OF SHEET METAL

2.1 Materials

The following six materials* were used in the work of this chapter and in Chapter 5 for the drawing of square cups:

A) AKDQ Steel - an aluminum-killed drawing quality steel, annealed and skin rolled.

B) 3003-H14 Utility Aluminum - a half-hard strain-hardened commercial quality aluminum-manganese alloy not intended for deep forming applications.

C) 3003-0 Draw Quality Aluminum - a fully annealed aluminum-manganese alloy specially processed to provide maximum formability.

D) 5182-0 Aluminum - a fully annealed drawing quality aluminum-magnesium alloy.

E) 5182-H111 Aluminum - same as D with the addition of a skin roll pass.

F) 2036-T4 - a drawing quality aluminum-copper-magnesium alloy, solution heat treated and then naturally aged at room temperature to a substantially stable condition.

---

* The sources were as follows: A - Dofasco, B - McMaster Engineering Machine Shop stores, C, D and E - Alcan Research in Kingston, F - Chrysler Corporation.

2.2 Mechanical Testing

2.2.1 Tensile Test

The tensile test is probably the most studied and most widely used test for determining mechanical properties today and a great deal of information can be gained from it. Basically the test, for sheet material, consists of pulling strips of metal, cut in different directions in the plane of the sheet, in uniaxial tension and determining the stress and the strain.

In addition to plots of true stess vs. true strain the following parameters were determined for the materials in this program; 0.2% Yield Stress (YS), Ultimate Tensile Stress (UTS), Total Elongation, Strain at Maximum Load, Strain Hardening Exponent (n), Plastic Strain Ratio (r), and Angle of Fracture.

The true stress-true strain values are calculated from the following relations

$$\sigma = \frac{P\ell}{A_o \ell_o} \qquad \epsilon = \ln\left(\frac{\ell}{\ell_o}\right)$$

where,

σ = true stress

ϵ = true strain

P = uniaxial tensile load

A_o = original cross-sectional area

ℓ_o = original gauge length

ℓ = instantaneous gauge length

0.2% yield stress is a measure of the stress required to cause plastic deformation for a material not having a definite yield point. The load used to calculate it is determined as shown in Figure 2.1. A line is drawn on the load-extension graph parallel to the initial slope but offset from it by an extension corresponding to 0.2% strain. The required load is found at the intersection of this line with the load-extension curve. The 0.2% yield stress is this load divided by the original area.

The ultimate tensile stress is the maximum load divided by the original cross-sectional area. It is an indication of the maximum strength of a material

The ratio of the ultimate tensile stress to the yield stress is a measure of the strain hardening capacity of the material.

The total elongation is measured by placing the two halves of the fractured specimen together and measuring the final gauge length, ℓ_f. Then,

$$\% \text{ elongation} = \frac{\ell_f - \ell_o}{\ell_o} \times 100\%$$

The total elongation is generally considered to be a measure of ductility but is dependent to some extent on the value chosen for ℓ_o. Total elongation is usually measured over a 2.0" gauge length. This was used for all materials in this chapter except the 2036-T4 aluminum and the AKDQ steel. For the 2036-T4 aluminum the gauge length was 2.5". The entire

FIG. 2.1 DETERMINATION OF 0.2% YIELD STRESS AND ULTIMATE TENSILE STRESS

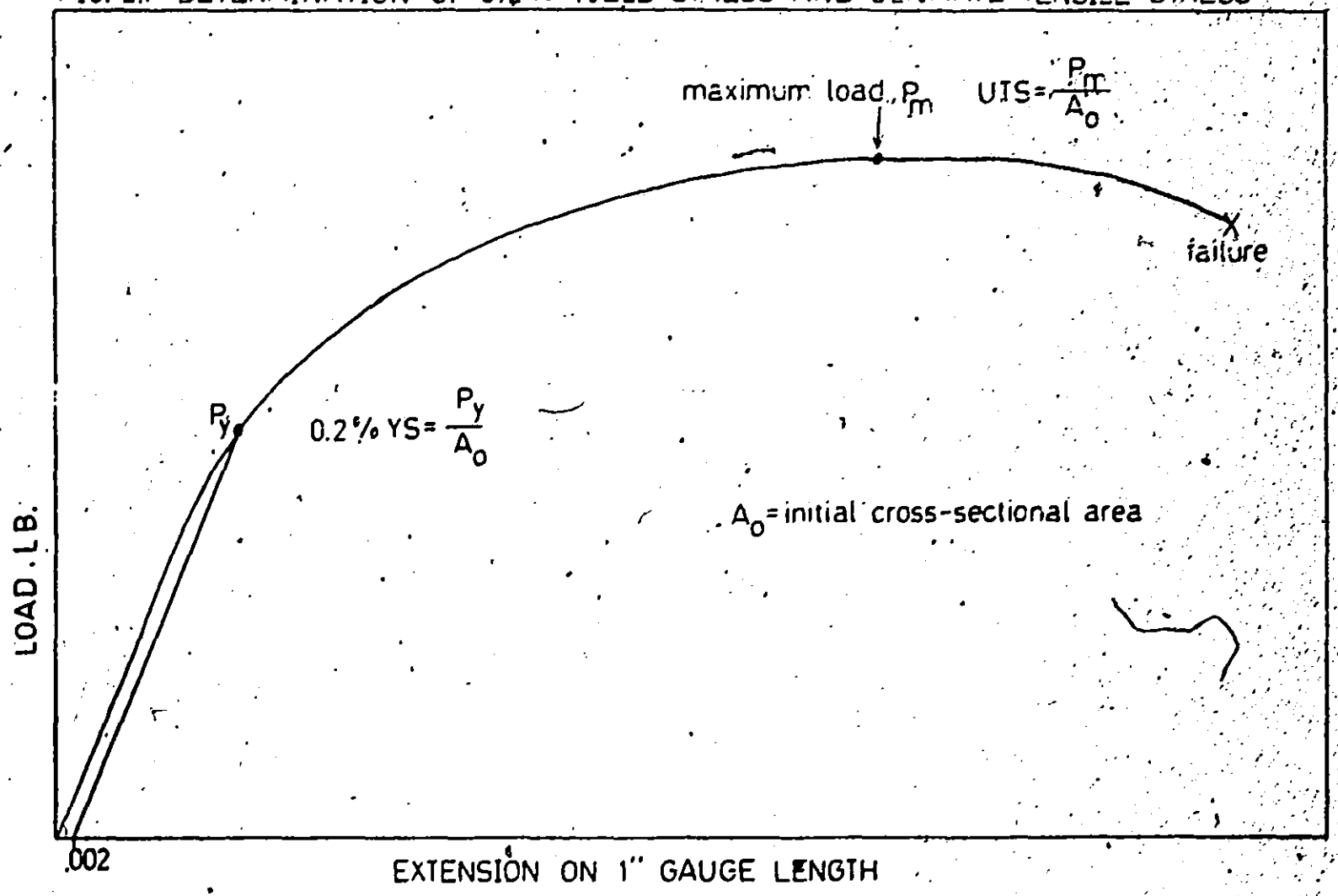

reduced section (3.9") was used on the steel specimen. The use of a longer gauge length results in lower values of total elongation.

The strain at maximum load is the true strain calculated at the point where the maximum load is first reached. Before this point the strain is uniform throughout the reduced section. After maximum load the straining process becomes unstable and a neck begins to form. The reason for the load drop is that the decrease in cross-sectional area is no longer balanced by an increase in flow stress. In other words, the rate of strain-hardening has dropped below a critical level. Thus strain at maximum load is a measure of strain-hardening ability.

The strain hardening exponent or n-value is a common measure of strain hardening ability. It is obtained by fitting the true stress-true strain data with the constitutive equation,

$$\sigma = K\varepsilon^n \tag{2.1}$$

where, K and n are material constants. This equation has been chosen for its mathematical convenience; it is easy to handle in theoretical analyses and it is able to fit many monotonically increasing curves quite reasonably. Theoretically for a material which obeys Equation (2.1) the strain at maximum load is numerically equal to n.

The plastic strain ratio, or r-value is defined as the ratio of the width strain to the thickness strain after tensile elongation. It can be described as a measure of the ability

of the material to resist thinning.

In these tests all r-value measurements were made on unloaded specimens. Most were measured after 10% tensile elongation. However the 2036-T4 aluminum was measured at slightly greater strain (13%) and the 3003-H14 utility aluminum was measured outside the necked region on failed specimens at 2-3% elongation. Due to the small strains, the r-values for the utility aluminum may contain large errors. An error estimate based on the propagation of reading errors places the limits at $\pm$ 15% for the low values (0° tests) and $\pm$ 60% for the higher values (45° and 90° tests). However duplicate samples do not seem to vary this much. A similar estimate for the steel values is $\pm$ 5% and for the 2036 aluminum $\pm$ 3%.

The angle of fracture was measured with a protractor as the angle, in the plane of the sheet, between the fracture edge and the axis of the specimen. This angle depends in part on the plastic anisotropy of the material. For 0° and 90° specimens it is possible to derive [11], using Hill's yield criterion for anisotropic materials, a simple relation between the angle of fracture θ and the r-value, namely

$$\theta = \tan^{-1}\left(\sqrt{1+\frac{1}{r}}\right)$$

Generally in the tensile testing of sheet materials, samples are cut at angles of 0°, 45° and 90° to the rolling direction. The average value for a property x is then taken

as:

$$\bar{x} = \frac{x_o + 2x_{45} + x_{90}}{4}$$

This assumes, quite reasonably, that samples cut at 45° and 135° to the rolling direction will have the same values. (Alternatively this may be regarded as an average based on an integral over 90°, which has been approximated by a composite trapezoidal rule.)

In this work the tensile tests on the steel, the utility aluminum and the 2036 aluminum were performed on an Instron Universal Testing Machine, model TT-C. Tensile data for the 3003-0 and 5182 aluminum alloys was supplied by the Alcan Research Laboratory in Kingston.

For the steel and the utility aluminum the specimen size was chosen to meet ASTM specification A370 (see Figure 2.2a). For the utility aluminum the smaller ASTM size (0.25" wide) was also tried but proved to be of little value due to the large effect of machining imperfections*. For the 2036 aluminum it was necessary, due to a shortage of material, to use a slightly smaller specimen size as shown in Figure 2.2b.

In order to get a rough idea of the type of fracture involved in the 3003-0 and 5182 aluminum alloys, quick tests

* As will be noted later, this material had a very low strain hardening rate which would make geometrical uniformity of the samples even more critical.

FIG. 2.2 TENSILE TEST SPECIMEN SIZES

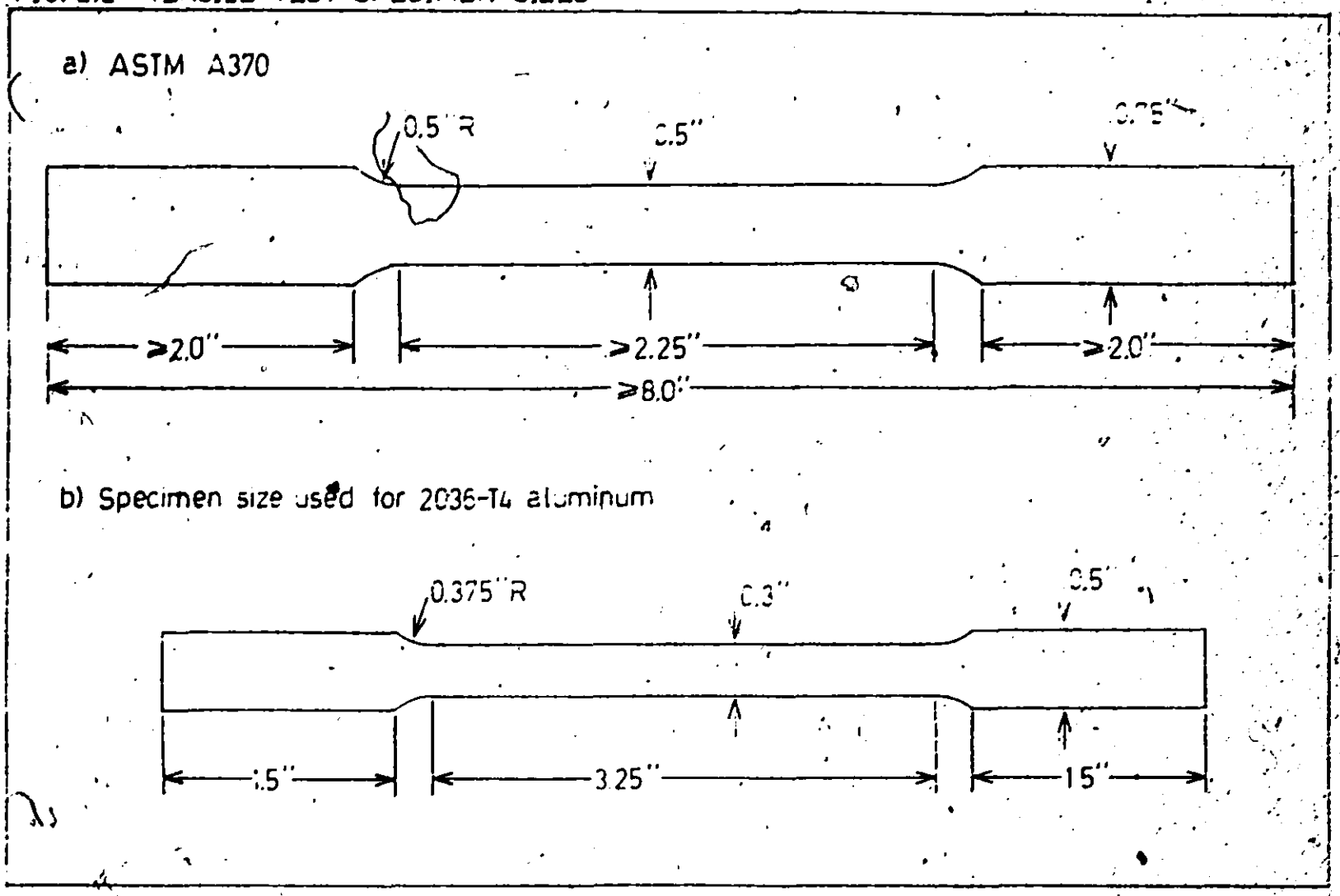

were made using shear-cut parallel-sided strips. The fracture angles quoted later for these materials were measured on such strips and may therefore be inaccurate.

The following paragraphs describe details of the test procedure used at McMaster.

Duplicate samples were cut at angles of 0°, 45° and 90° with respect to the rolling direction.

Gauge marks were made on the specimen with a ball-point pen. This leaves a visible indentation but does not cut a deep notch the way a regular metal scriber does, particularly in the soft aluminum alloys.

The original width and thickness and the width after tensile straining for r-value determination were measured with a hand micrometer having a vernier scale reading to .0001". At least three measurements were made at different points along the gauge length.

The length strain for r-value determination was calculated from measurements of the initial and final distances between gauge marks (≈ 1.0") using a travelling microscope. At least two sets of gauge marks were measured on each sample. The maximum error in one length measurement was estimated, from repeated measurements of one sample, to be .0014".

The extension of the sample required for calculating stress and strain values was obtained in two ways. The first, and most accurate, was by means of an Instron strain gauge extensometer clamped to the specimen. The second, which was used as a check on the first and in place of it when there was

evidence that the extensometer had slipped, was to keep track of the time with a watch sweep second hand and mark the chart every 30 or 60 seconds. This time multiplied by the cross-head travel speed of the machine gives the overall extension. An estimate of the appropriate initial gauge length, (approximately equal to the length of the reduced section) was obtained by calculating back, using the times, cross-head rates and extensometer readings from a duplicate specimen for which no slipping occurred.

2.2.2 Bulge Test

In the bulge test an 8" octagon of material is clamped in a 6.5" diameter circular ring and bulged by hydraulic oil pressure on one side. (Figure 2.3) The material at the centre of the blank is strained equi-biaxially and the dome is approximately spherical. A mechanical extensometer and spherometer sit on top of the material.

True stress-true strain values may be calculated from the following formulae;

$$\sigma = \frac{P\ r}{2\ t_o} \cdot \left(\frac{\ell}{\ell_o}\right)^2$$

$$\varepsilon = 2\ \ln\left(\frac{\ell}{\ell_o}\right)$$

where

P = hydraulic oil pressure

r = radius of curvature of the dome - determined from the spherometer

FIG. 2.3 SCHEMATIC DIAGRAM OF THE BULGE TEST

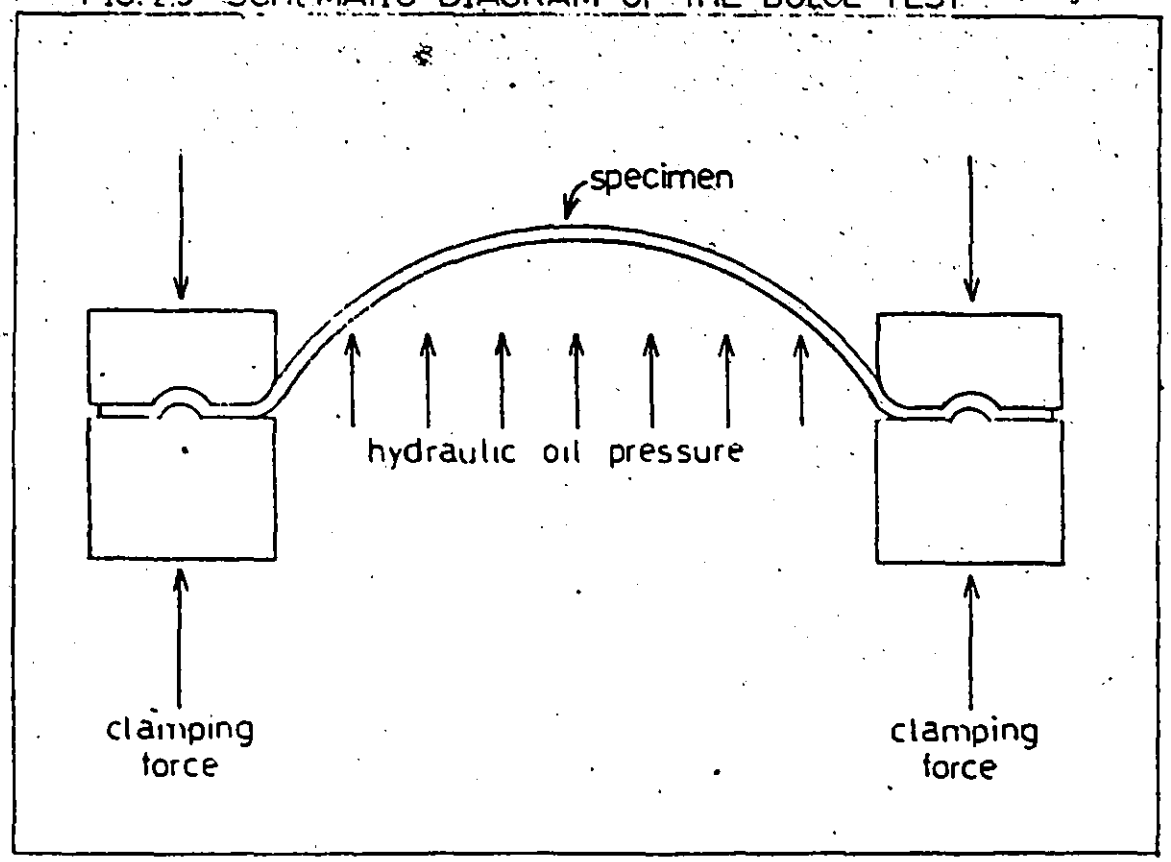

t_o = initial thickness of sample

ℓ_o = initial separation of extensometer points

ℓ = instantaneous separation of extensometer points

A value of the strain hardening exponent, n may be determined from the stress-strain data in the same way as for the tensile test.

The main advantage of the bulge test is that samples can be quickly cut on a shear and no machining is required. This means that stress-strain data can be produced very quickly.

In addition since the straining is equi-biaxial, much greater strains can be attained before failure. Whereas for the tensile test instability theoretically begins when $\varepsilon = n$, for the bulge test it should occur at $\varepsilon = \frac{4}{\pi}(2n+1)$.

Finally, in commercial stamping operations, the strain, particularly near failure points, is often a biaxial stretch so the stress-strain data from a bulge test may be more relevant than tensile test data.

2.2.3 Torsion Test

The in-plane torsion test has been developed [12, 13] to provide a quick and reliable way of measuring the n-value. and the equivalent thickness strain at fracture, ε_f. The deformed material consists of a ring, clamped securely at its inner and outer edges which is twisted in its plane until shear fracture occurs at the inner edge. The n-value is

determined from the shape of an originally straight radial line after twisting. The fracture strain is calculated from the shear angle at fracture at the inner edge.

Marciniak's torsion testing machine* has two angle measuring rings which contact the specimen at different radial distances from the centre. By measuring the angular displacement of two radial points (B and D, Figure 2.4a) it is possible to determine n and ϵ_f. Tables are provided to eliminate the necessity of calculation.

Unfortunately for most of the aluminum alloys studied here, deformation was concentrated in a region very close to the inner ring. In this case the angular displacement of B is extremely small and the standard method can not be used.

As an alternative radial lines were drawn on the specimen before deformation and then examined after fracture. The quantities measured were θ, the angle of the line with the tangent to the inner circular ring and d, the distance from the inner ring to the point where the line became straight. (Figure 2.4b) θ was measured at eight positions around the circumference using the protractor built into a tool maker's microscope. The standard deviation of the mean of these measurements was generally 3 or 4 degrees. d was measured with a small plastic scale, resulting in a reading error of $\pm$ 0.2 mm. The formulae to calculate ϵ_f and n are;

$$\epsilon_f = \frac{1}{\sqrt{3}} \text{ cotan } \theta$$

* Figure 2.4c.

FIG.24 TORSION TESTING

a) material suited for measurement in the Marciniak machine

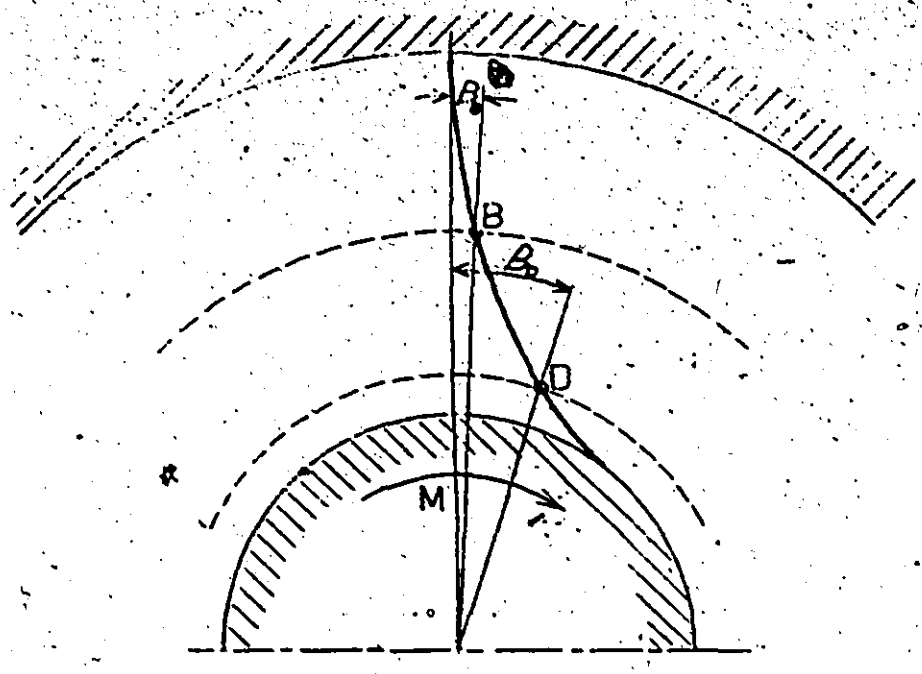

b) material which must be measured by alternate method

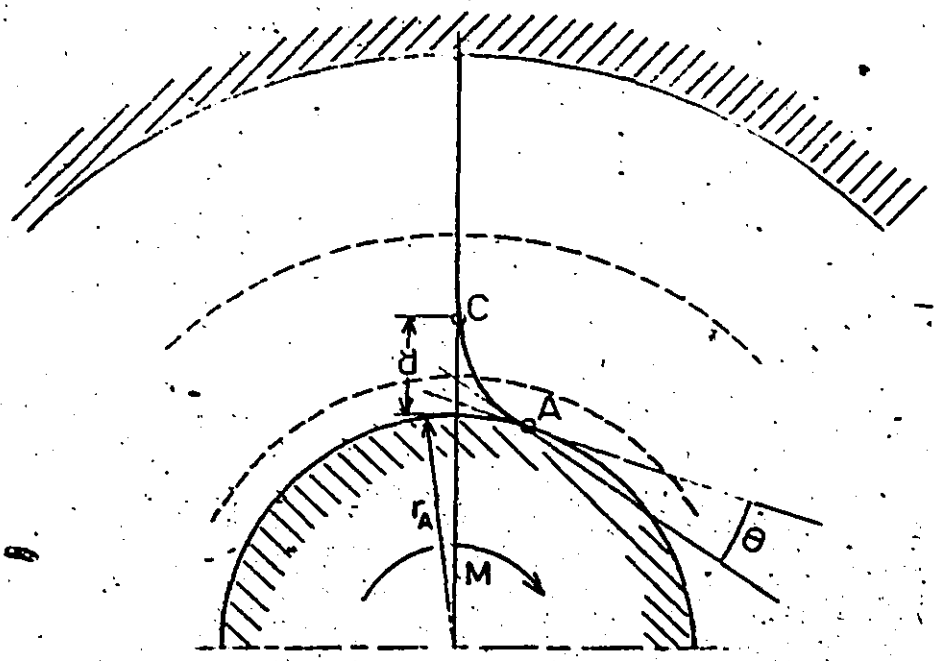

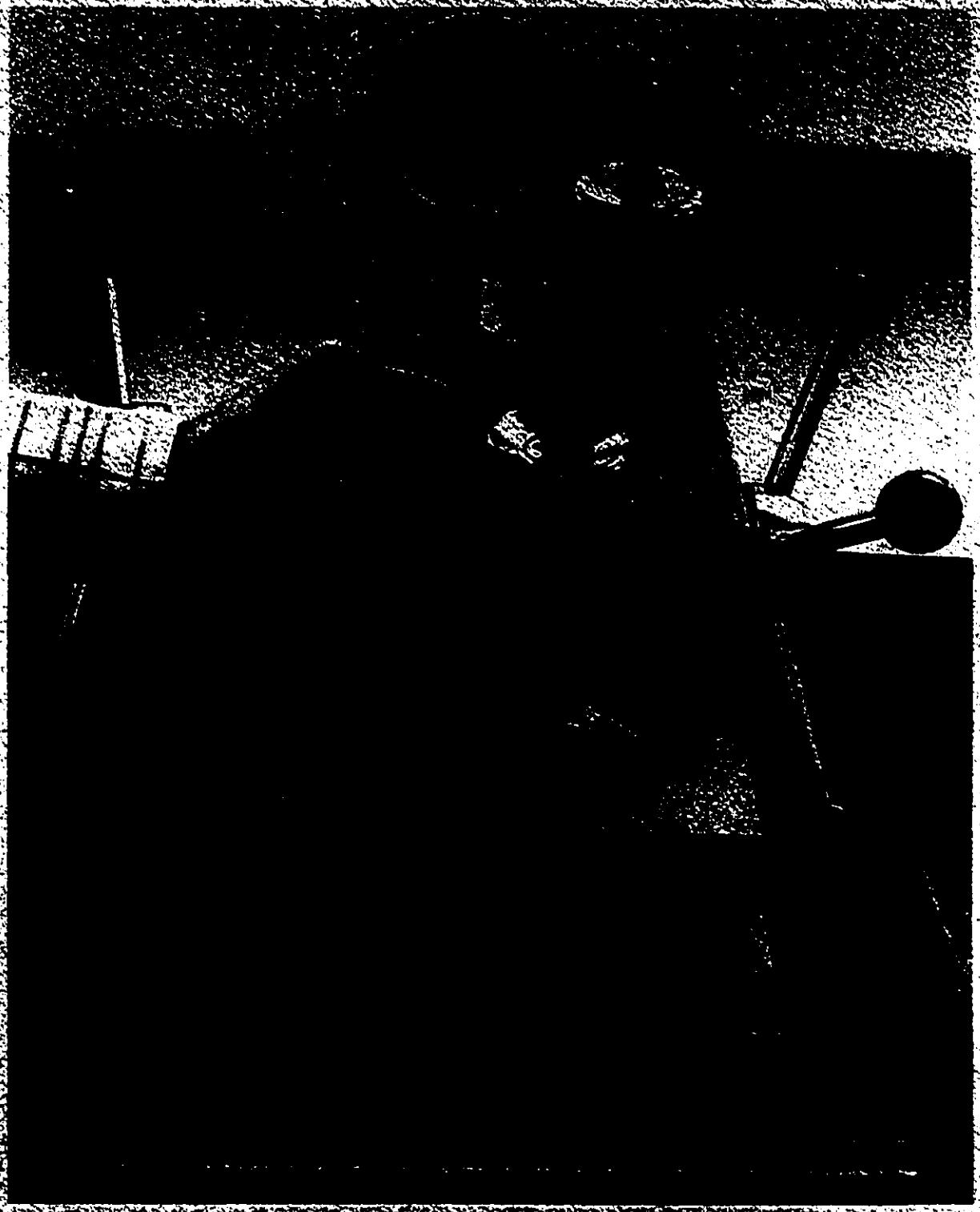

Figure 2-10. Marshall Torsion Pendulum System

$$n = \frac{2 \ln \left(\frac{r_A + d}{r_A}\right)}{\ln \left(\frac{\cot\text{an}\ \theta}{\tan \gamma_c}\right)}$$

where,

r_A = radius of inner clamp = 8 mm.

γ_c = an assumed value of the small angle between the deformed line and the radial direction at point c. A value of 2° was used since this seemed to be the smallest deviation which could be detected. Varying this angle $\pm 1^o$ produces 9% - 22% variation in the n-value.

2.2.4 Swift Circular Cup Test

The Swift circular cup test is a virtually pure drawing operation. The quantity measured is the limiting drawing ratio, LDR, which is the diameter of the largest circular blank which can be successfully drawn divided by the punch diameter, (2.0"). The tooling used in these tests is designed with generous punch-die clearance and punch and die radii so that tool geometry has as little effect as possible on failure.

LDR is considered to be a measure of drawability and is found to correlate well with r-value. This is explained as follows. The failure in a circular cup test commonly occurs over the punch radius due to thinning of the material in plane strain (since it cannot strain in the circumferential direction). The wall of the cup must support the load

necessary to draw in the flange, which deforms primarily in the plane of the sheet. Thus a material with a high r-value, which resists thinning, and strains preferentially in the plane of the sheet, should yield deeper cups before failure.

The earing behaviour in circular cup drawing is related to the anisotropy in the plane of the sheet, which may be seen in two ways; by the variation of r-value and by the variation of strength (Y.S, UTS.) with test direction. Large variations in these properties results in larger ears for the same diameter blank. Earing is also more pronounced in deeper cups.

The limiting blank diameter is found by drawing a series of blanks of various sizes and bracketting as closely as possible the critical size. It is sometimes possible to use a plot of the maximum or failure loads against blank diameter to aid in finding the critical size. (Figure 2.5) This is based on the assumptions that the maximum load in successfully drawn blanks varies directly with the blank size and that the maximum load in a failed cup is independent of the blank size. These assumptions are not really valid, particularly for the soft aluminum alloys near the critical blank diameter, but the method is still useful in cutting down on the number of blanks which must be drawn.

In this work the critical size was bracketted closely enough that the maximum error in the limiting drawing ratio is $\pm$ .03.

To be very precise, the blanks used for the Swift

FIG. 25 DETERMINATION OF LIMITING BLANK DIAMETER

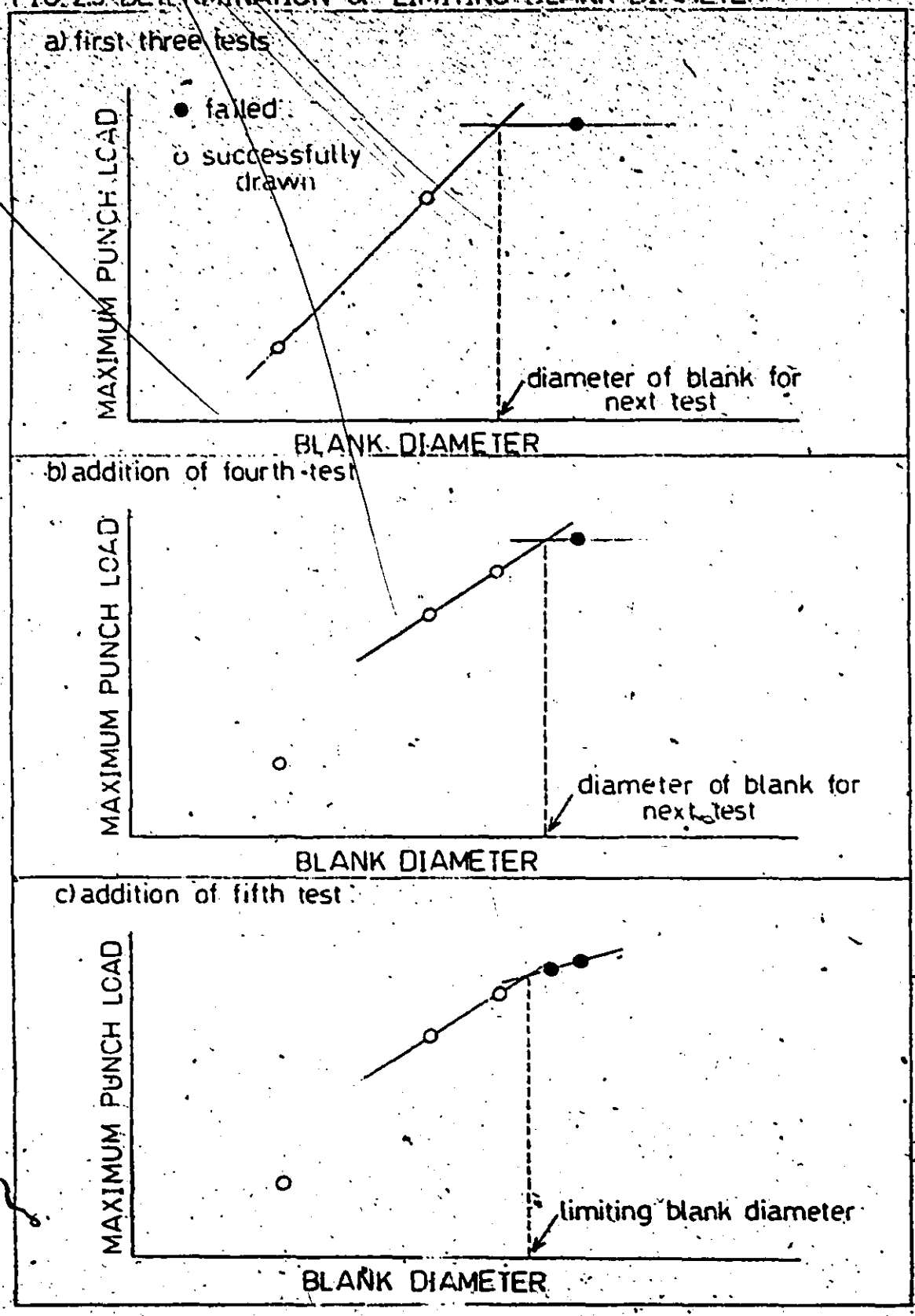

test should be perfectly round and have machined edges. However since this is extremely time consuming, the blanks for these tests were simply marked with a compass scriber and cut out with aircraft-type tinsnips. These snips were found to produce relatively clean sharp edges. The slight burr was removed with a file. It is true that this method leaves a ring of work-hardened material at the edge of the blank; however it is small in comparison with the rest of the flange and should contribute very little to the punch load. Since failure depends on the punch load it is expected that the sheared edge will have negligible effect on the results.

The blanks in these tests were lubricated on both sides with polyethylene film coated with a heavy gear lubricant.

2.3 Test Results

The test results are shown in Tables 2.1-2.5 and Figures 2.6 - 2.13.

In each of the following sections the values are repeated with the materials listed in rank order according to the parameter under consideration.

Table 2.1 Tensile Test Results

Material and Thickness	Test Direction	0.2% YS (ksi)	UTS (ksi)	UTS / 0.2% YS	Elong. (%)	r	Fracture Angle	n	Strain at Max. Load
AKDQ Steel (.032")	0	24.9	43.3	1.74	38.3	1.999	67	.219	.217
	45	26.7	44.9	1.68	35.9	1.572	67	.210	.204
	90	25.2	42.9	1.70	32.6	2.529	70	.205	.193
	Av.	25.9	44.0	1.70	35.7	1.918	68	.211	.205
3003-H14 Aluminum (.032")	0	20.3	22.0	1.08	3.5	0.40	72	--	.012
	45	20.3	21.6	1.06	2.5	1.40	60	--	.010
	90	22.4	23.4	1.04	2.8	1.30	59	--	.009
	Av.	20.8	22.2	1.06	2.8	1.10	63	--	.010
3003-0 Aluminum (.036")	0	7.3	16.6	2.27	32.0	0.565	65	.251	NA
	45	7.0	15.4	2.20	35.8	0.802	--	.245	
	90	6.7	15.0	2.24	34.3	0.411	65	.245	
	Av.	7.0	15.6	2.23	34.5	0.645	65	.247	
5182-0 Aluminum (.033")	0	22.6	44.1	1.95	23.2	0.636	65	.318	NA
	45	22.2	42.1	1.90	27.2	0.881	--	.320	
	90	22.4	42.2	1.88	27.0	0.740	57	.311	
	Av.	22.4	42.6	1.91	26.2	0.785	61	.317	
5182-H111 Aluminum (.033")	0	24.2	44.3	1.83	22.3	0.726	62	.239	NA
	45	22.0	42.5	1.93	28.2	0.943	59	.252	
	90	22.0	42.6	1.94	26.7	0.822	62	.241	
	Av.	22.6	43.0	1.91	26.4	0.854	61	.246	
2036-T4 Aluminum (.033")	0	28.6	52.8	1.85	21.8	0.638	64	.232	.168
	45	29.3	50.8	1.73	24.0	0.765	65	.241	.200
	90	29.4	51.0	1.73	24.7	0.849	62	.240	.199
	Av.	29.2	51.4	1.76	23.6	0.754	64	.239	.192

Table 2.2 Bulge, Torsion and Swift Test Results

Material	Bulge Test				Torsion Test		Swift Cup Test
	n	$\frac{4}{\pi}(2n+1)$	Strain at Max. Load	Strain at Failure	ε_f	n	LDR
AKDQ Steel	.233	.533	.491	.624	2.194 (2.05)*	.239 (.245)*	2.52
3003-H14 Aluminum	.057	.405	.419	.419	1.358	.045	2.04
3003-0 Aluminum	.234	.534	.585	.675	0.710 (.742)*	.209 (.235)*	2.20
5182-0 Aluminum	.312	.591	.270	.270	0.356	.222	2.30
5182-H111 Aluminum	.254	.548	.314	.314	0.352	.190	2.29
2036-T4 Aluminum	.215	.520	.399	.442	0.245	.179	≥ 2.19

* Calculated from angles read on the Marciniak Torsion Testing Machine.

Table 2.3 Tensile Test Failures

Material	Diffuse Neck	Local Neck
AKDQ Steel	large amount	ductile failure
3003-H14 Aluminum	not visible	ductile failure
3003-0 Aluminum	small amount	ductile failure
5182-0 Aluminum	not visible	brittle failure
5182-H111 Aluminum	not visible	brittle failure
2036-T4 Aluminum	not visible	brittle failure

Table 2.4 Comparison of n-value Fits for Alloys Supplied by Alcan

Material	Alcan's Value	McMaster unweighted fit, $\varepsilon > .03$	McMaster best weighted fit
3003-0 Aluminum	.251	.261	.221
5182-0 Aluminum	.318	.313	.313
5182-H111 Aluminum	.239	.253	.257

Table 2.5 Rank Order of Strain Hardening Parameters

Material	UTS/YS	Tensile n		Bulge n	Torsion n
		McMaster	Alcan		
5182-0 Aluminum	2	1	1	1	2
3003-0 Aluminum	1	4	2	3	3
5182-H111 Aluminum	3	2	3	2	4
AKDQ Steel	5	5	5	4	1
2036-T4 Aluminum	4	3	4	5	5
3003-H14 Aluminum	6	-	-	6	6

FIG. 2.6 TENSILE TEST RESULTS

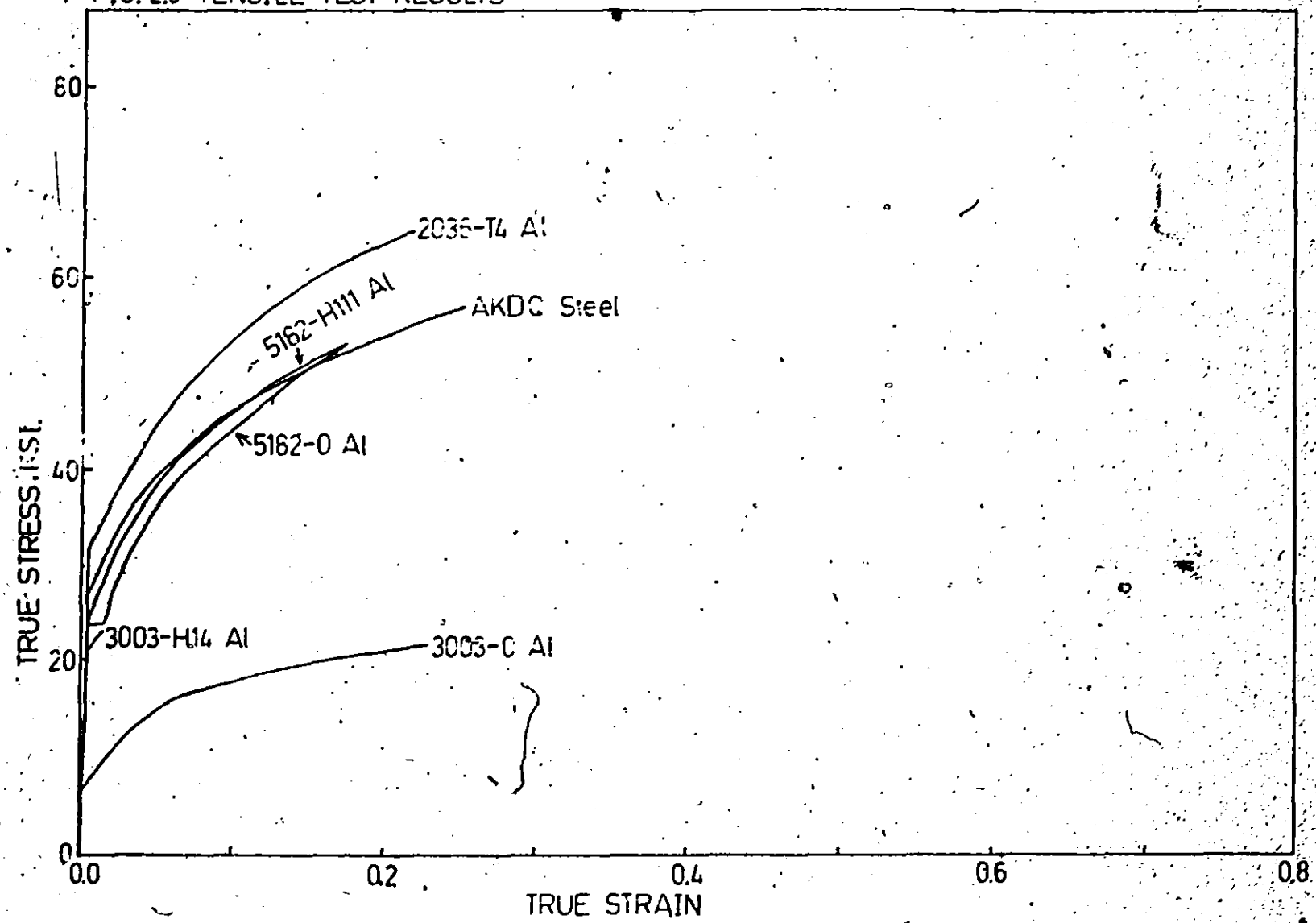

FIG. 27 BULGE TEST RESULTS

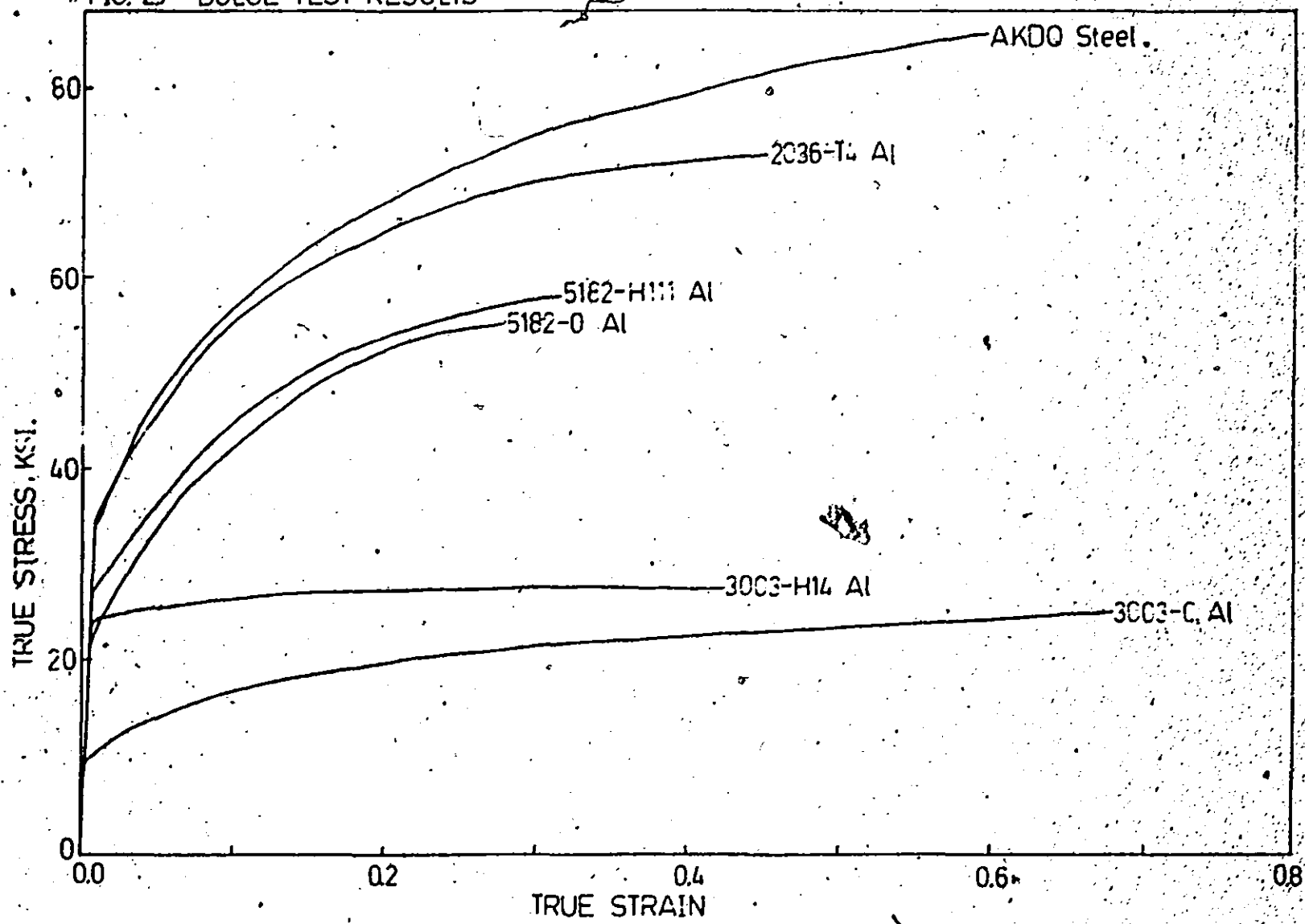

FIG. 2.8 AKDQ STEEL

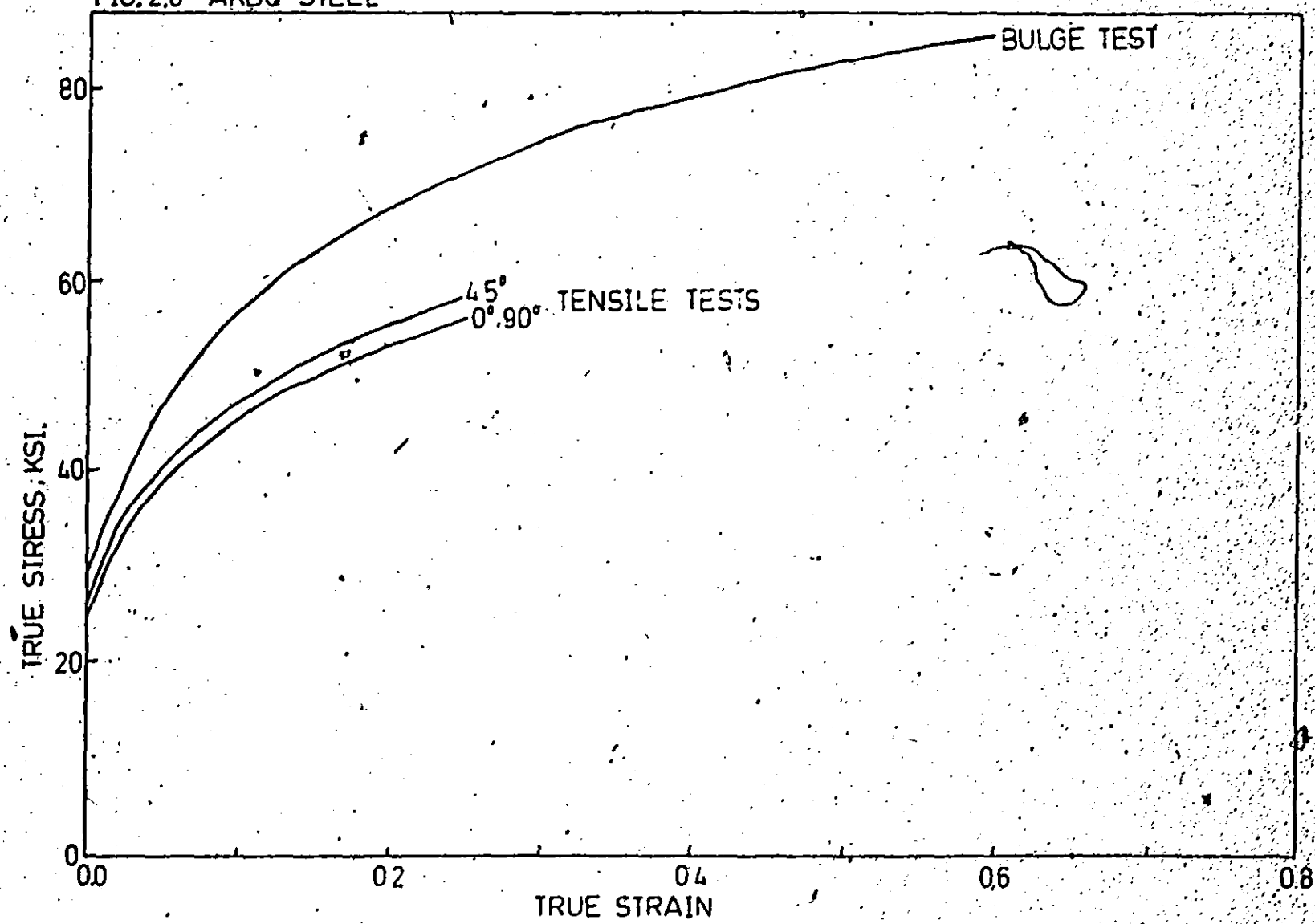

FIG. 2.9 3003-H14 UTILITY ALUMINUM

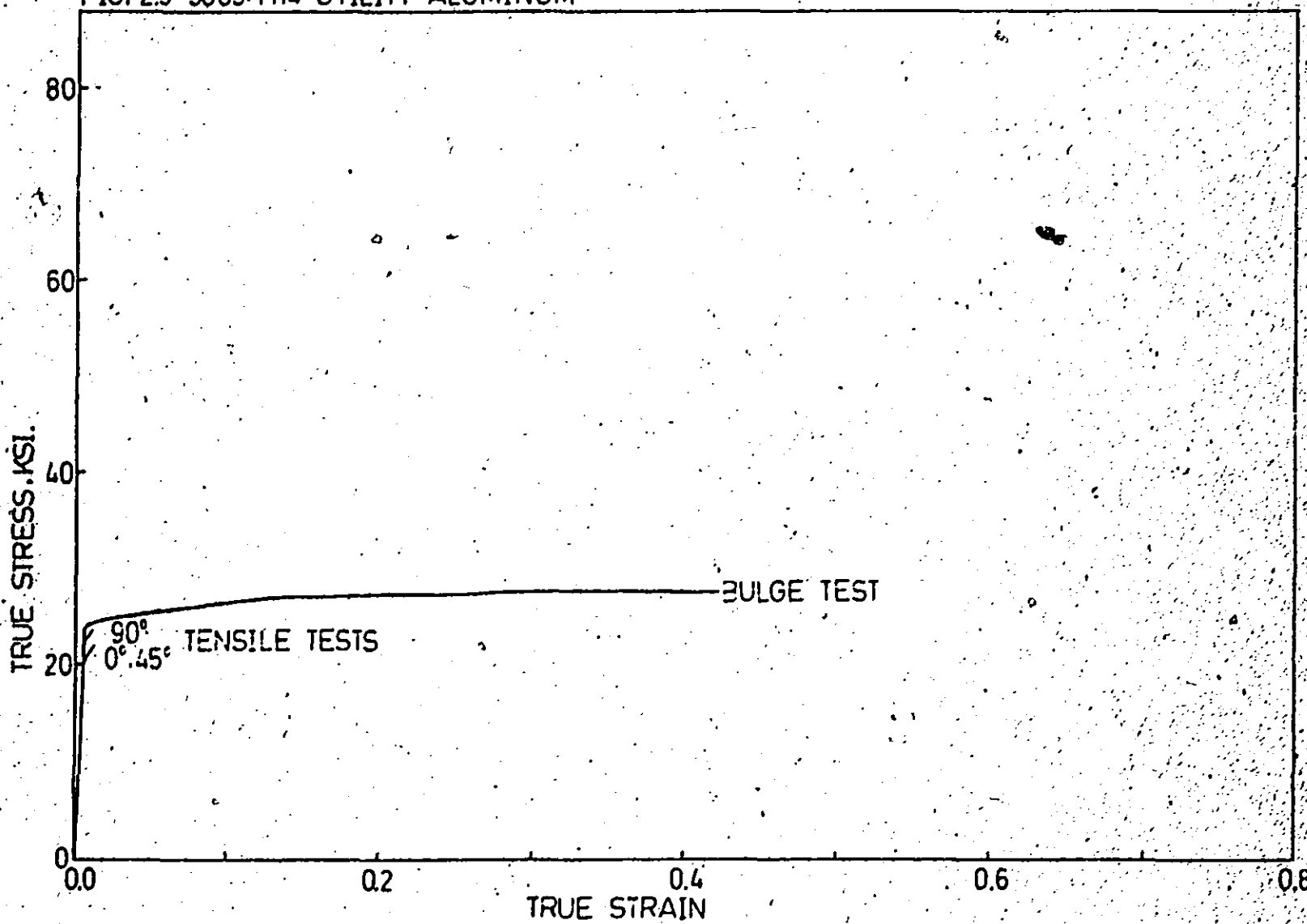

FIG. 2.10 3003-0 ALUMINUM

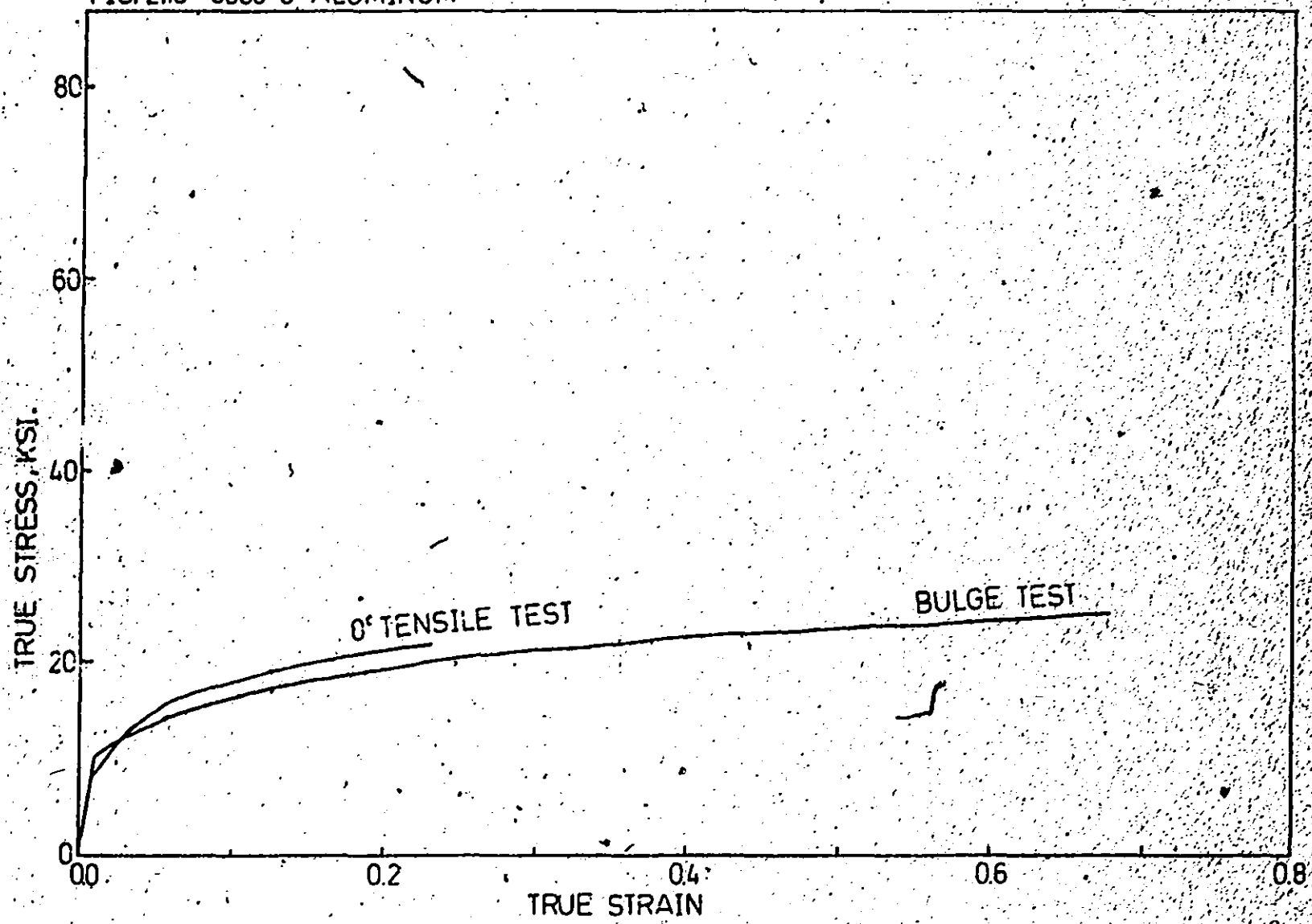

FIG. 2.11 5182-0 ALUMINUM

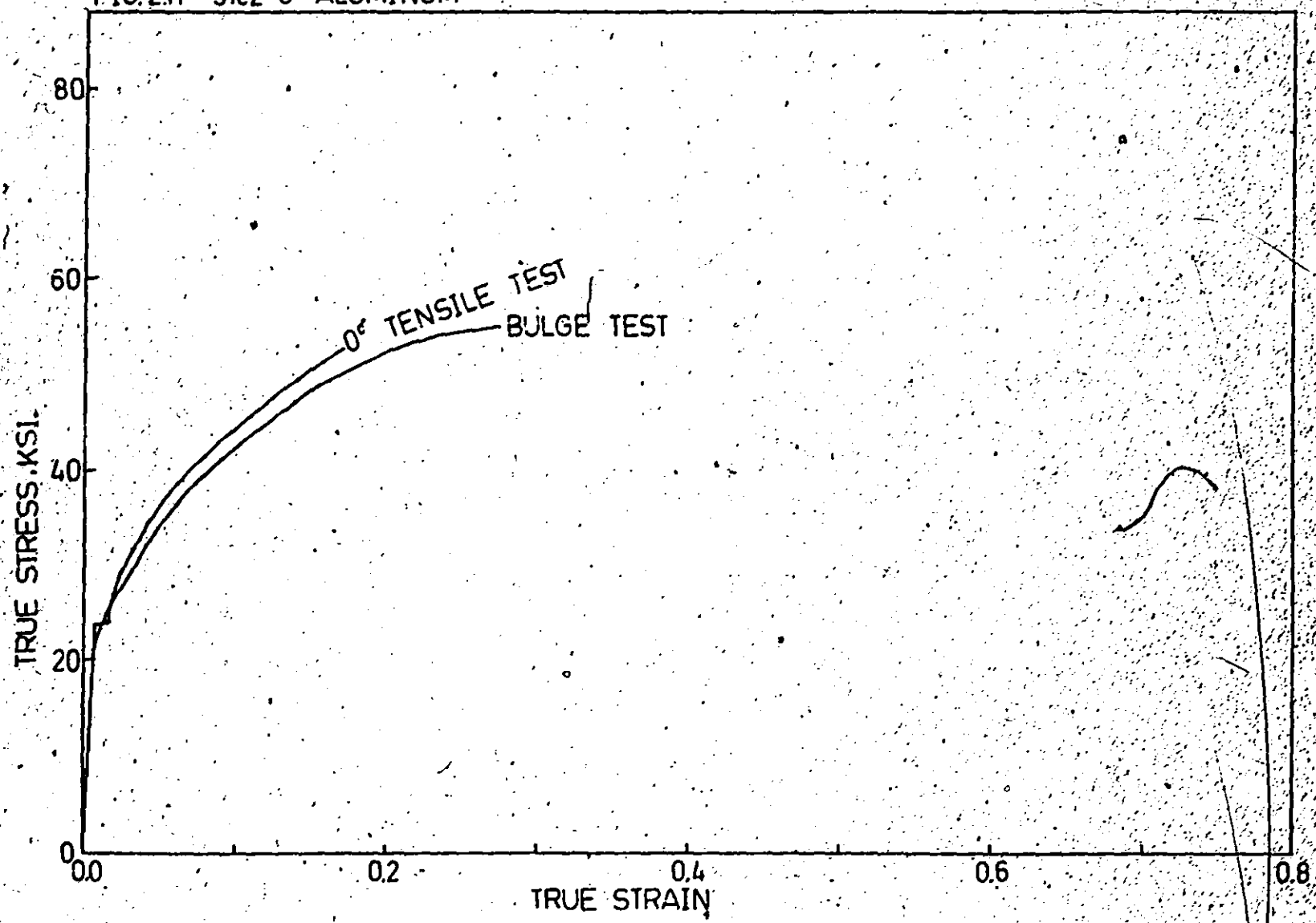

FIG. 2.12 5182-H111 ALUMINUM

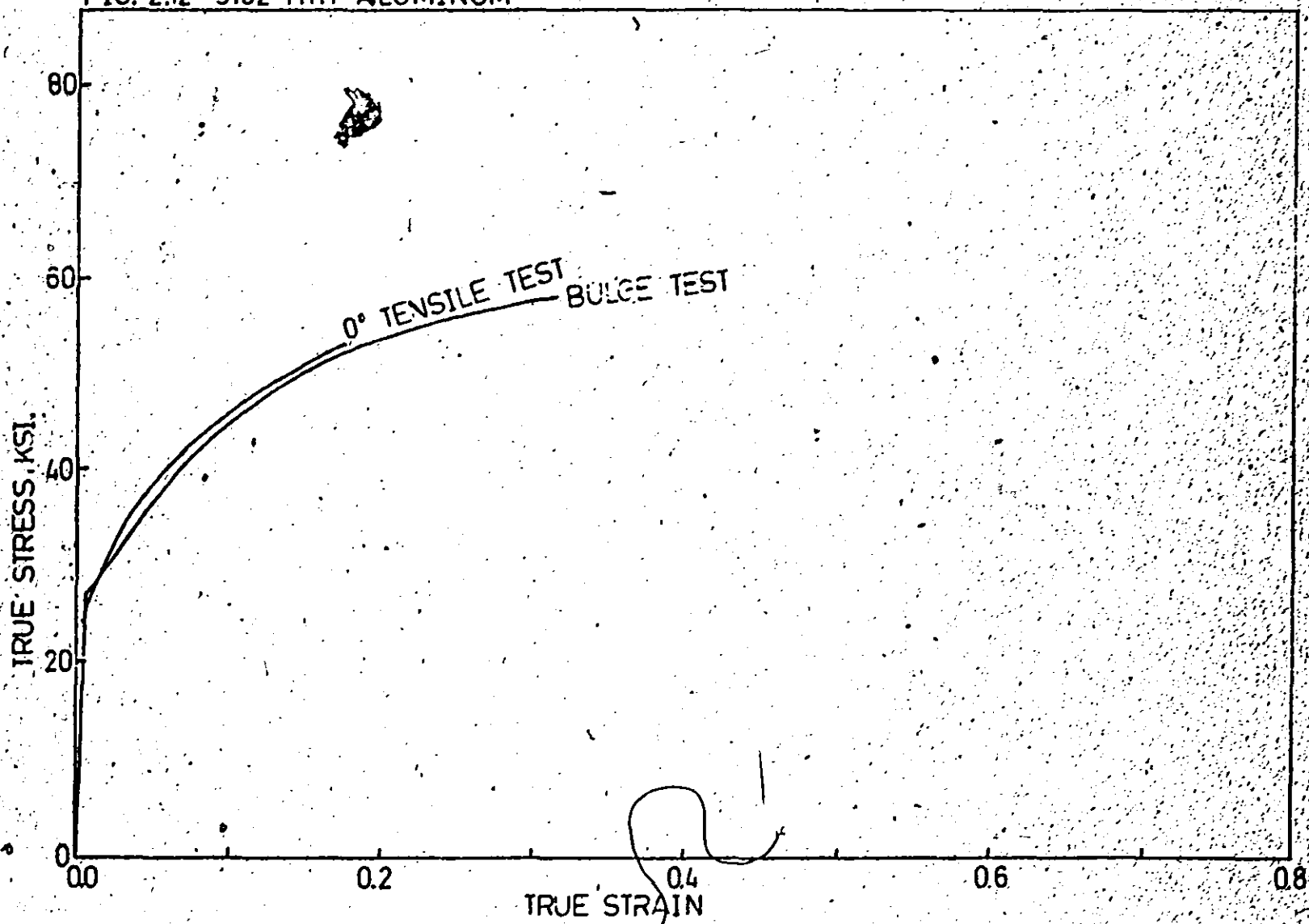

FIG. 2.13 2036-T4 ALUMINUM

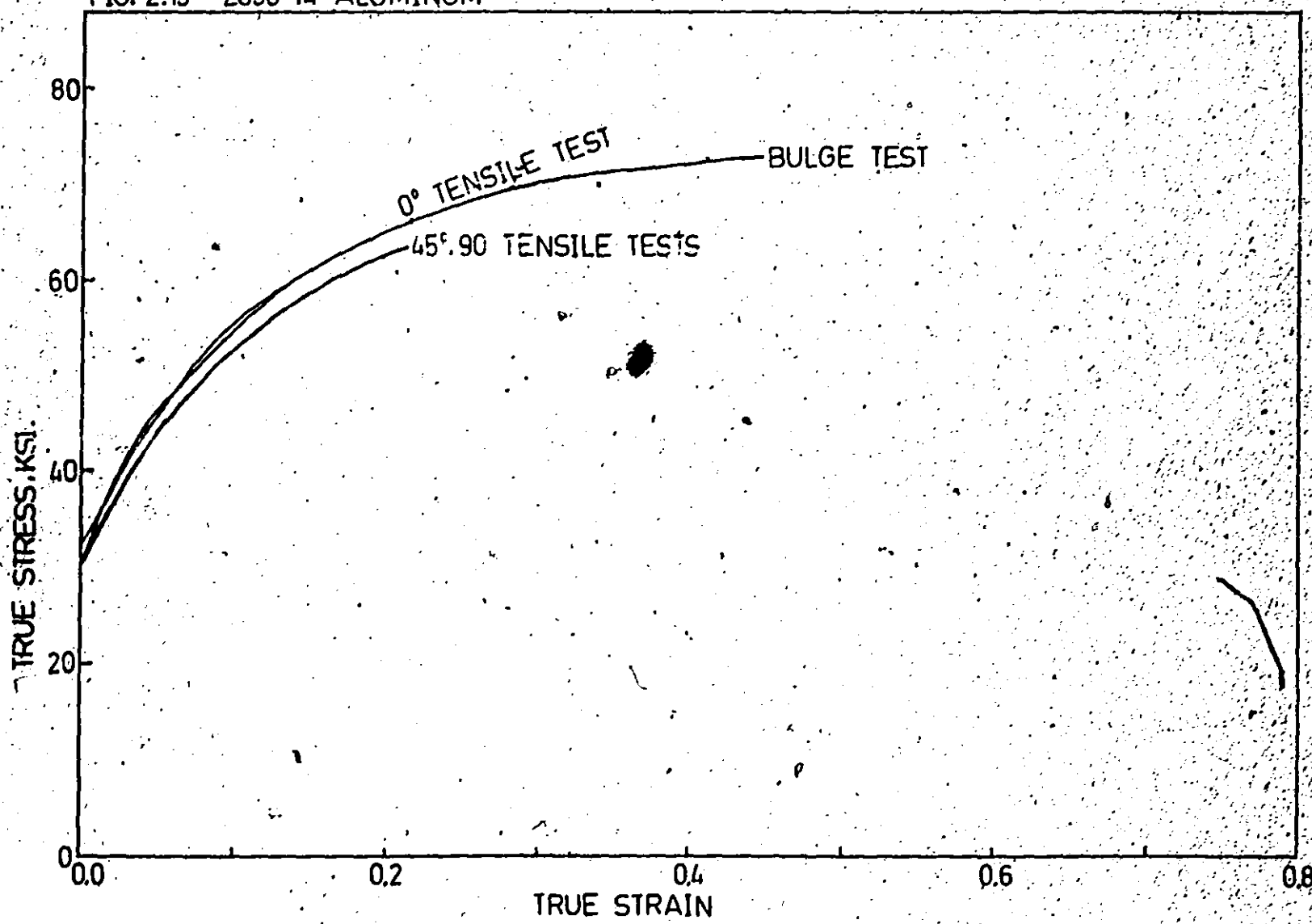

2.3.1 Tensile Test - 0.2% Yield Stress

2036-T4	29.2 ksi.
AKDQ steel	25.9
5182-H111	22.6
5182-0	22.4
3003-H14	20.8
3003-0	7.0

The 3003-0 aluminum has a much lower yield stress than any other material.

It should also be noted that the 5182-0 exhibited a small yield point elongation (≈ 1%). This was eliminated by the skin roll pass (5182-H111).

Both tempers of the 5182 aluminum exhibited serrated yielding (Figure 2.14) but it seemed to be suppressed at the beginning of the curve in the skin rolled (H111) material. The local shear bands which appeared concurrently with the serrated yielding (similar to Luder's strains) were at an angle of 55° with the specimen axis, i.e., not parallel to the fracture surface (≈ 61°).

2.3.2 Tensile Test - Ultimate Tensile Strength

2036-T4	51.4 ksi.
AKDQ steel	44.0
5182-H111	43.0
5182-0	42.6
3003-H14	22.2
3003-0	15.6

The 2036-T4 aluminum has the greatest maximum strength while the 3003-0 alloy is significantly weaker than the others.

FIG. 2.14 TENSILE LOAD-EXTENSION PLOT OF A MATERIAL EXHIBITING SERRATED YIELDING

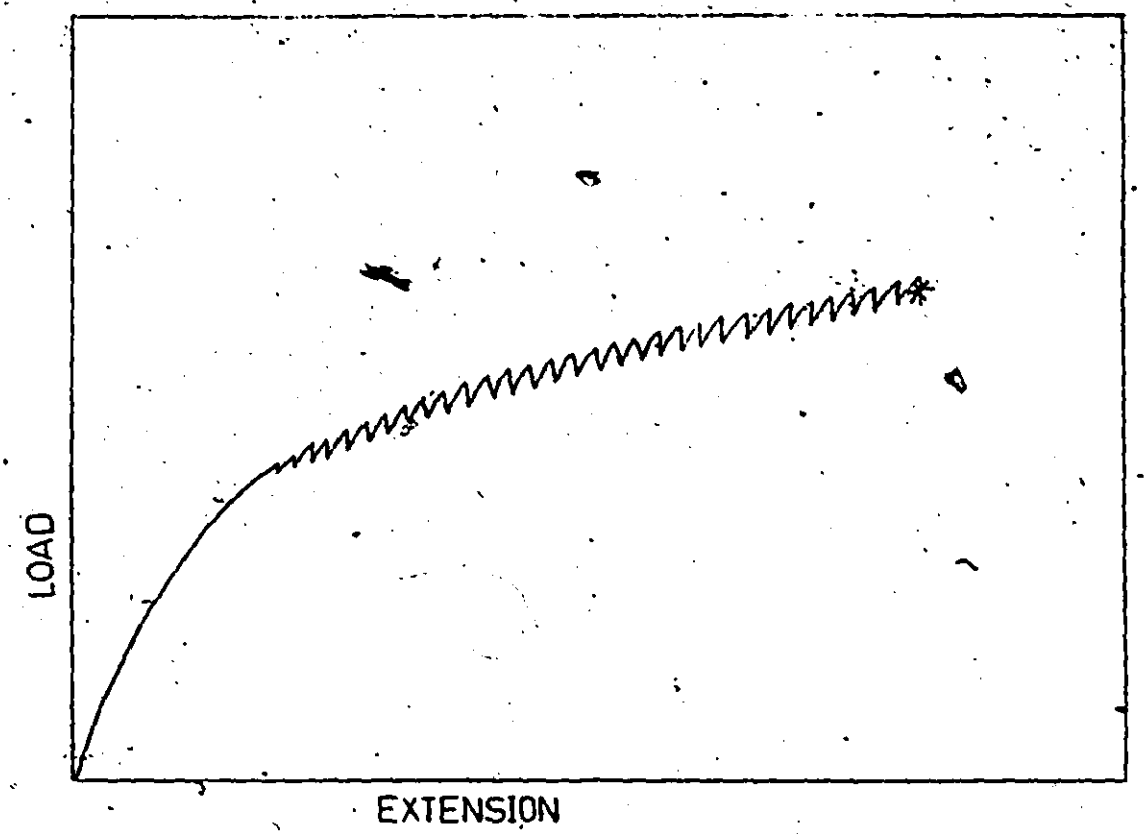

2.3.3 Tensile Test - Ultimate to Yield Strength Ratio, UTS/0.2% YS

3003-0	2.23
5182-0	1.91
5182-H111	1.91
2036-T4	1.76
AKDQ steel	1.70
3003-H14	1.06

This parameter shows that the heavily cold-worked 3003-H14 has the lowest strain-hardening capacity, as would be expected.

2.3.4 Tensile Test - Total Elongation

AKDQ steel	35.7%
3003-0	34.5
5182-H111	26.4
5182-0	26.2
2036-T4	23.6
3003-H14	2.8

The steel and the 3003-0 aluminum have the greatest total elongation. The 3003-H14 seems to have almost no ductility.

2.3.5 Tensile Test - Strain at Maximum Load

AKDQ steel	.205
2036-T4	.192
3003-H14	.010

Figures were not available for the 3003-0 and 5182 alloys since Alcan did not determine this parameter.

The 3003-H14 aluminum has extremely low strain at maximum load.

2.3.6 Tensile Test - Strain Hardening Exponent, n

(McMaster fits)		(Alcan fits marked *)	
5182-0	.313	5182-0	.317*
5182-H111	.257	3003-0	.247*
2036-T4	.239	5182-H111	.246*
3003-0	.221	2036-T4	.239
AKDQ steel	.217	AKDQ steel	.211

These results indicate that the strain hardening ability of the aluminum alloys is better than that of the steel.

The quoted n-values for the bulge and tensile tests are the result of weighted least squares fits of the natural logarithms of true stress and true strain to:

$$\ln \sigma = n \ln \varepsilon + \ln K$$

The weighting factor $w_i = (\sigma_i)^2$ is used to counteract the inherent weighting of the logarithms. The goodness of fit was evaluated on the basis of the standard deviation of n and on the appearance of a plot of the deviations of points from the fitted line vs. strain. Points were discarded from the beginning of the curve until a good fit was obtained, since the latter part of the stress-strain curve is considered to be more important in assessing formability. The standard deviation of the n-values given (variance weighted averages of duplicates) varied between .001 and .008 and averages about .003).

A copy of the computer program is given in Appendix I.

The tensile test values given for the 3003-0, 5182-0 and 5182-H111 aluminum alloys were provided by Alcan and are unweighted logarithmic least squares fits to data for greater than 3% strain. Alcan also provided stress-strain plots for the 0° tensile tests of these three samples. Points were taken from these graphs, and weighted and unweighted fits performed with the results shown in Table 2.4. It is shown that the difference between the weighted and unweighted fits can be significant.

2.3.7 Tensile Test - Plastic Strain Ratio, r

AKDQ steel	1.918
3003-H14	1.10
5182-H111	0.854
5182-0	0.785
2036-T4	0.754
3003-0	0.645

The steel has much higher r-value than any of the aluminum alloys.

2.3.8 Tensile Test - Fracture Angle

5182-0	61°
5182-H111	61
3003-H14	63
2036-T4	64
3003-0	65
AKDQ steel	68

No large variation in fracture angle was observed.

2.3.9 Bulge Test - Strain Hardening Exponent, n

5182-0	.312
5182-H111	.254
3003-0	.234
AKDQ steel	.233
2036-T4	.215
3003-H14	.057

This index suggests that, except for the 3003-H14 alloy, the aluminum alloys equal or better the steel in strain hardening ability.

2.3.10 Bulge Test - Strain at Maximum Load

3003-0	.585
AKDQ steel	.491
3003-H14	.419
2036-T4	.399
5182-H111	.314
5182-0	.270

The 3003-0 aluminum and the steel exhibit the highest strains at maximum load while the 5182 aluminums exhibit the lowest.

2.3.11 Bulge Test - Strain at Failure

3003-0	.675
AKDQ steel	.624
2036-T4	.442
3003-H14	.419
5182-H111	.314
5182-0	.270

The 3003-0 aluminum and the steel exhibit the largest strains at fracture and the 5182 aluminum the lowest.

2.3.12 Torsion Test - n-Value

AKDQ steel	.239
5182-0	.222
3003-0	.209
5182-H111	.190
2036-T4	.179
3003-H14	.045

This index also indicates that the 3003-H14 utility aluminum has drastically less strain hardening ability than the other materials.

2.3.13 Torsion Test - Fracture Strain

AKDQ steel	2.194
3003-H14	1.358
3003-0	0.710
5182-0	0.355
5182-H111	0.352
2036-T4	0.245

The steel and the 3003-0 aluminum have the highest fracture strains. The 2036-T4 and 5182 aluminum alloys have much lower fracture strains.

2.3.14 Swift Circular Cup Test - LDR

AKDQ steel	2.52
5182-0	2.30
5182-H111	2.29
3003-0	2.20
3003-H14	2.04

2036-T4 $\geq$ 2.19

The steel has the highest LDR and the 3003-H14 the lowest.

For the steel, large ears occur in the 0° and 90° directions. The earing in the aluminum alloys occurred in the

45° directions and except for the 3003-H14 utility aluminum was less pronounced. (Since no cups were successfully drawn from the 2036 aluminum, no comments can be made about its earing behaviour.)

The failures for the steel and the 3003 aluminum alloys were of the common type, i.e., over the punch radius. The fractures appeared to be of a ductile nature. Large blanks of the 5182 aluminum alloys also failed over the punch radius but less necking occurred before fracture.

Due to the generous die radius of the Swift tooling, the outer edge of the blank is not supported during the last part of the draw (Figure 2.15) and some wrinkling is inevitable. For smaller blanks of the 5182 alloys splitting occurred due to shear in these wrinkles. For LDR determination this type of failure was ignored as it was felt that it did not relate to the "drawability" in the anisotropy or r-value sense. Blank size was increased until the common type of failure over the punch radius occurred and the maximum was considered to be the limiting blank diameter.

Only one blank was drawn with the 2036 aluminum due to a shortage of material and this also failed in a non-standard manner. A shearing split occurred, in the plane of the sheet, beginning at the top of the cup wall and propagating out across the flange.

FIG. 2.15 SCHEMATIC DIAGRAM OF SWIFT CIRCULAR CUP TEST SHOWING UNSUPPORTED EDGE IN FINAL STAGE OF DRAW

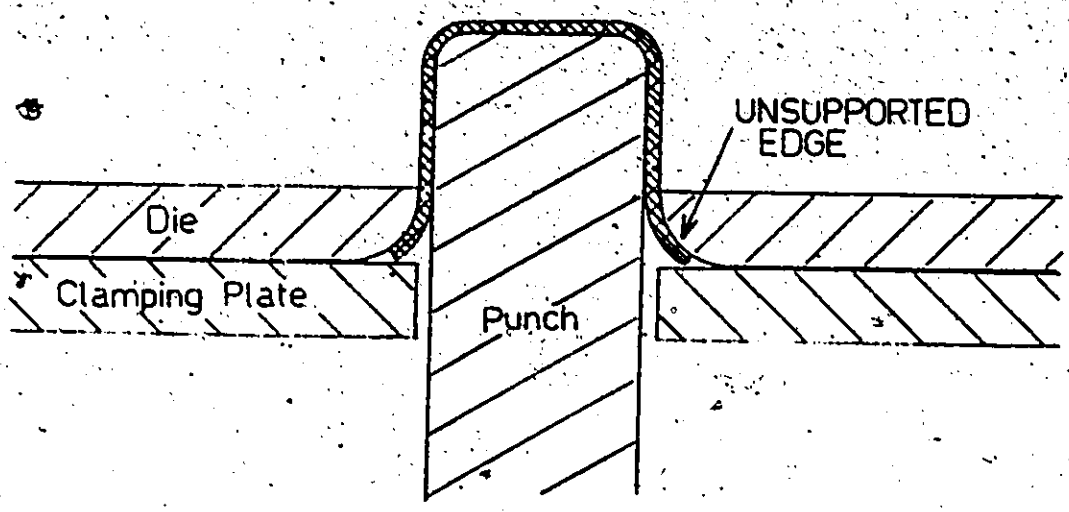

2.4 Correlations and Discussion

2.4.1 Parameters Related to Anisotropy

Figure 2.16 shows a plot of limiting drawing ratio vs. r-value. Except for the 3003-H14 aluminum, the values show the expected increase in LDR with increasing r-value. The low LDR for the 3003-H14 may be due to the very poor strain hardening ability, resulting in early failure in the material which is initially stretched between the punch and the die before the flange begins to draw in. This view is supported by the correlation of r with fracture angle and by the relationship of the bulge and tensile stress-strain curves, as discussed later in this chapter.

Figure 2.16 also shows experimental and theoretical curves produced by Whitely [14], Ikeshima [15] and Thomson [16]. These all lie below the results of this work. The explanation probably lies in differences in tool geometry and lubrication.

The observations of earing behaviour generally support the theory that higher relative r-value or lower relative strength in a given direction will result in ears in that direction in a successfully drawn cup.

As mentioned earlier the fracture angles should correlate with the r-values; larger r-values coinciding with smaller fracture angles. Bearing in mind that these angles are not easy to measure since the fracture edge is not really straight, this seems to be generally true particularly when individual test directions rather than averages are considered. The steel does not fit the general pattern but this is not.

FIG. 2.16 LIMITING DRAWING RATIO VS. PLASTIC STRAIN RATIO

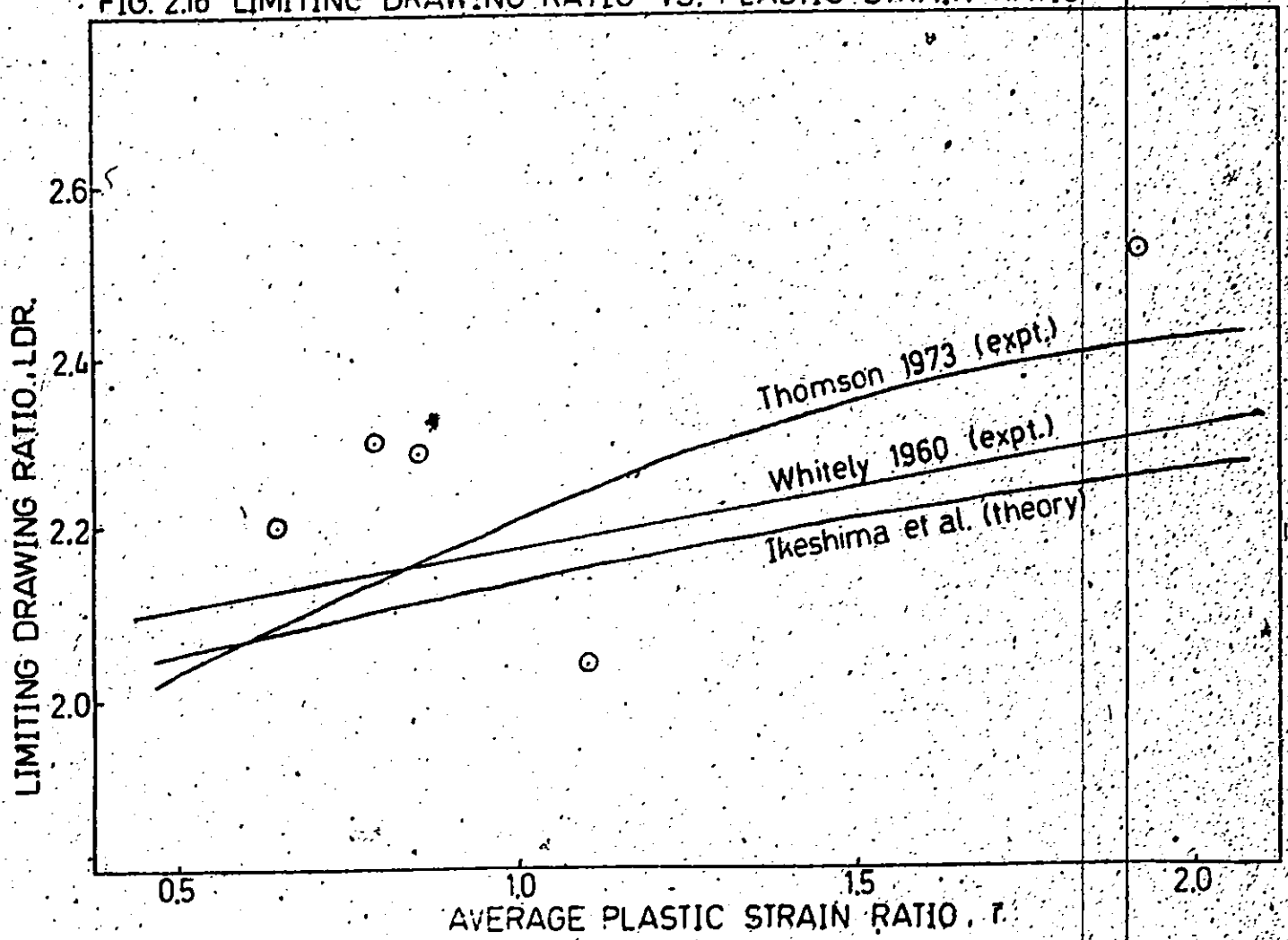

surprising since the theory considers a 2-dimensional model in the plane of the sheet whereas the real situation, particularly near fracture after diffuse necking, has a definite 3-dimensional character.

The bulge and tensile test stress-strain curves do not, in general, coincide. This is explained as a result of the anisotropy. In terms of r-values - a higher r-value means greater resistance to thinning and therefore higher flow stress in biaxial tension than in a uniaxial test. The following formulae express this correlation [17].

$$\sigma_z = \left[\frac{1+\bar{r}}{2}\right]^{1/2} \sigma_{av} \quad ; \quad \varepsilon_z = \left[\frac{2}{1+\bar{r}}\right]^{1/2} \varepsilon_{av}$$

where,

σ_z, ε_z = predicted bulge test stress and strain

σ_{av}, ε_{av} = average tensile test stress and strain

$\bar{r}$ = average r-value

These relations were checked by calculating the predicted bulge stress and strain for one point near the end of the tensile test curves. The fit to the actual bulge test results was very good for the steel and slightly improved for the 3003 alloys. For all other materials the fit was made worse. The 5182 alloys were over compensated and the correction moved the curve in the wrong direction for the 2036 aluminum.

2.4.2 Parameters of Strain Hardening and Fracture

Table 2.5 shows the rank order of the materials in the parameters related to strain-hardening, i.e., UTS/YS, tensile test n, bulge test n and torsion test n. It may be seen that although correlation is not perfect, a general trend is visible. The 3003-H14 is definitely the poorest material as far as strain hardening is concerned. The 3003-0 and 5182 alloys appear to have slightly greater strain hardening ability than the steel and the 2036-T4 slightly less.

In the bulge test, comparison of the strain at maximum load with $\frac{4}{\pi}(2n + 1)$ shows that the agreement is quite good for the steel and the 3003 aluminum but poor for the 5182 and 2036 aluminum alloys.

The strain at failure in the bulge test is equal to the equi-biaxial limit strain* which is defined as the strain near the fracture but clear of any zone of localized plastic deformation. It has been suggested [18], based on the Marciniak hypothesis which associates failure in biaxial tension with pre-existing inhomogeneities, that the limit strain is dependent on the size of the initial inhomogeneities, the strain hardening exponent (n) and the fracture strain (ε_f). This seems to be supported here. The steel and the

* Actually the values quoted in Table 2.2 will be underestimates of the limit strain. Accurate determination requires measurement of grid markings near the fracture site whereas the given values are simply the last available extensometer reading.

3003-0 aluminum, which have reasonably high n and ε_f, have large failure strains. The 5182 and 2036 aluminum alloys, which have much lower fracture strains, have low biaxial limit strains. The 3003-H14 aluminum also had a low limit strain, probably due to its very low n-value.

In order to explain the types of tensile test fractures (Table 2.3), it is useful to consider another factor - strain rate sensitivity. The rate sensitivity in conjunction with the work hardening ability determines to a large degree the amount of diffuse necking which occurs before local necking begins. Ghosh [6] has suggested that 3003-0 aluminum has very low strain rate sensitivity compared to steel and that 2036-T4 aluminum has a small negative rate sensitivity. The 5182 alloys exhibit serrated yielding (Portevin-Le Chatelier Effect [19]) which has been suggested to be an indication of negative rate sensitivity [5].

Before going further it should be noted that rate sensitivity is difficult to measure particularly when it is as small as suggested. Tensile tests at McMaster were performed at two strain rates for the 2036-T4 aluminum, (10^{-4} sec^{-1} and 2.5×10^{-3} sec^{-1}), and no difference was found. Ghosh's value of strain rate sensitivity would predict a stress difference of 700 p.s.i., i.e., 1.5%, which could have easily been missed. Therefore the following discussion is offered as a suggestion only.

The steel exhibits a large amount of diffuse necking before a local neck develops, which is consistent with high

strain hardening and considerable positive rate sensitivity. The 3003-0 aluminum has less diffuse necking due to its smaller rate sensitivity. The utility aluminum, with both low strain hardening and low rate sensitivity, exhibits virtually no diffuse necking. The 5182 and 2036 alloys also have no diffuse neck but in this case it may be due to negative strain rate sensitivity in spite of high strain hardening.

The failure type in the local neck depends on the fracture strain. The materials with higher fracture strains in the torsion test (AKDQ steel, 3003-0 and 3003-H14 aluminum) neck down to sharp points, i.e., fracture in a ductile fashion. The materials with lower fracture strains fracture in a brittle* fashion, i.e., with relatively less necking.

* The term brittle is not used here in a strictly correct sense; it is meant to imply fracture after very little local necking.

CHAPTER 3

CONSTRUCTION OF SQUARE CUPPING TOOLS

3.1 Design

A punch and die set for drawing square cups was designed for use in the Hille 20 ton Universal Sheet Metal Testing Machine. (Figure 3.1).

Figure 3.2 is a schematic diagram showing the critical dimensions of the finished tooling. The punch and die radii and the punch-die clearance were not generously chosen as it was desired to generate failures. They were selected to agree with commercial practice.

The maximum blank diameter which can be accommodated in the Hille Press is 6.5". Based on the work of Thomson, Hobbs and Brammar [7] with steel, it was decided that the maximum cup width for which a significant number of failures could be generated was about 2.0 inches.

The tooling was designed for 0.03" thick material. Recommended punch [20] and die [8] radii are 4t to 10t. The values measured on the completed tools were about 7t. The suggested punch-die clearance [20] is 1.15-1.20t. The value chosen was .05" = 1.2t.

The tools were machined from mild steel which was then case-hardened. After hardening it was necessary to grind and polish to restore flat and true surfaces.

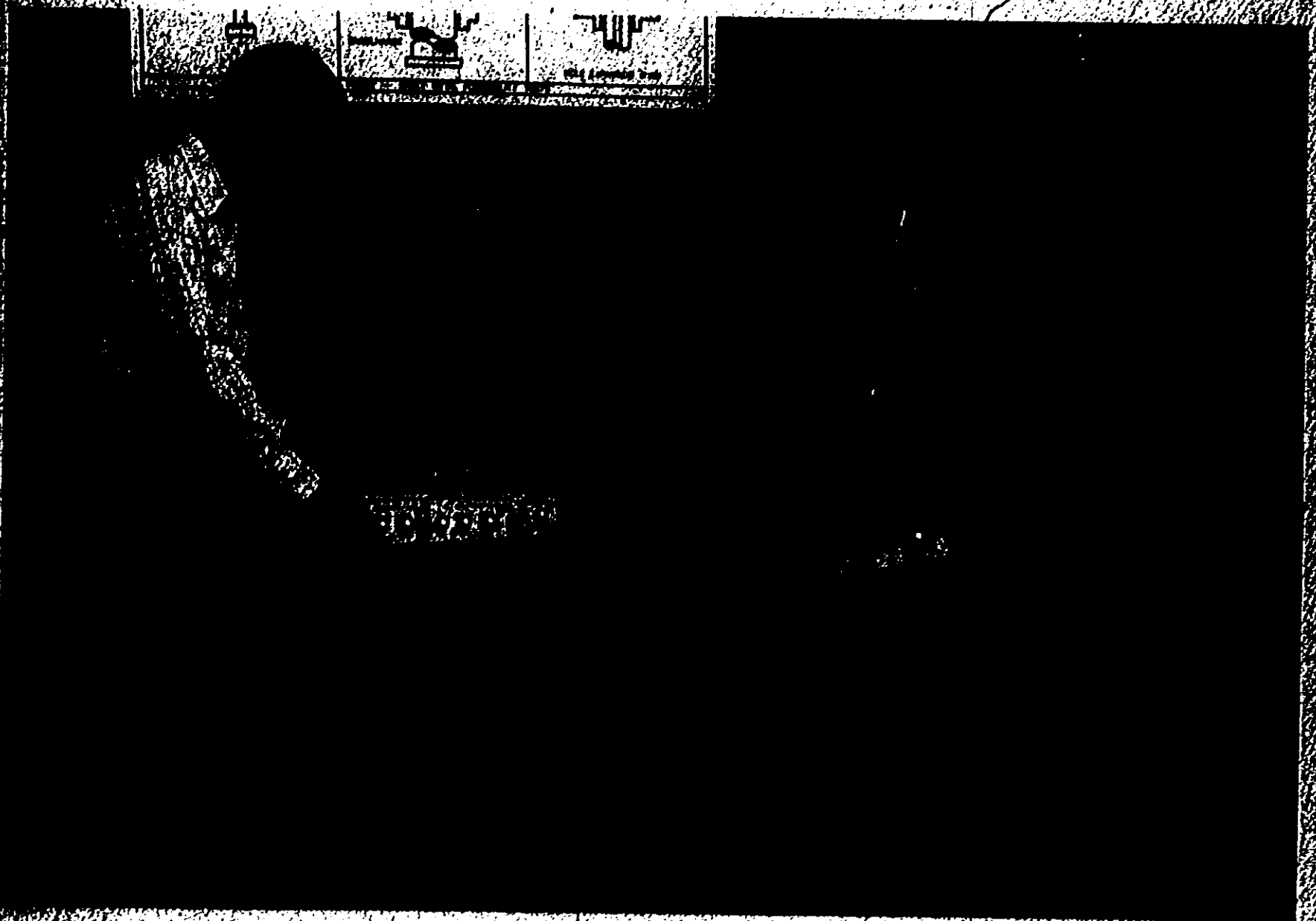

Figure 3.1a Hille 20 Ton Universal Sheet Metal Testing Machine.

FIG. 3.2 SCHEMATIC DIAGRAM OF SQUARE CUPPING TOOLS

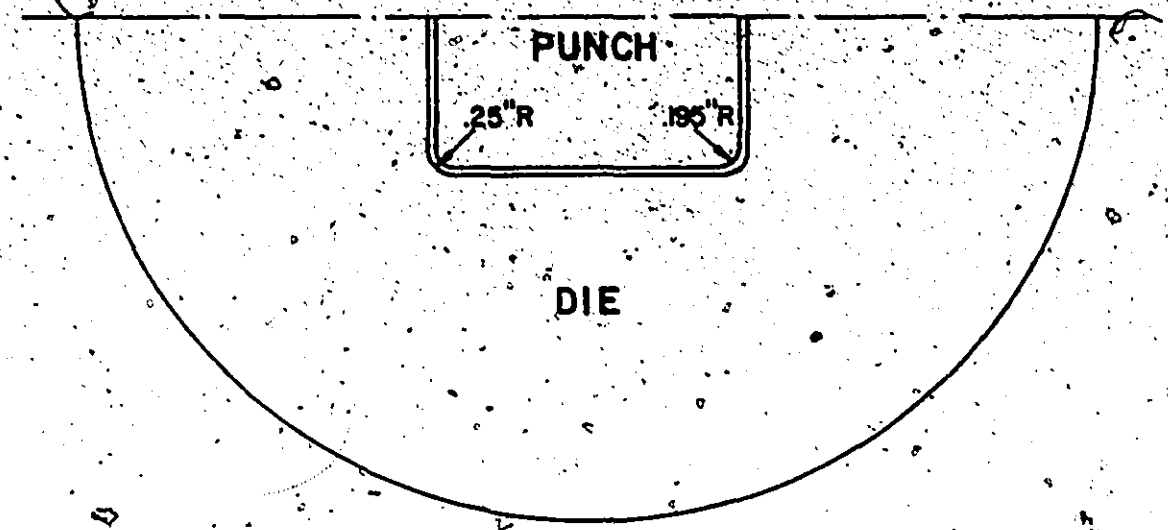

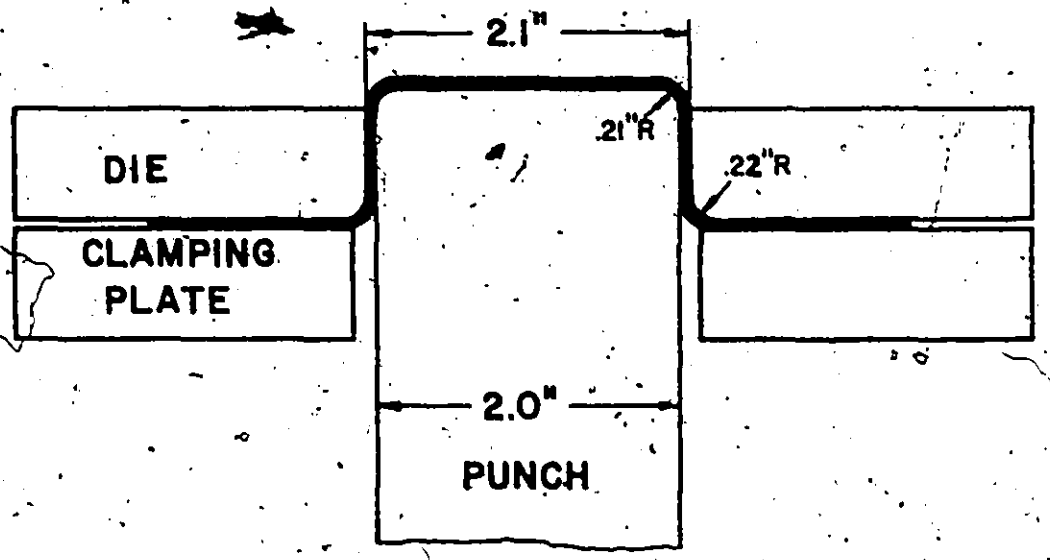

3.2 Installation and Initial Testing

The initial tests were performed with 3.5" diameter circular blanks of .017" thick commercial quality steel. This material exhibits very large yield point elongation, about 6%. As a result there is a sharp visible line dividing the elastically and plastically deformed areas on the bottom of a formed cup.* If the die, punch and clamping plate are symmetrically machined and properly aligned the plastic zone should extend equally from all four sides and failure should occur simultaneously at all four corners as shown in Figure 3.3a.

The first trials were performed with dry blanks and high clamping load (17,000 lb.). The extension of the plastic zone and the location of the failures was not symmetric. (Figure 3.3b). In addition, the edge of the blank was polished more on the sides where the material did not stretch, indicating that the clamping pressure was not even all around the blank.

By experimenting with different relative orientations of the tools and by polishing some areas it was possible to achieve much more symmetric stretching and failure. The addition of minimal lubrication (hydraulic oil) then led to virtually perfect symmetry and the tooling was considered to be ready for further tests.

---

* stretcher strain marks

FIG. 3.3 TOP VIEW OF PARTIALLY DRAWN BLANK SHOWING PLASTIC-ELASTIC BOUNDARY AND FAILURE LOCATION

a) optimum tooling

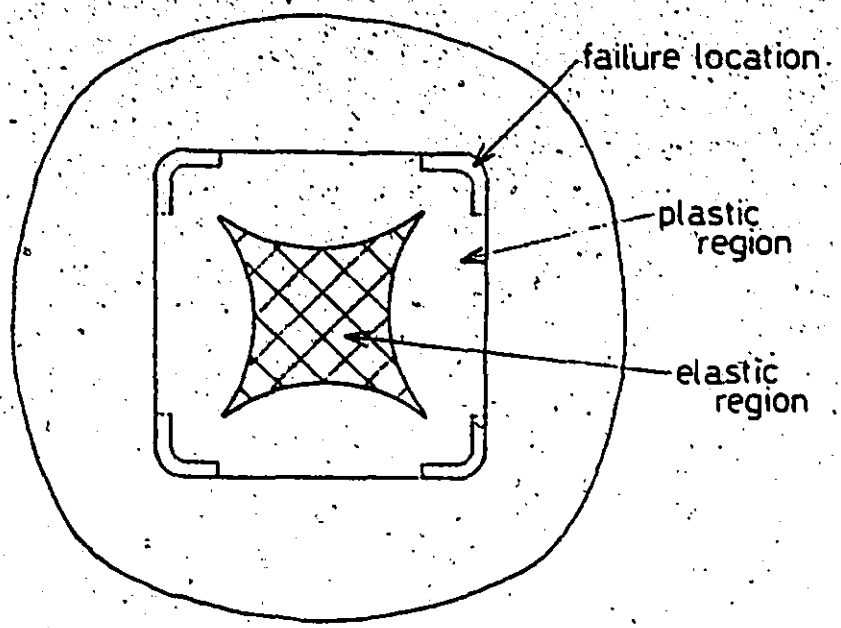

b) uneven clamping pressure

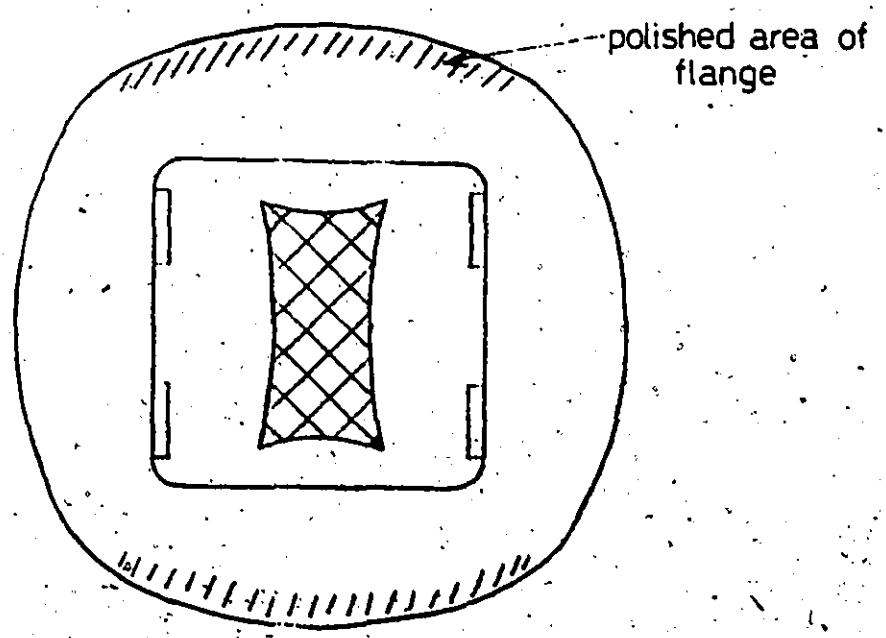

CHAPTER 4

LUBRICATION STUDIES

4.1 Introduction

Generally lubricants for deep drawing are chosen by trial and error at the press and on the basis of measurements of the coefficient of friction. It has also been suggested that maximum drawing force may be a good criterion for evaluating lubricants [21].

The purpose of this work was to select a suitable lubricant for deep drawing experiments using the square punch and die set. Several possible criteria for assessing lubricants were examined, namely: -

i) maximum clamping pressure for near-critical blank size,
ii) load at failure,
iii) depth of draw failure, and
iv) maximum load in successfully drawn cups.

4.2 Materials and Lubricants

The materials used for these tests were 0.0315" utility grade aluminum (3003-H14) and 0.0310" commercial grade galvanized steel. The blanks were circular with lathe-turned edges and were set in the die with the rolling direction of the material parallel to the sides of the square die.

The punch speed in all tests was approximately 0.04 in./sec.

Tests were performed with four basic lubricants and several combinations of two of them. The basic lubricants chosen were:

a) polythylene sheet, 0.004" thick,

b) hydraulic oil - Shell Tellus Oil 25, lighter than SAE 10 (150-165 SSU @ 60°F),

c) motor oil - Veedol non-detergent motor oil, SAE 50,

d) gear oil - Motormaster all-purpose E.P. gear lubricant, SAE 140.

4.3 Experiments

4.3.1 Maximum Clamping Load for Near-Critical Blank Size

This series of tests was conducted with 4.50" diameter aluminum blanks which could be successfully drawn at low clamping loads but which failed at high clamping load. The parameter used to compare the lubricants was the maximum clamping load for which a blank could be successfully drawn.

A blank with no lubrication at only 1000 lb. clamping load failed at the bottom of the side wall where material was stretched over the punch radius. Almost no drawing occurred.

When hydraulic oil was applied to both sides of the blank and to the punch, die and clamping plate, failure still occurred with 1000 lb. clamping but the cup was deeper and the fracture was located at the top of the side wall.

With gear oil similarly applied, a blank was successfully drawn with 6000 lb. clamping except that the very tips

of the ears at the corners were broken off. At 7000 lb. failure occurred at the bottom corner of the cup.

When polyethylene sheet was placed on both sides of the blank, a successful cup was drawn with a clamping load of 18000 lb.

It may be concluded that the hydraulic oil produces only a slight reduction in friction compared to the dry blank. The thick gear oil is much better but significantly inferior to the polyethylene sheet.

One further phenomena was observed. When gear oil was used with a clamping load of only 1000 lb. the blank failed due to sudden severe wrinkling of the flange. This suggests that friction between the flange surface and the tooling acts as a constraint against wrinkling.

4.3.2 Maximum Load and Depth of Draw at Failure

This group of tests was performed with 5.25" diameter steel blanks which failed at the bottom corner of the cup for all lubrication combinations. The depth-at-failure and maximum load (at failure) were examined as measures of the lubrication effectiveness. These values were determined from the autographic record of punch load vs. punch travel as shown in Figure 4.1.

Two clamping loads were used; 3000 lb. and 6000 lb.

The lubrication combinations are shown in Table 4.1.

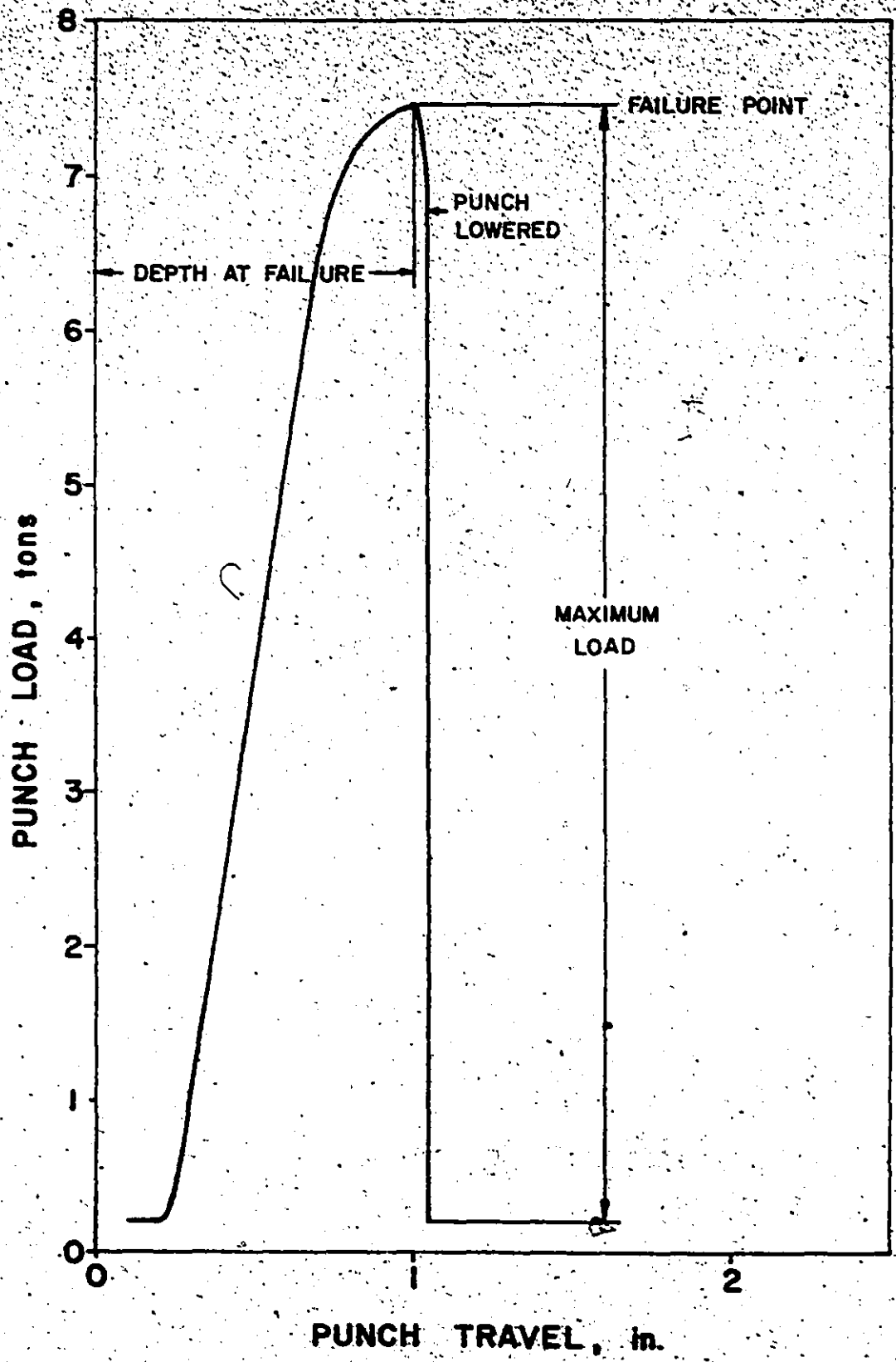

Figure 4.1. Autographic record for deep drawing operation.

Code	Lubricant
	Shell Tellus Oil 25 and polyethylene sheet
1	- sheet oiled on both sides
2	- sheet oiled on blank side only
	Veedol Non-detergent Motor Oil and polyethylene sheet
3	- sheet oiled on both sides
4	- sheet oiled on blank side only
	MotorMaster E.P. Gear Lubricant and polyethylene sheet
5	- sheet oiled on both sides
6	- sheet oiled on blank side only
7	Polyethylene sheet only

Table 4.1. Lubrication conditions for tests on blanks lubricated on both sides.

The maximum load (at failure) is shown in Figure 4.2. The range of failure loads is only 3% and this suggests that this parameter is not a discriminating one.

The depth at failure as shown in Figure 4.3 indicates greater variation. Except for one case, lubrication on both sides of the polyethylene film increased the depth. At the lower clamping pressure, the motor oil gave a deeper draw and at higher pressure, the gear oil gave a deeper draw.

One disadvantage of lubricating the film on both sides was that the blank tended to slide off-centre during clamping.

4.3.3 Maximum Load in Successfully Drawn Cups

In this series of tests all blanks were successfully drawn and the maximum punch load was used as a measure of lubrication effectiveness. Three lubrication conditions were tested with two clamping loads (3000 lb., 6000 lb.). The results are shown in Figure 4.4.

The results of the three groups of tests can be only roughly compared due to the differences in blank diameter but it is clear that both the motor oil and the gear oil additions are a definite improvement over the polyethylene film alone and the gear oil is more effective than the motor oil

This last conclusion differs from the results of the depth of failure tests. This probably means that the gear oil is in fact better for the reduction of friction and that in

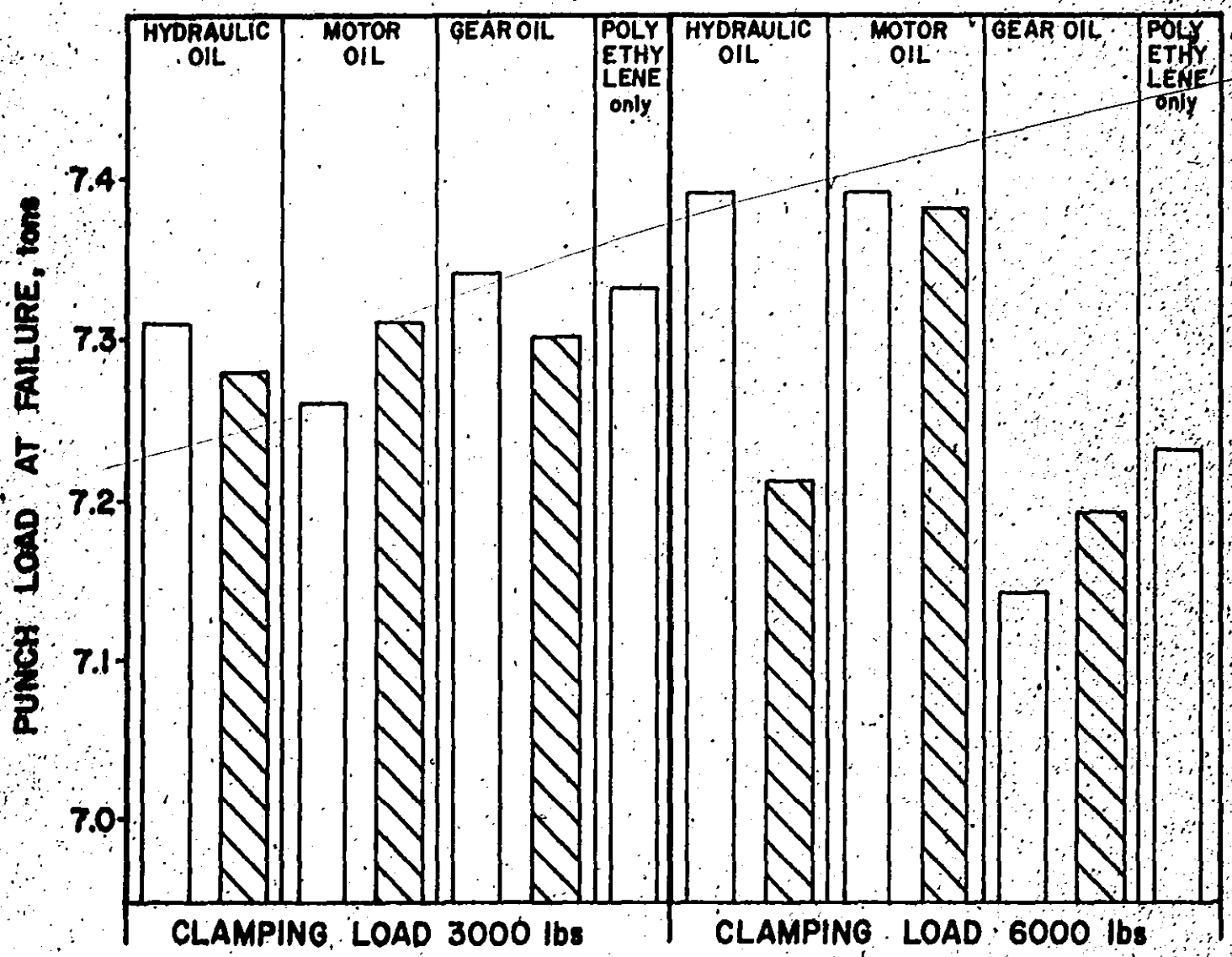

Figure 4.2. Blanks lubricated on both sides; open bars - polyethylene film oiled on one side only; solid bars - oiled on both sides.

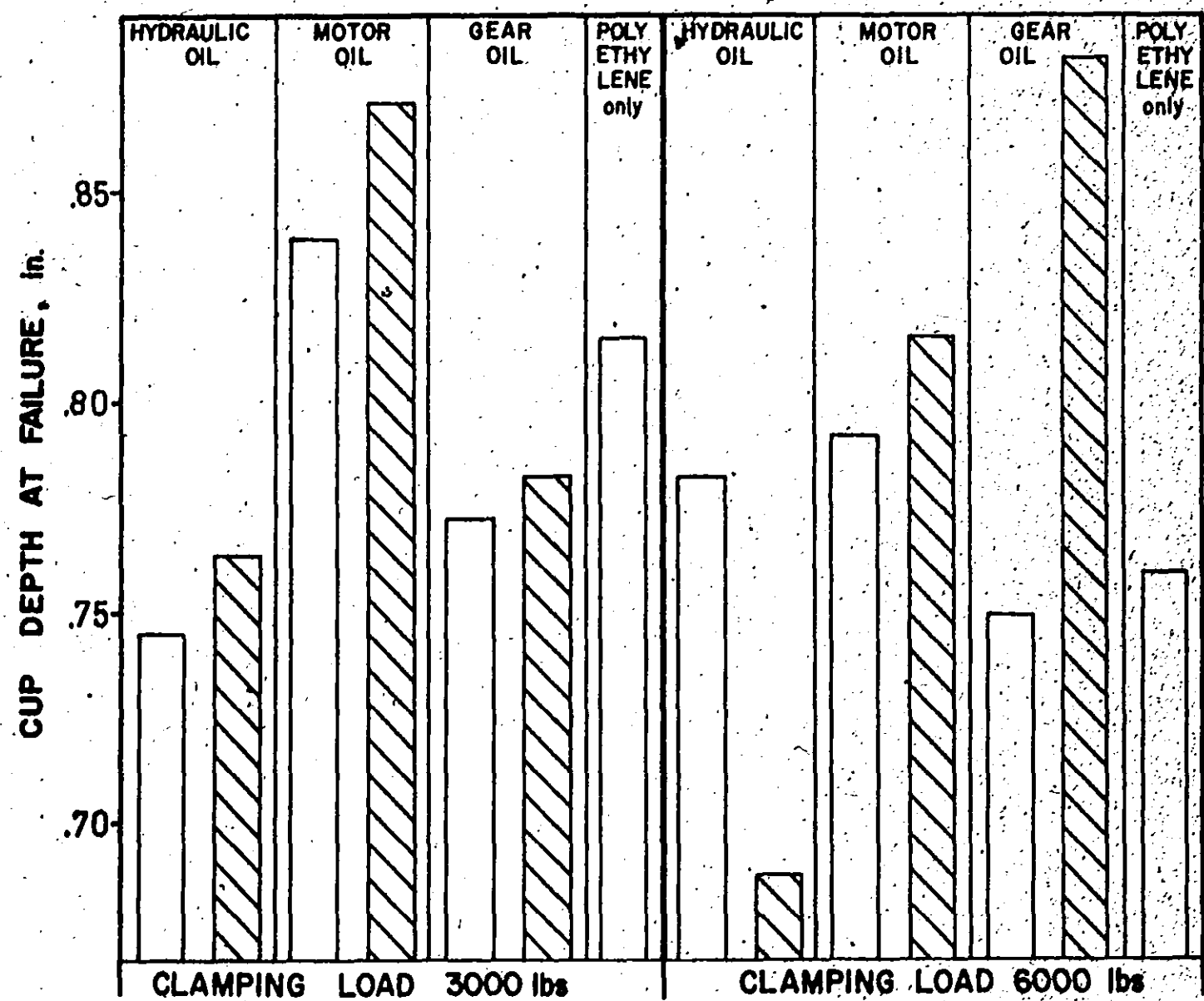

Figure 4.3. Depth of cup at failure for the same blanks as Figure 4.2.

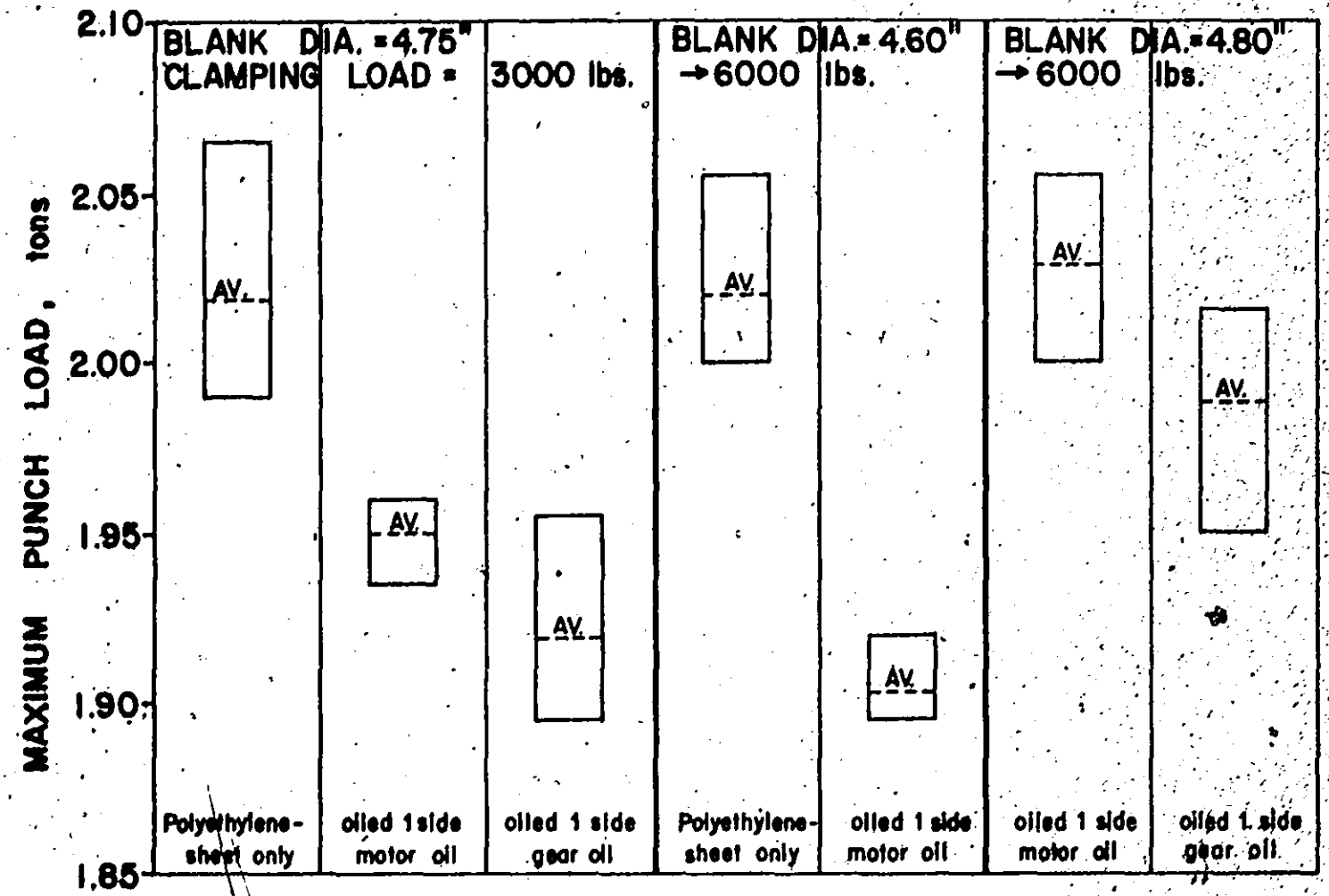

Figure 4.4. Average and range (3-4 tests) of maximum load in successful drawing of aluminum blanks lubricated on both sides as indicated.

the depth at failure test the greater frictional load with the motor oil caused more stretching of the material. In this case, a slightly poorer lubricant may yield a deeper cup.

4.3.4 Effect of Different Lubrication on Each Side of the Blank

It has been suggested that the greatest contribution of friction comes from the contact over the die radius [32] and at the edge of the blank where material has thickened due to the flange deformation [21]. In some cases the punch is roughened to increase friction between the punch and the cup so that the material will not stretch as much and larger blanks can be drawn without failure [23].

An investigation of the effects of lubrication on only one side of the blank was therefore made for the conditions shown in Table 4.2. The clamping load was 3000 lb. The blanks were mild steel, 5.25" in diameter. They all failed at the bottom corner.

The depth-at-failure results are shown in Figure 4.5. As expected, lubrication on the top only (i.e., on die radius) is more effective than on the bottom only. However the blank lubricated on both sides is much better than either indicating that the effect of friction over the whole blank surface is not negligible compared with friction load over the die radius.

In the one test where the flange was lubricated on both sides but the punch was dry, the failure depth was lower than might be expected. There are two possible explanations;

Code	Lubrication
1	No lubrication
2	Polyethylene and gear oil - die side only
3	Polyethylene and gear oil - punch side only
4	Polyethylene and gear oil - both sides
5	Polyethylene and gear oil on the die side and polyethylene with a hole cut around the punch on the clamping plate side.

Table 4.2. Lubrication conditions for tests on blanks lubricated on one side only.

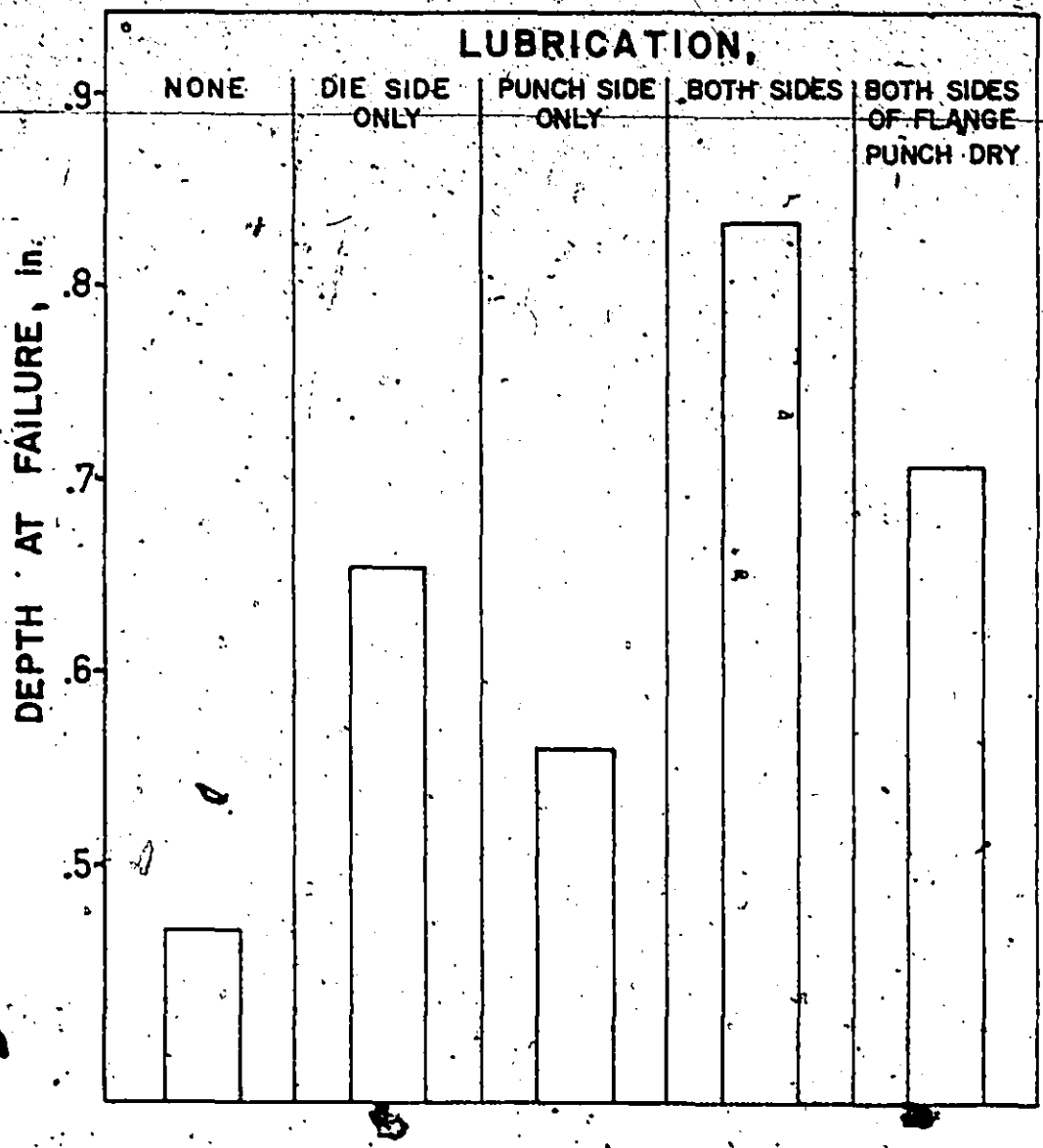

Figure 4.5. Depth at failure for different lubrication conditions; where used the lubricant was polyethylene sheet oiled on one side with gear oil.

i), the lack of lubrication on the punch corners prevented distribution of the strain and led to early failure and,
ii) the bottom lubrication was polyethylene only, i.e., no oil as in the previous test.

4.3.5 Effect of Clamping Load

Tests were performed on 4.99" diameter aluminum blanks which were drawn successfully with a variety of clamping loads. In all tests the blanks were lubricated on both sides with a sheet of polyethylene coated one side with gear oil.

The maximum punch load results (Table 4.3) indicate that increasing the clamping pressure in a small scale operation such as this, has negligible effect on the punch load with this lubrication. The reason may be a reduction in the coefficient of friction with increasing contact pressure [22].

4.4 Conclusion

The tests for maximum clamping load for near-critical blank size indicated that polyethylene sheet was a far better lubricant than any of the oils alone. This test is probably only useful for distinguishing between the poorer lubricants and since in practice very high clamping loads are not used, the test is not representative.

The maximum punch load at failure does not seem to vary much with lubrication. The depth-of-draw at failure does vary with the effectiveness of lubrication but results may be

Clamping Load (lb.)	Maximum Punch Load (Tons)
3000	2.04
6000	2.11
9000	2.13
12000	2.11
20500	2.12

Table 4.3 Maximum punch loads measured for different clamping loads in drawing aluminum blanks lubricated on both sides with gear oil and polyethylene sheet.

confusing due to increased stretching with poorer lubricants.

The maximum punch load for successfully drawn cups appears to be the best way of ranking lubricants. The results are repeatable and clearly indicate variations in lubrication effectiveness. On the basis of this criterion polyethylene film plus gear oil was used in further studies with the square die.

CHAPTER 5

SQUARE CUPPING TESTS

5.1 Observation of Strain History

The strain development within the flange during the deep drawing of a square cup was determined by successive observations of an initially orthogonal grid scribed on the surface of the material. The test was interruped at several points and a record made, of the grid pattern on the flange, and of the position of the edge of the flange. These records were then used to construct pictures of material flow. Due to the symmetry of the cup and assuming planar isotropy in the material it is only necessary to consider 1/8 of the surface of the blank. However, to assist in visualization of the flow, the section between the die diagonals is taken, so the situation is similar to drawing through a straight-sided die with semi-angle 45° (Figure 5.1).

Two types of grid were tried in preliminary tests; a square grid of straight lines, 0.5 cm apart, aligned parallel to the sides of the die opening, and a grid of circles and radial lines. It was found that while the circular grid is better for strain measurement at the cup corners, the square grid provides a better general picture of the flow pattern, so it was chosen for further tests.

The grids were marked on the blanks with a metal

FIG 5.1 VISUALISATION OF SQUARE CUP DRAWING AS DRAWING THROUGH A STRAIGHT-SIDED DIE OF SEMI-ANGLE 45°

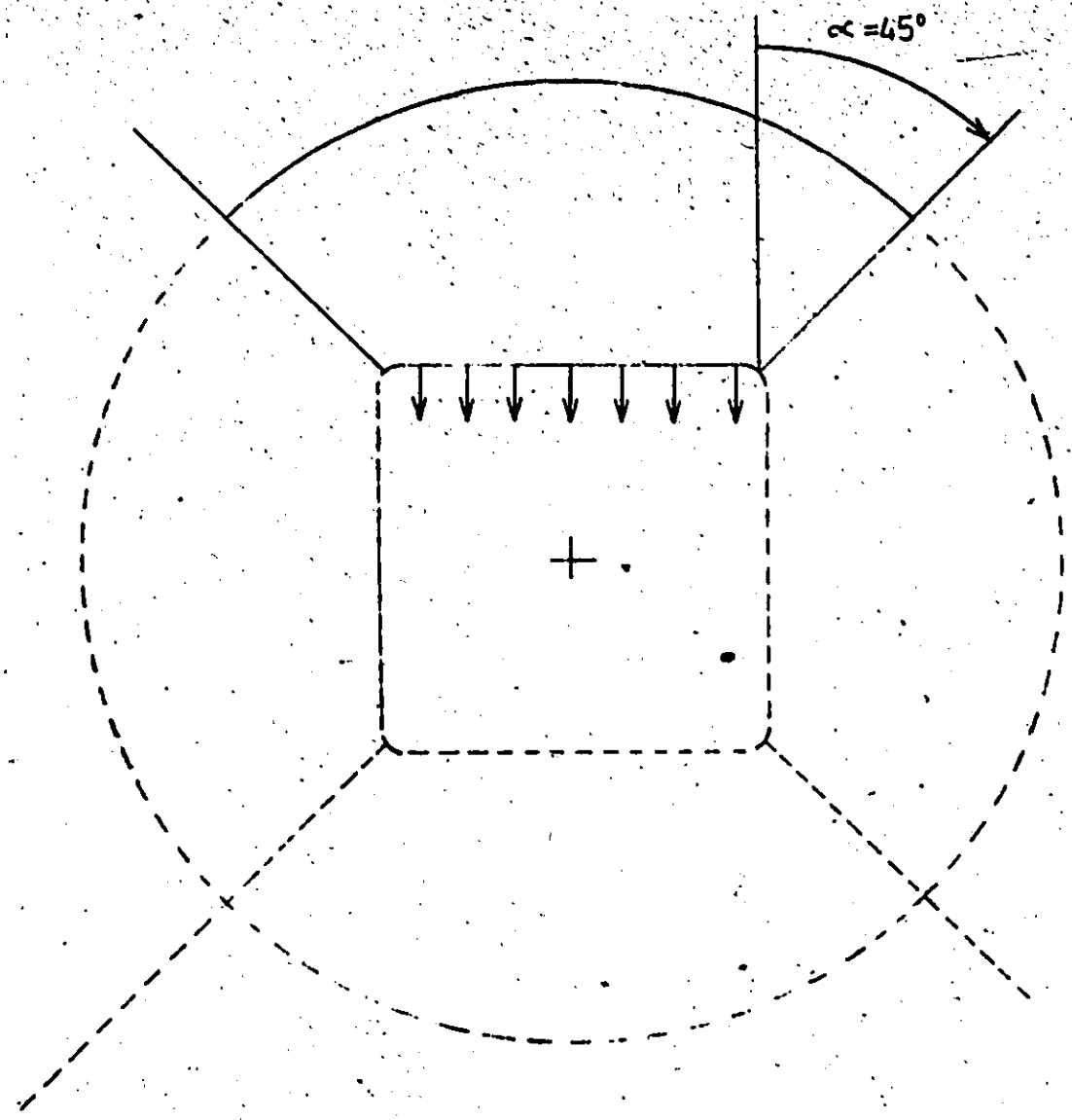

scriber. Some initial trials were made with grids applied by the photo-resist technique but this proved unsatisfactory since the severe straining and ironing at the cup corners removed the grid lines. Mechanical scribing was then used because it is simple, inexpensive and required no additional equipment.

The first tests were made with 3003-H14 utility aluminum and in this case the records at the intermediate stages of drawing were made with a polaroid camera. It proved to be quite difficult to get clear pictures of the grid lines unless they were deeply scribed; good diffuse lighting was essential. In order to improve the presentation of data, diagrams of deformed grids were traced from the photographs. This resulted in drawings very close to 1/2 full size.

The grid lines do have some effect on the drawing process. Occasionally fracture was initiated at a grid line but more frequently, it appeared that friction was increased. In these cases a blank which drew successfully without a grid, failed when a grid was applied, even though fracture was not on a grid line.

In order to avoid the photographic difficulties and to permit the use of lightly scribed grids a second technique was adopted for later tests. In this case the intermediate record was made by tracing the grid on a fine tracing paper laid over the sample.

For some of the interrupted tests with steel blanks it was necessary to increase clamping pressure to avoid

wrinkling in the flange. This indicates that friction was reduced compared to the uninterrupted test. This would be expected since fresh oil was applied after each stage.

Interrupted tests were not performed for the other alloys and only the grid pattern on the completed cup was observed. In the case of the 3003-0 material it was again noted that the grid lines, even though they were lighter than with the 3003-H14 aluminum, seemed to affect friction since it was necessary to reduce blank size to successfully draw a gridded specimen.

It should also be noted that accurate strain measurements are not possible from a manually scribed grid such as used here. The grids serve only to give a general idea of the material flow.

The "depth" values quoted on the diagrams of material flow are actually punch travel, measured on the autographic record, between the position when the punch first contacted the undeformed blank and the position when the test was stopped.

Figure 5.2 shows a collection of blanks drawn in the work of this chapter. The materials used were the same as were tested in Chapter 2.

All blanks were cut out using aircraft-type tinsnips and the burrs removed with a file.

The maximum useful height was measured to the lowest point on the edge of the cup (Figure 5.3). Minor wrinkling and oil canning effects occurred in some tests but

Figure 5.2a Collection of Cups Drawn in Square Cupping Tests.

FIG. 53 MEASUREMENT OF MAXIMUM USEFUL HEIGHT OF SQUARE CUPS

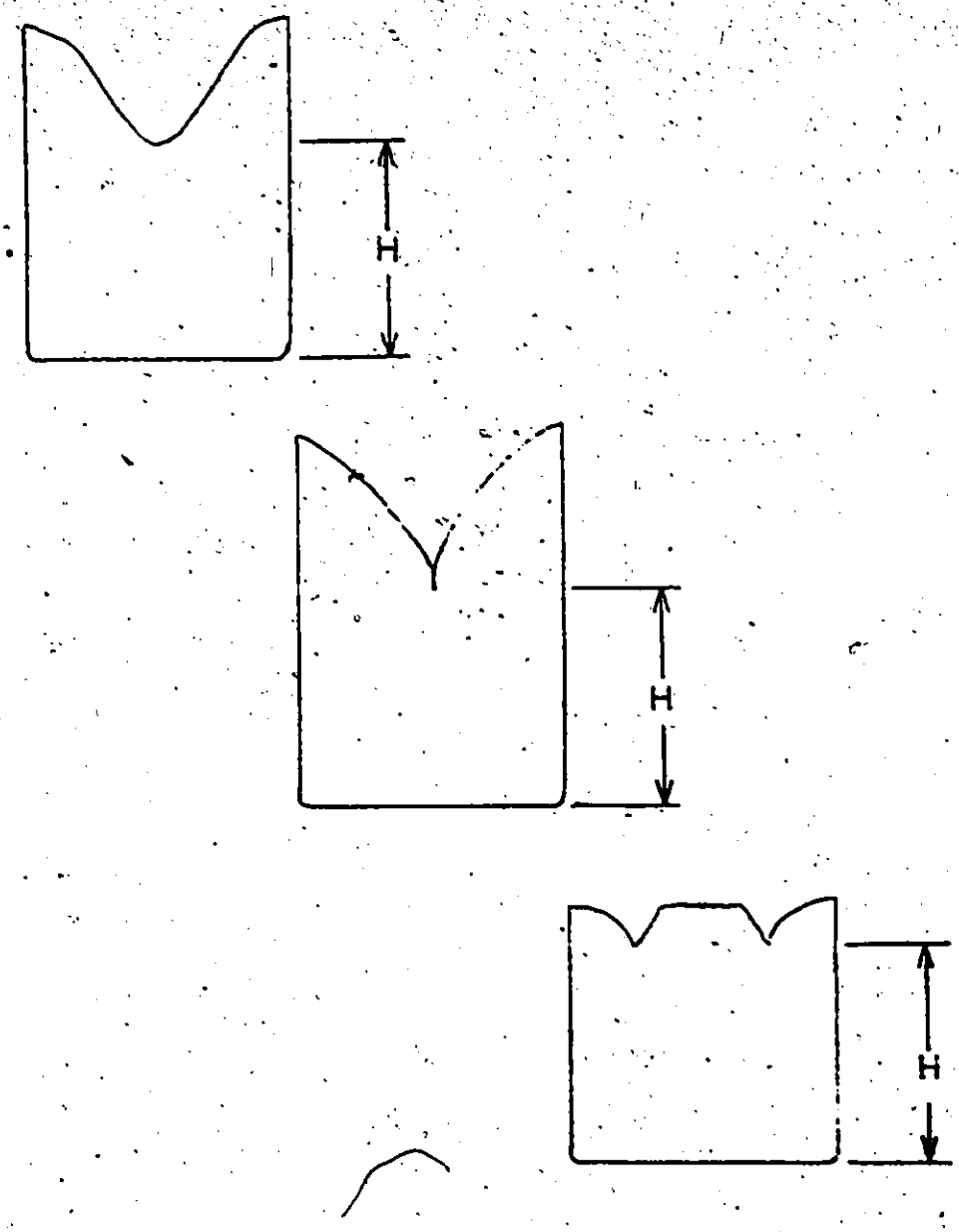

these were ignored for the purpose of this measurement. These effects are difficult to measure and their appearance in larger commercial pressings is not simply related to these small scale tests. Height measurements were made on all four sides of the cup and an average taken.

5.2 Tests with Circular Blanks

The first square cups were drawn from circular blanks since this is an easy shape to produce and has been claimed to be nearly ideal for square cups [3, 9]. All materials were tested at two different orientations, (except the 2036-T4 aluminum of which only a small quantity was available). The first orientation, 0°, was with the rolling direction of the material parallel to the sides of the die opening. The second, 45°, was with the rolling direction aligned with a diagonal of the die opening.

Table 5.1 lists the results and Figures 5.4 and 5.5 illustrate the types of failure observed. Figure 5.6 shows the deepest cup drawn from each material.

The steel gives the deepest cups. When failure occurs it is a ductile fracture at the bottom corner, parallel to the cup bottom (Figures 5.4a and 5.5a). The failure occurs at the point when maximum punch load is reached.

The 3003 aluminum alloys produce shallower cups. Failure in the 3003-0 material is similar to the failure in steel (Figures 5.5a and 5.4c). The 3003-H14 utility aluminum also exhibited ductile fracture at maximum punch load, but in

Table 5.1 Results of Square Cupping Tests with Circular Blanks

Material	Optimum Orientation	Maximum Blank Diameter	Maximum Useful Height of Drawn Cup	Type of Failure
AKDQ Steel	45°	5.74 in.	2.39	ductile fracture at bottom corner parallel to bottom Figures 5.3a, 5.4a.
3003-H14 Aluminum	0°	5.25 in.	1.82	ductile fracture along bottom edge, Figures 5.3c, 5.4b.
3003-0 Aluminum	0°	5.01 in.	1.84	ductile fracture at bottom corner parallel to bottom Figures 5.3a, 5.4c.
5182-0 Aluminum	0°,45°	3.75 in.	0.92	brittle split in corner wall parallel to bottom, propagate into flange Figures 5.3b, 5.4d.
5182-H111 Aluminum	0°, 45°	3.75	0.92	brittle split in corner wall parallel to bottom, propagate into flange Figures 5.3b, 5.4e.
2036-T4 Aluminum	all tests at 0°	3.29	0.55	inclined, brittle split in corner wall, propagate into flange Figures 5.3f, 5.4g.

FIG. 54 FRACTURE PROFILES OF FAILED SQUARE CUPS

d) 5182-0 Aluminum, split in side wall at corner

e) 5182-H111 Aluminum, split in side wall at corner

f) 5182-H111 Aluminum, failure at bottom corner at angle to bottom

g) 2036-T4 Aluminum, shear-type split in side wall at corner

10 mm

FIG. 54 FRACTURE PROFILES OF FAILED SQUARE CUPS

a) AKDQ Steel, failure at bottom corner parallel to bottom

b) 3003-H14 Utility Aluminum, failure along bottom edge over punch radius

c) 3003-0 Aluminum, failure at bottom corner parallel to bottom

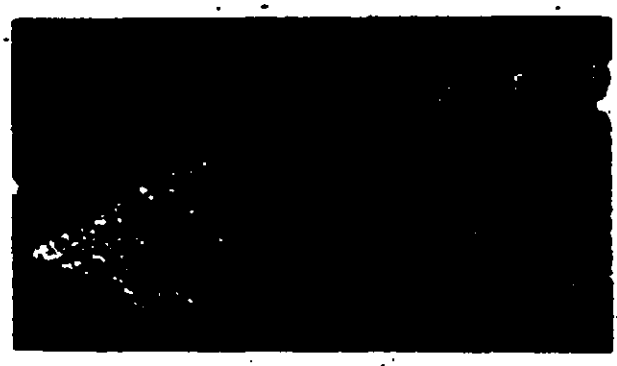

10 mm.

FIG. 55 FAILURE TYPES IN SQUARE CUPS

a)

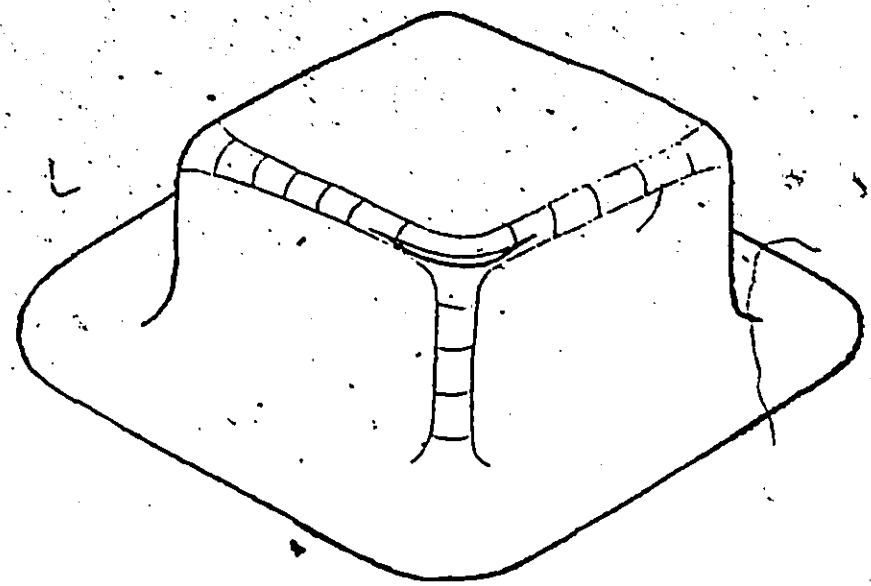

fail at bottom corner, parallel to bottom

b)

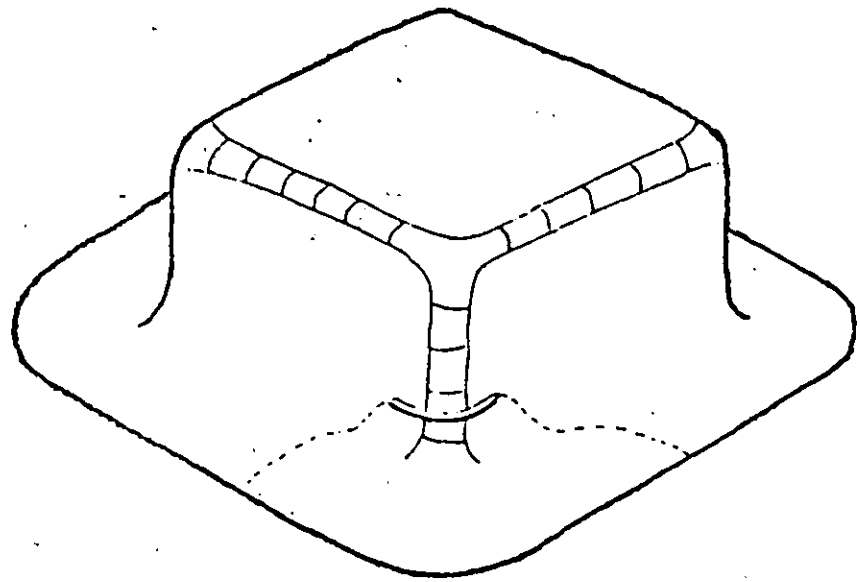

split inside wall, at corner, propagate into flange

FIG.55 FAILURE TYPES IN SQUARE CUPS

c)

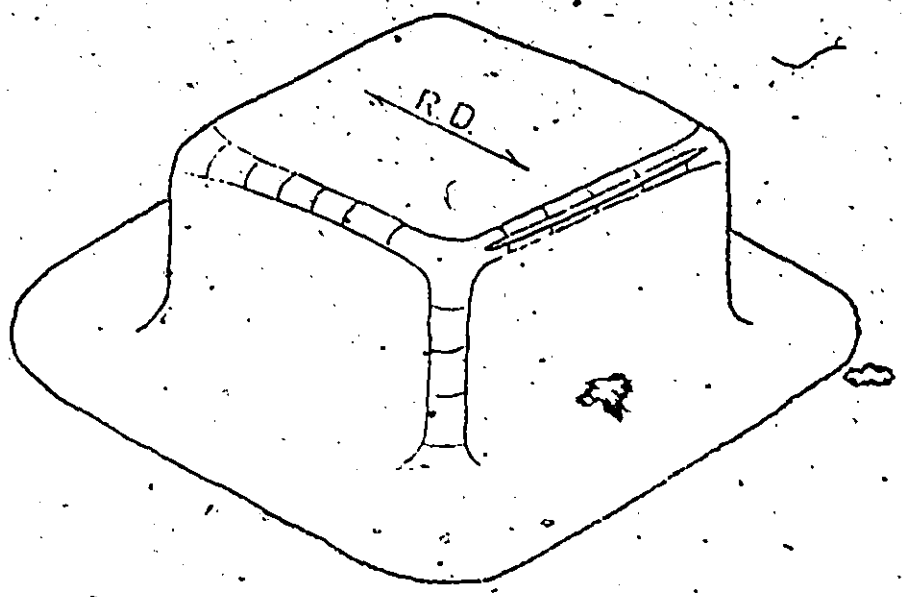

fail on bottom edge over punch radius

d)

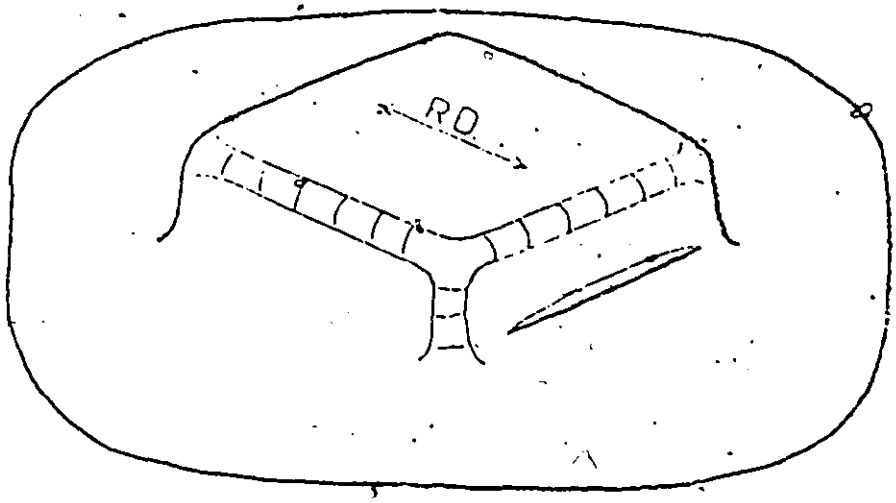

fail at top of side wall over die radius.

FIG 55 FAILURE TYPES IN SQUARE CUPS.

e)

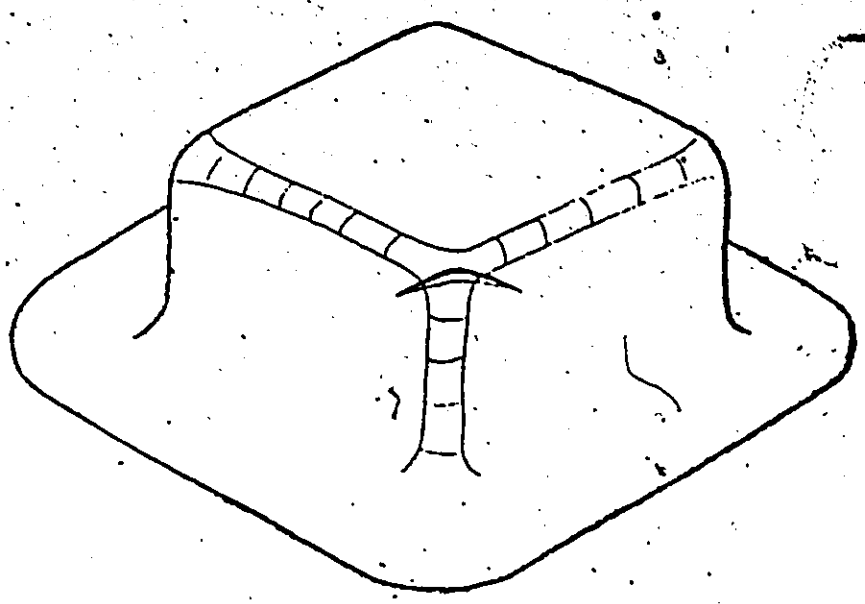

fail at bottom corner, at angle to bottom

f)

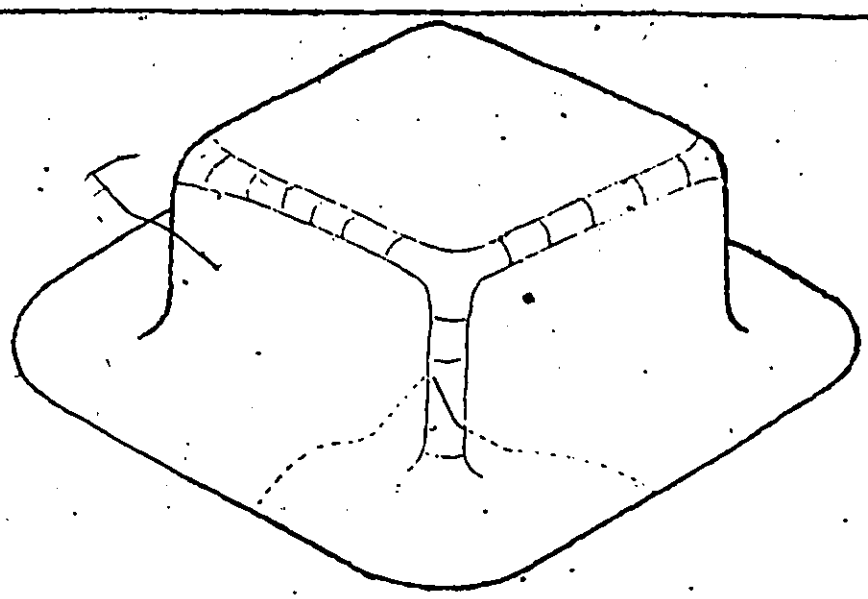

inclined split in side wall at corner, propagate into flange

FIG. 5.5 FAILURE TYPES IN SQUARE CUPS

g)

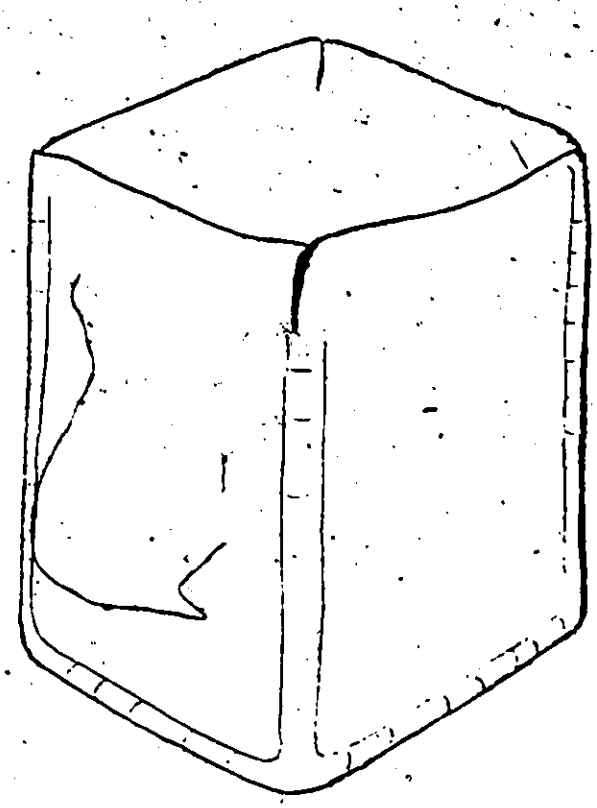

corner split, in fully developed blank

Figure 5.6a Deepest Cups Drawn from Circular Blanks of Different Materials.

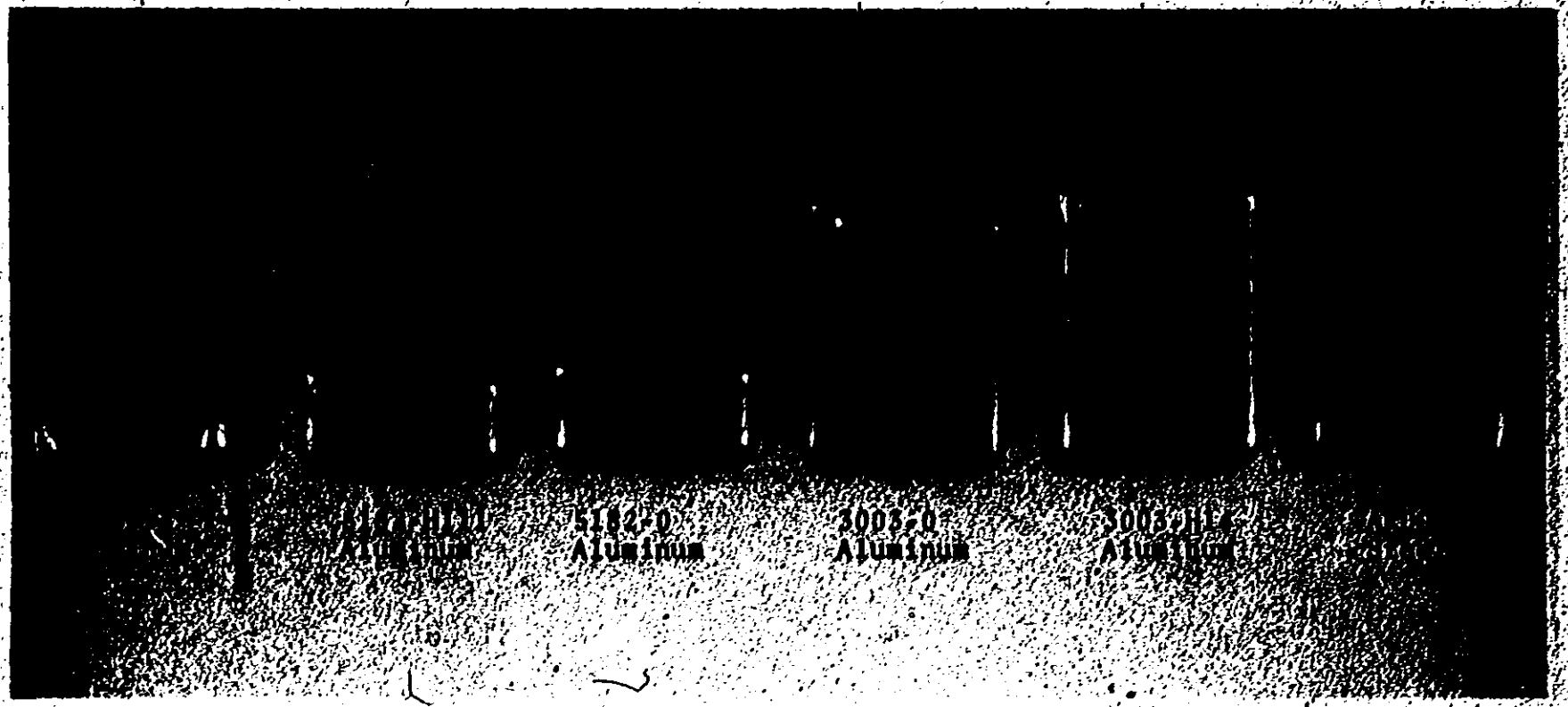

FIG. 5.6 DEEPEST CUPS DRAWN FROM CIRCULAR BLANKS OF DIFFERENT MATERIALS
b)

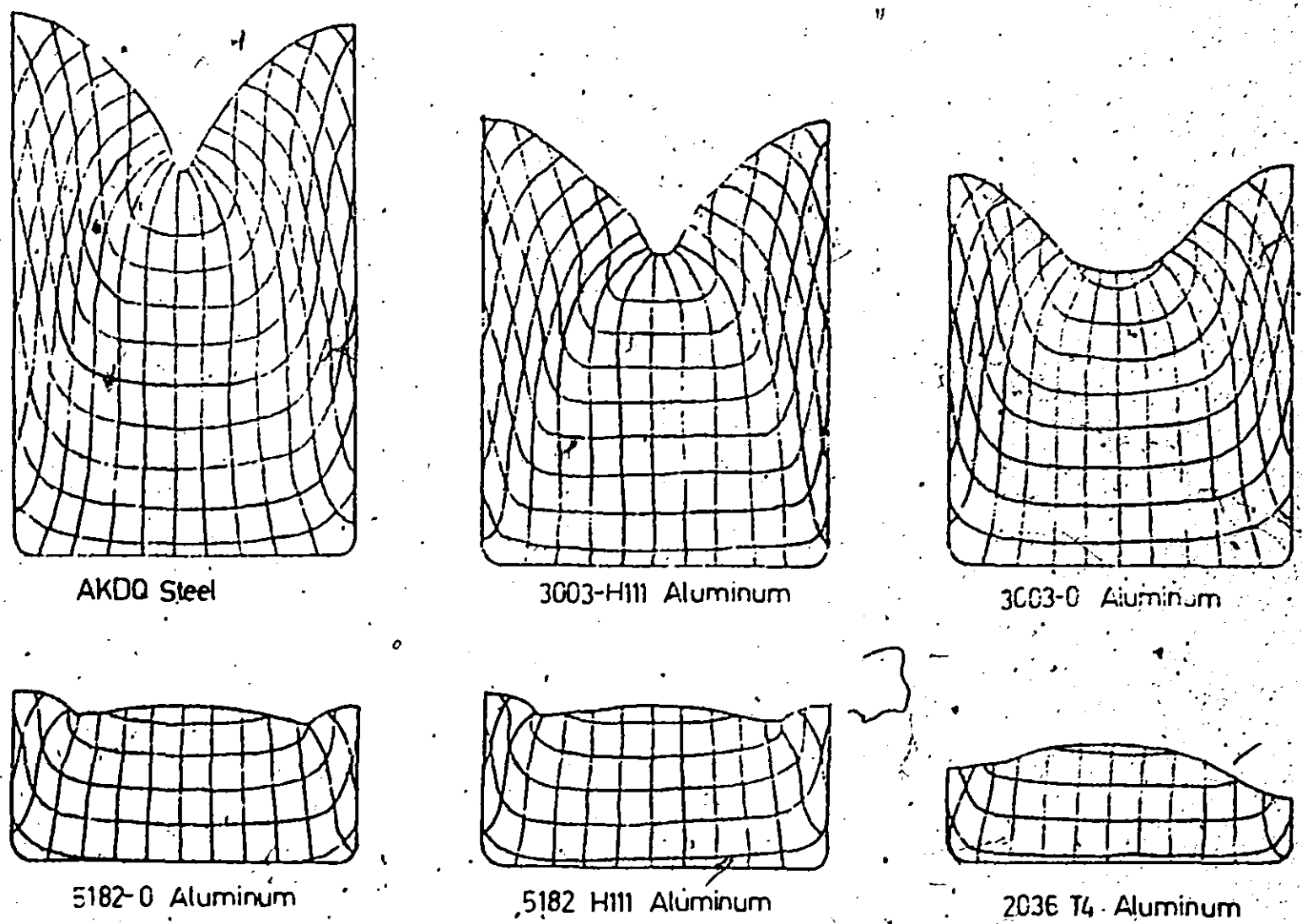

this case it occurred along the bottom edge at one side of the cup (Figure 5.5c).

The 5182 and 2036-T4 aluminum alloys gave much shallower cups and failed in a very different fashion. The fractures appeared to be of a brittle nature inasmuch as there was very little local thinning (Figure 5.4 d, e, g) and they were located in the corner of the wall of the cup. The 5182 aluminum split parallel to the cup bottom (Figure 5.5b) while the 2036-T4 alloy split at an angle to the cup bottom (Figure 5.5f). Both types of fracture propagated quickly all the way across the flange, along lines which are probably parallel to planes of maximum shear. The 2036-T4 aluminum failed at maximum load but the 5182 material did not fail until after the maximum load point.

When very large blanks of 2036-T4 or 5182 aluminum were tested failure occurred by brittle fracture over the punch radius at the bottom corner. The transition to this failure type occurred at 5.15" diameter for the 5182 aluminum, i.e., at a diameter comparable to the maximum blank diameter of the other materials.

The steel produced deeper cups in the 45° orientation; whereas the 3003 aluminum alloys were better when oriented at 0°. With the 5182 aluminum, orientation did not seem to be very important. Slightly larger blanks could be drawn at 0° before the transition to failure at the bottom corner occurred, but no difference was found as far as the critical corner wall splitting was concerned.

The occurrence of stretcher strain marks was noted on some 5182-0 aluminum cups.

The material flow pictures are shown as Figures 5.7-5.16.

Figures 5.7 and 5.8 show the development of strain within the flange for the steel and the utility aluminum respectively. The solid lines within the flange represent grid lines originally straight and parallel to the edge of the die. The shaded areas represent parts of the blank which are undeformed.

Figures 5.9 and 5.10 show the progressive positions of the edge of the blank as the cup is drawn, and the grid pattern on the completed cup. In Figures 5.11-5.16 only the initial blank shape and the final grid pattern are shown.

It may be seen that large undeformed regions exist in the flange of the utility aluminum cup. These are separated by areas of high shear strain. The transition between the two is very sharp and is readily visible on the sample due to the presence of roll marks. The material in the side of the cup is virtually undeformed except for the bending and straightening over the die radius. Another block of rigid material exists at the corners but this decreases in size as the cup is drawn.

In the other materials, which were previously observed to have higher strain hardening rates, undeformed areas do not exist in the completed cups. However the material at the sides is much less heavily deformed and lightly deformed areas exist in the early stages of drawing near the outside

FIG. 57 AKDQ STEEL.CIRCULAR BLANK

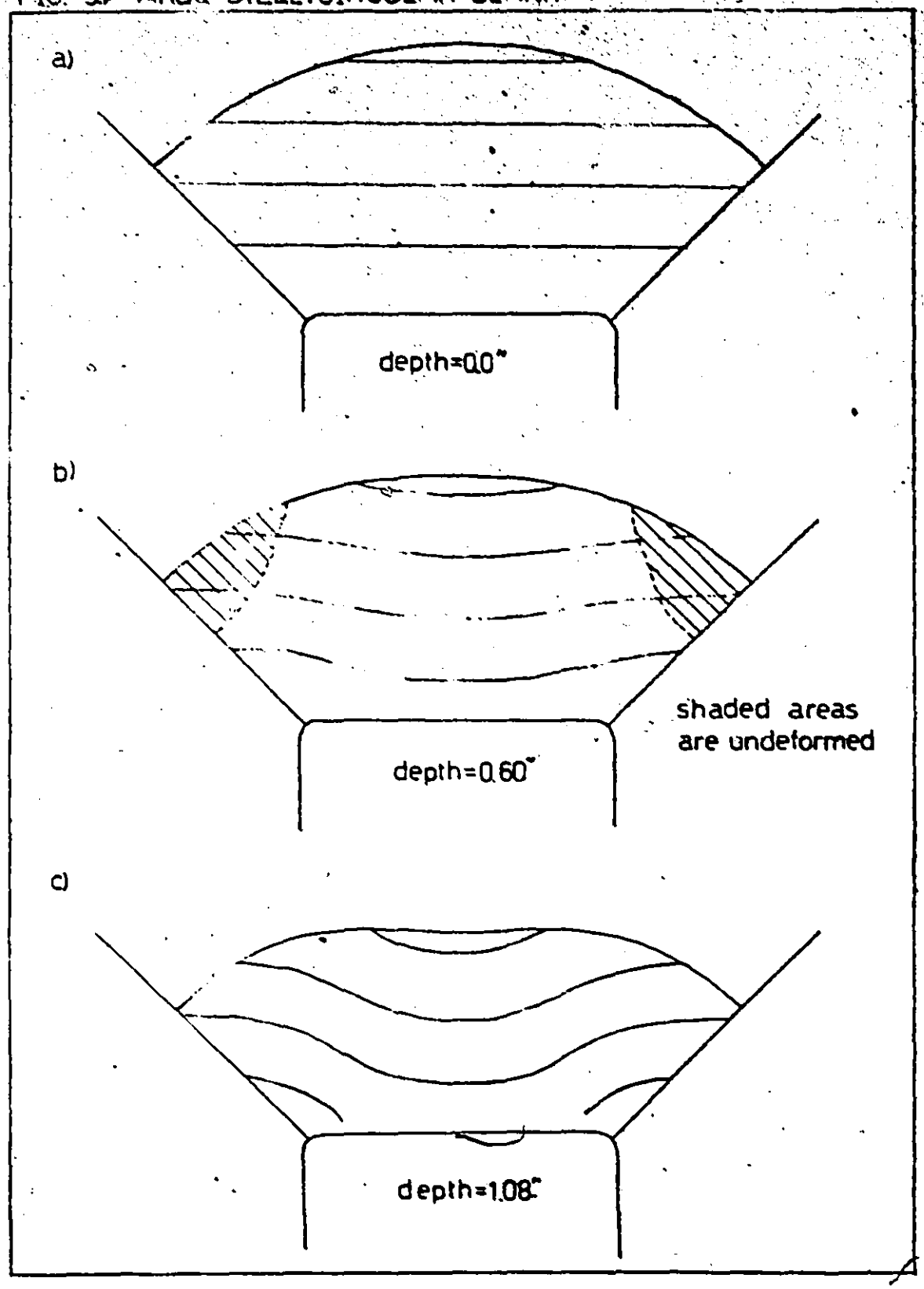

FIG. 57 AKDQ STEEL.CIRCULAR BLANK

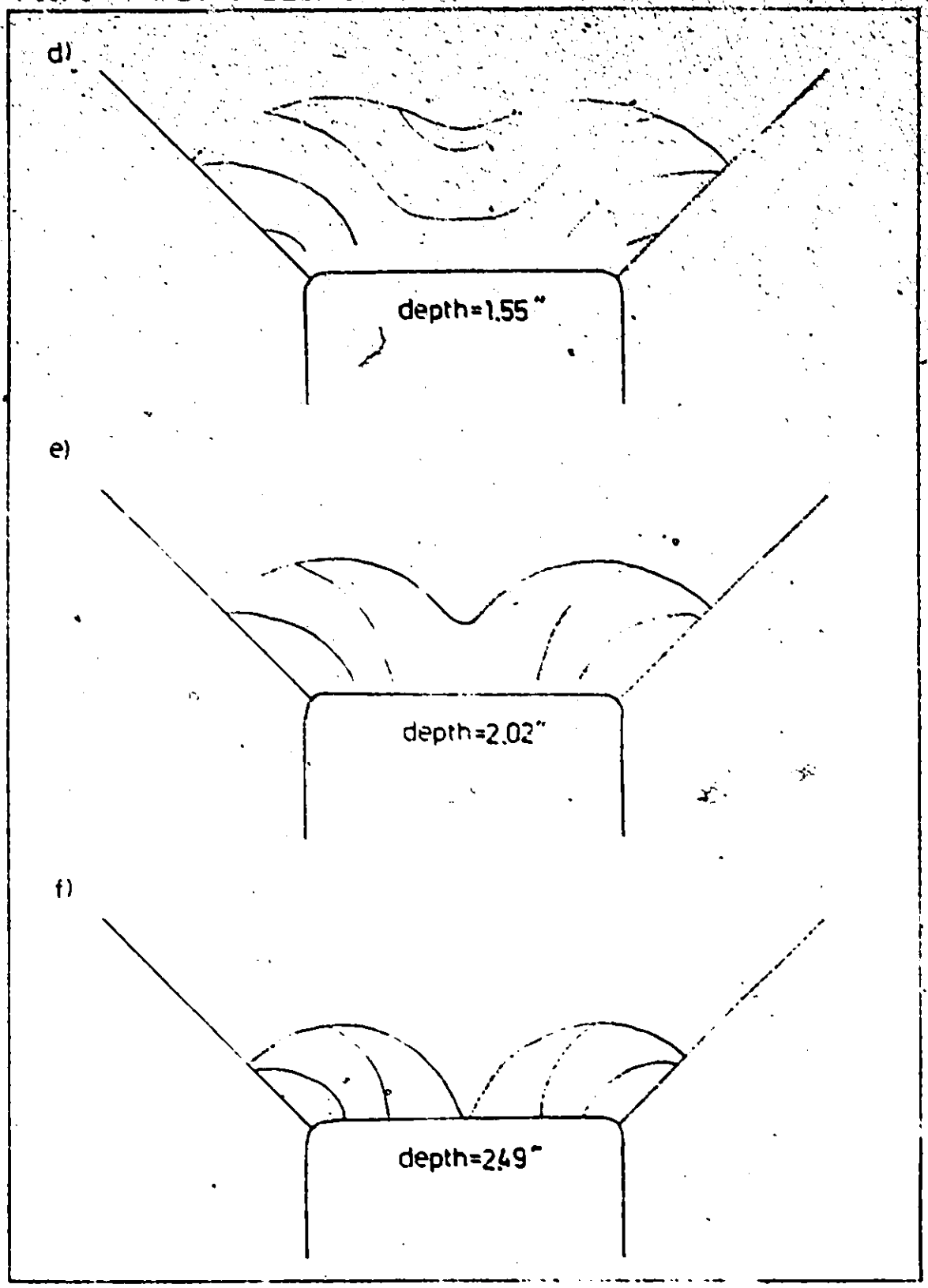

FIG. 5.8 3003-H14 UTILITY ALUMINUM, CIRCULAR BLANK, ½ SIZE

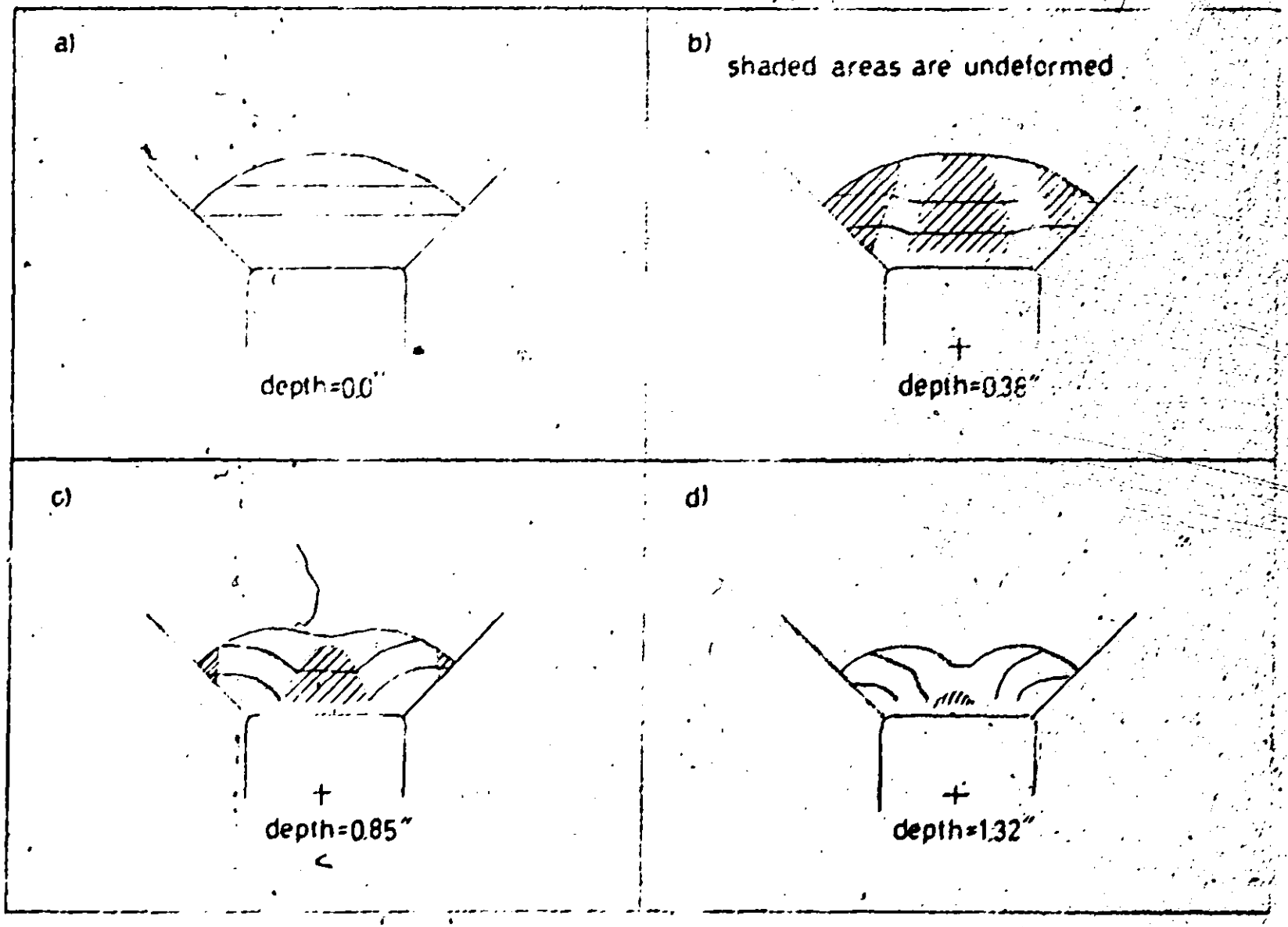

FIG. 5.8 3003-H14 UTILITY ALUMINUM CIRCULAR BLANK, ½ SIZE

FIG. 5.9 AKDQ STEEL CIRCULAR BLANK

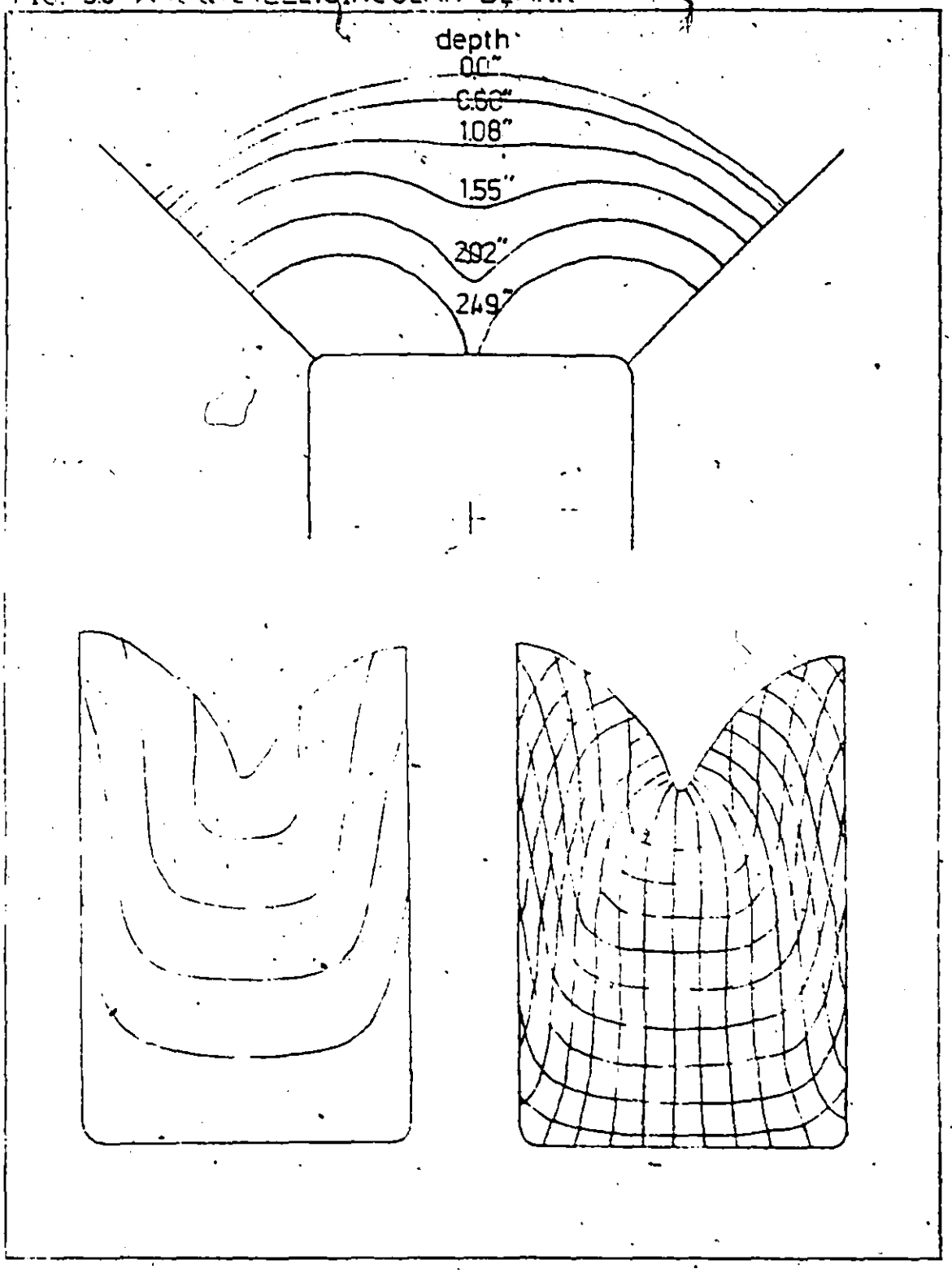

FIG. 5.10 3003-H14 UTILITY ALUMINUM CIRCULAR BLANK

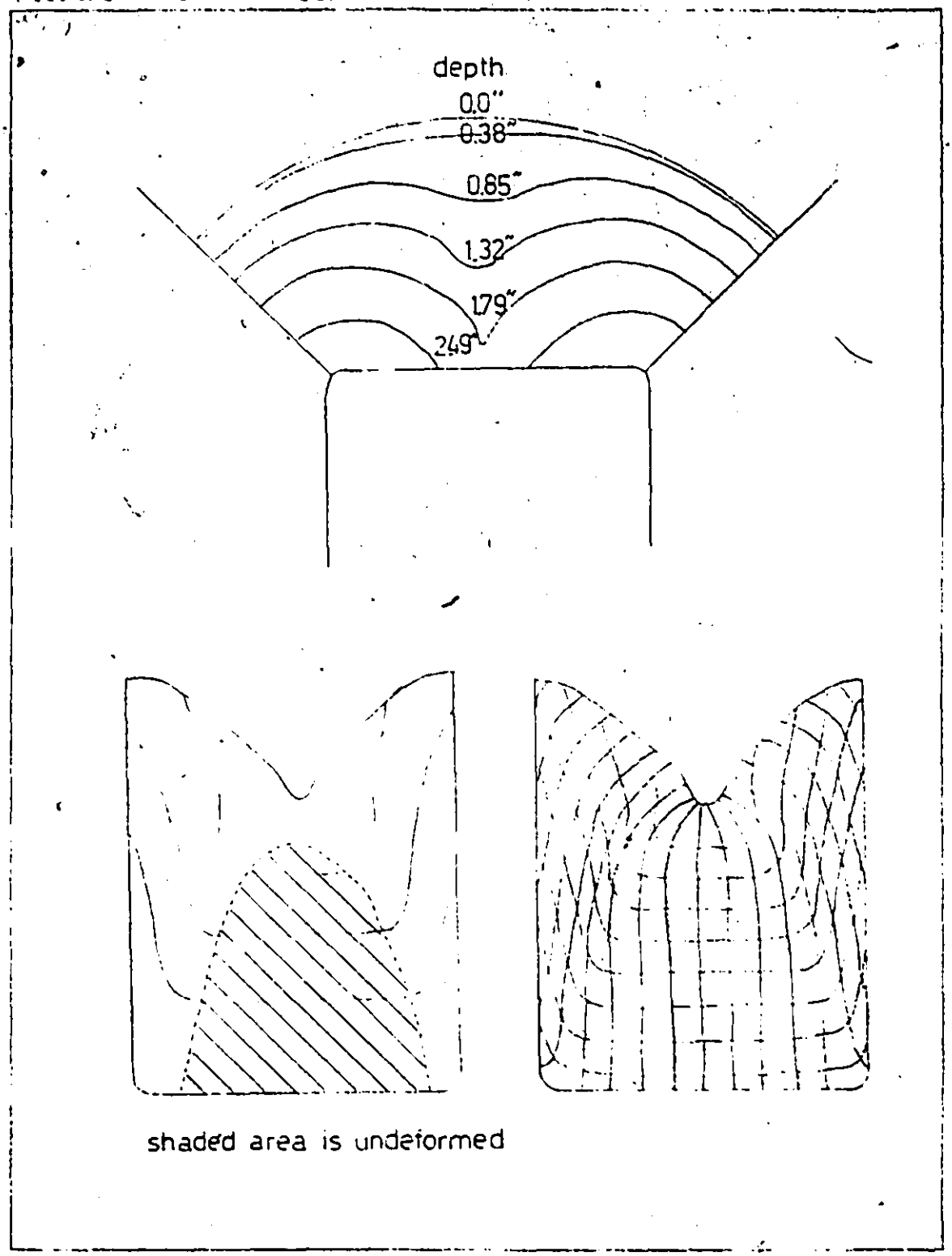

FIG.5.11 3003-0 ALUMINUM. CIRCULAR BLANK

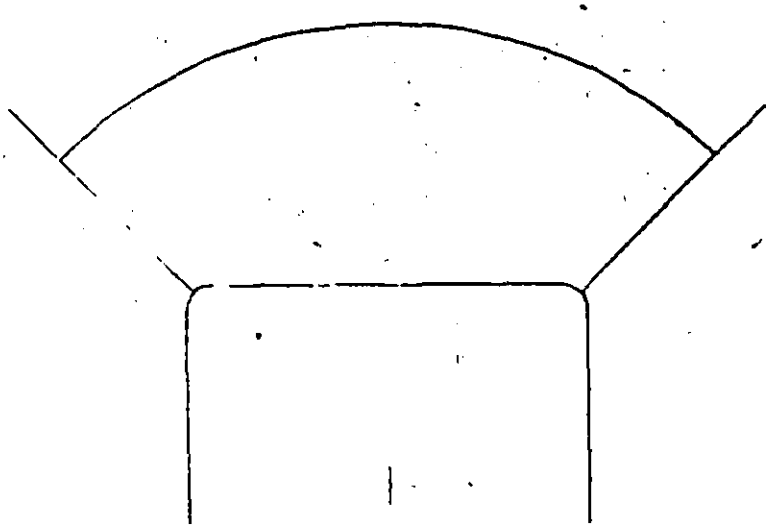

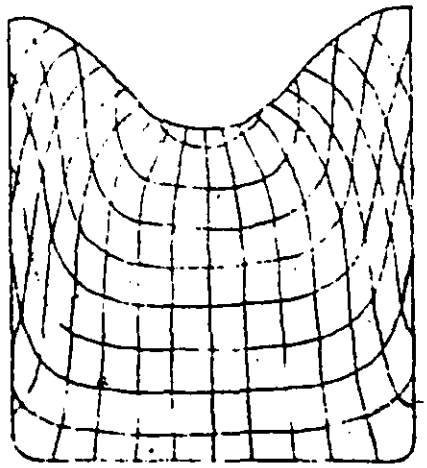

FIG 5.12 5182-0 ALUMINUM CIRCULAR BLANK

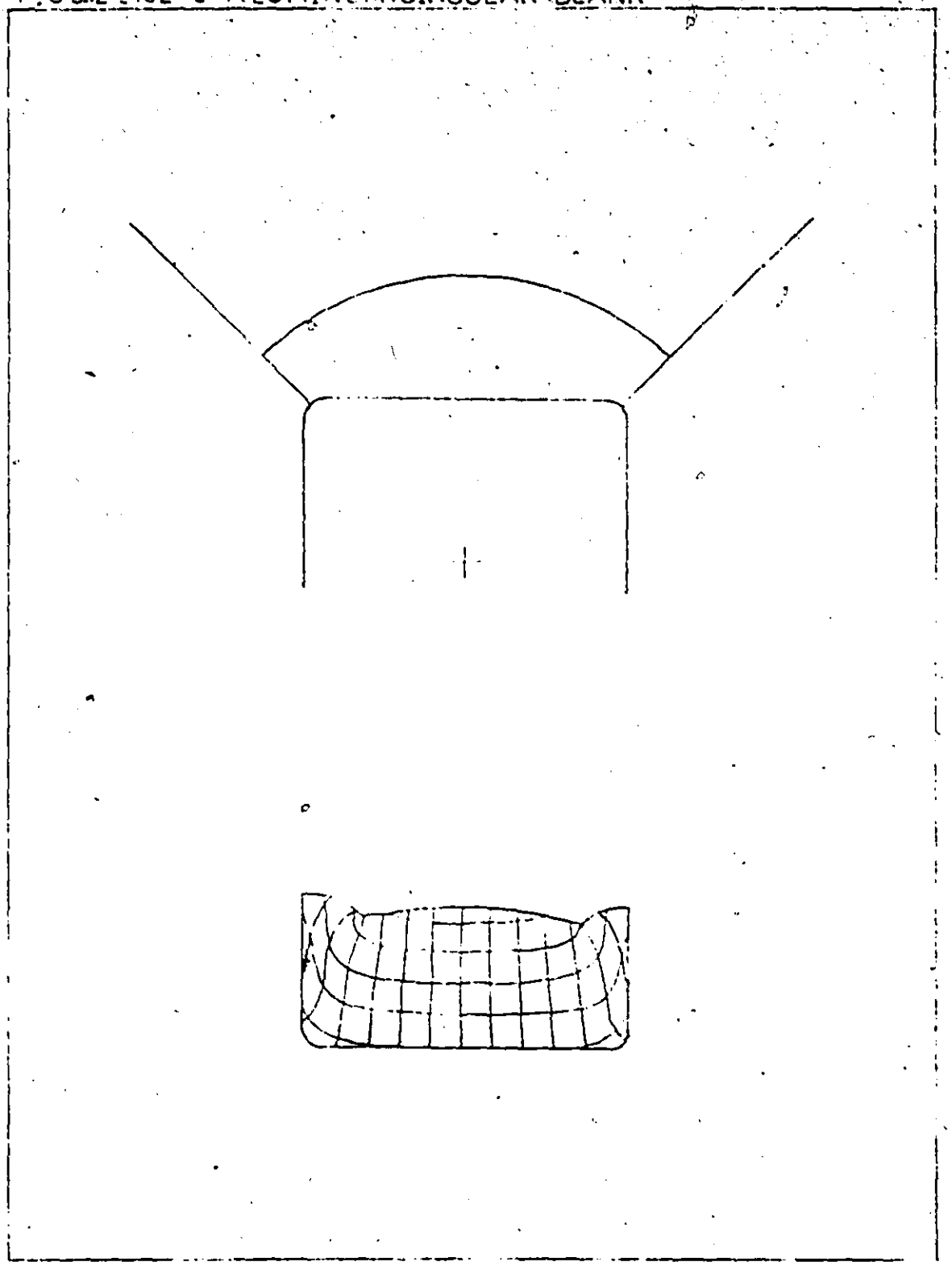

FIG. 5.13 5182-H111 ALUMINUM. CIRCULAR BLANK

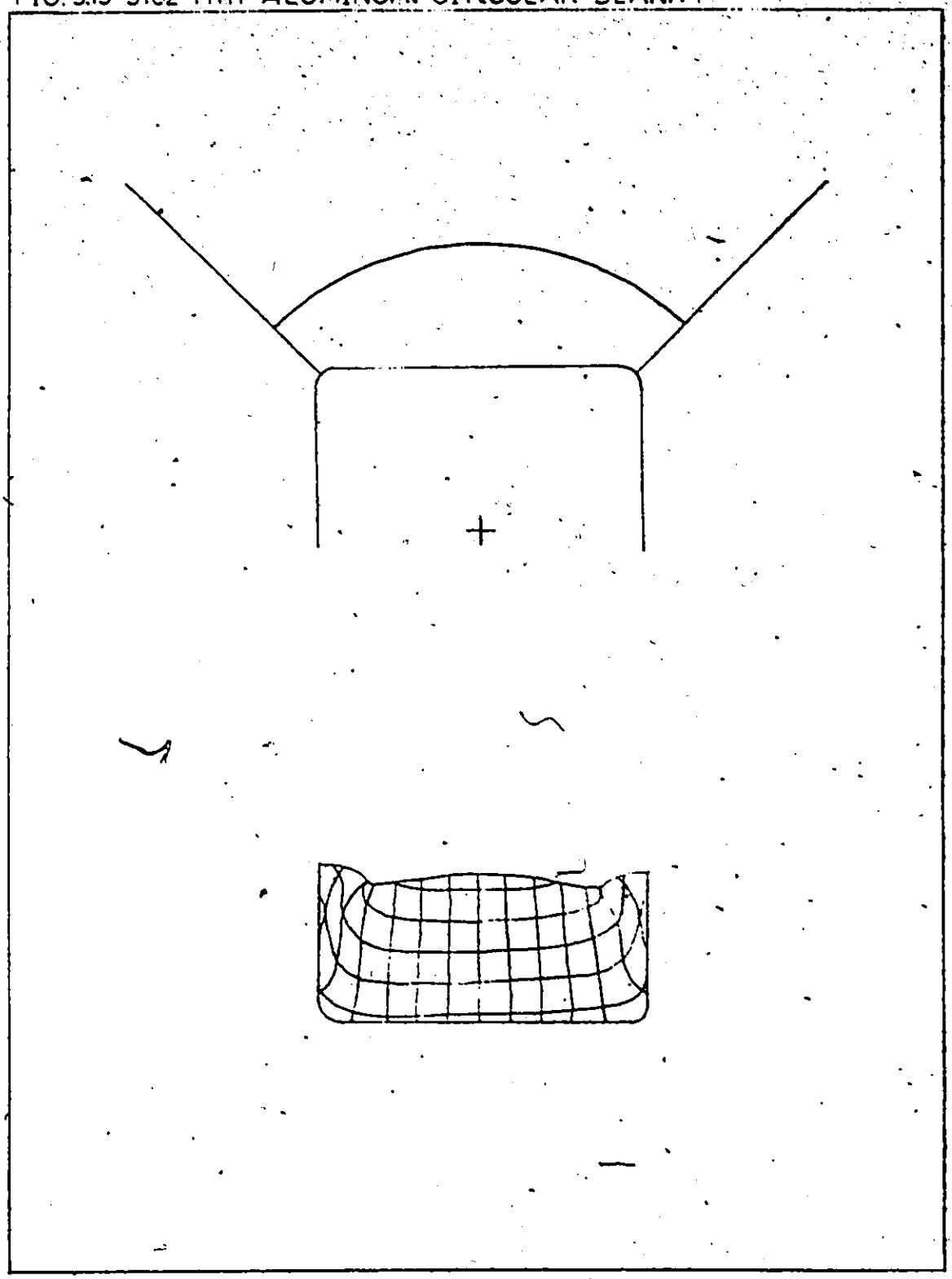

FIG. 5.14 5182-H111 ALUMINUM. FAILED CIRCULAR BLANK

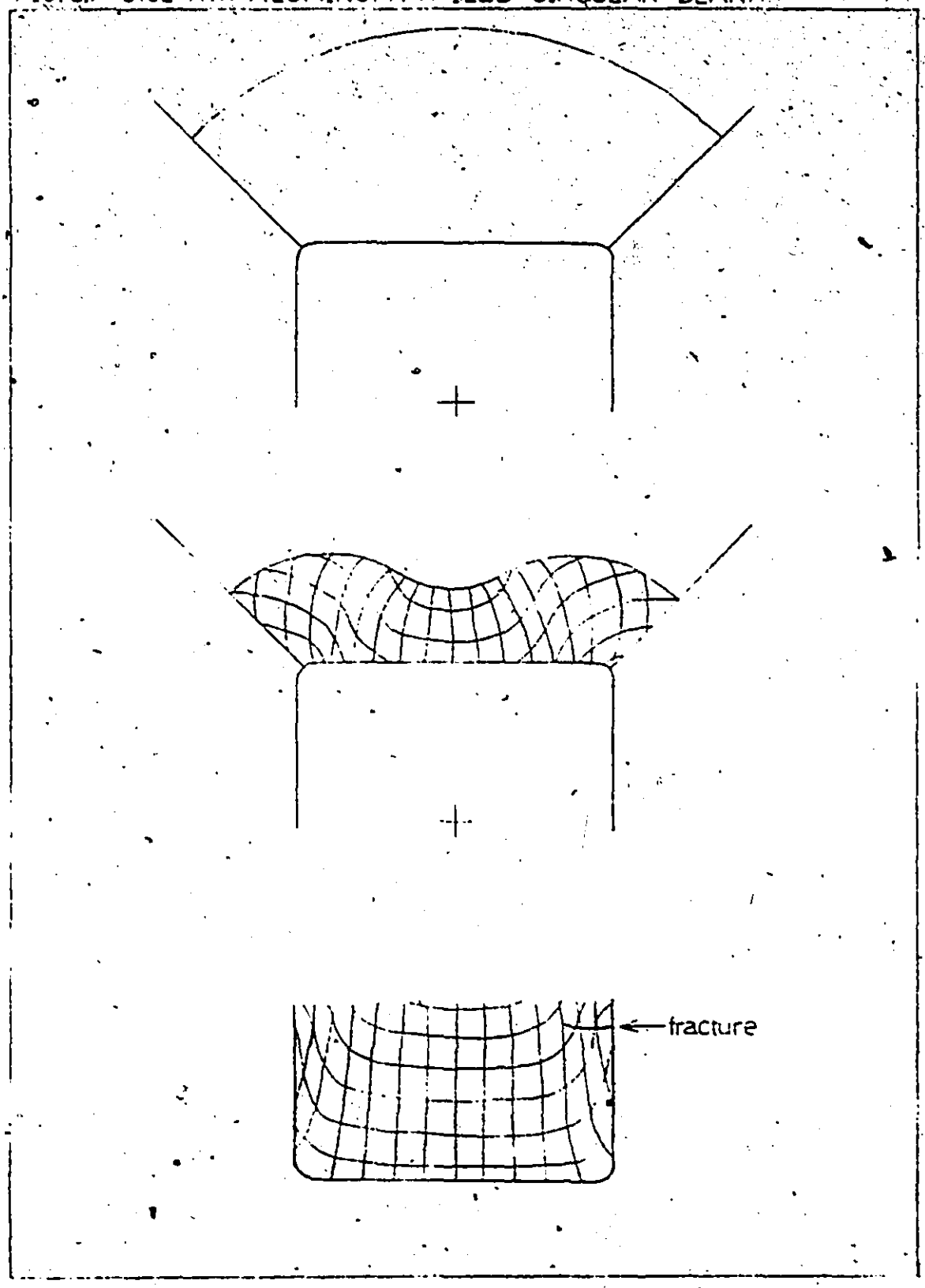

FIG.5.15 2036-T4 ALUMINUM. CIRCULAR BLANK

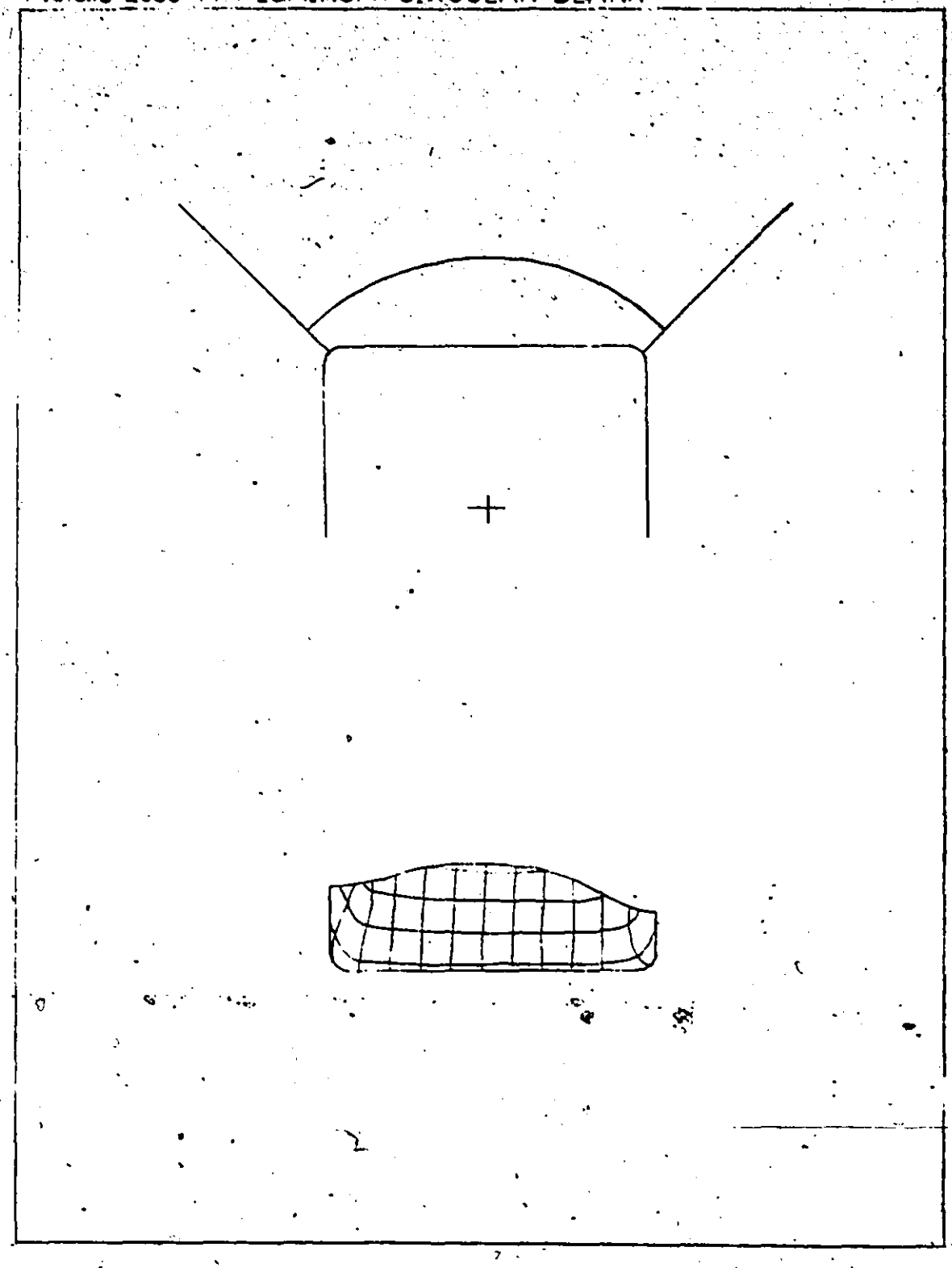

FIG. 5.16 2036-T4 ALUMINUM. FAILED CIRCULAR BLANK

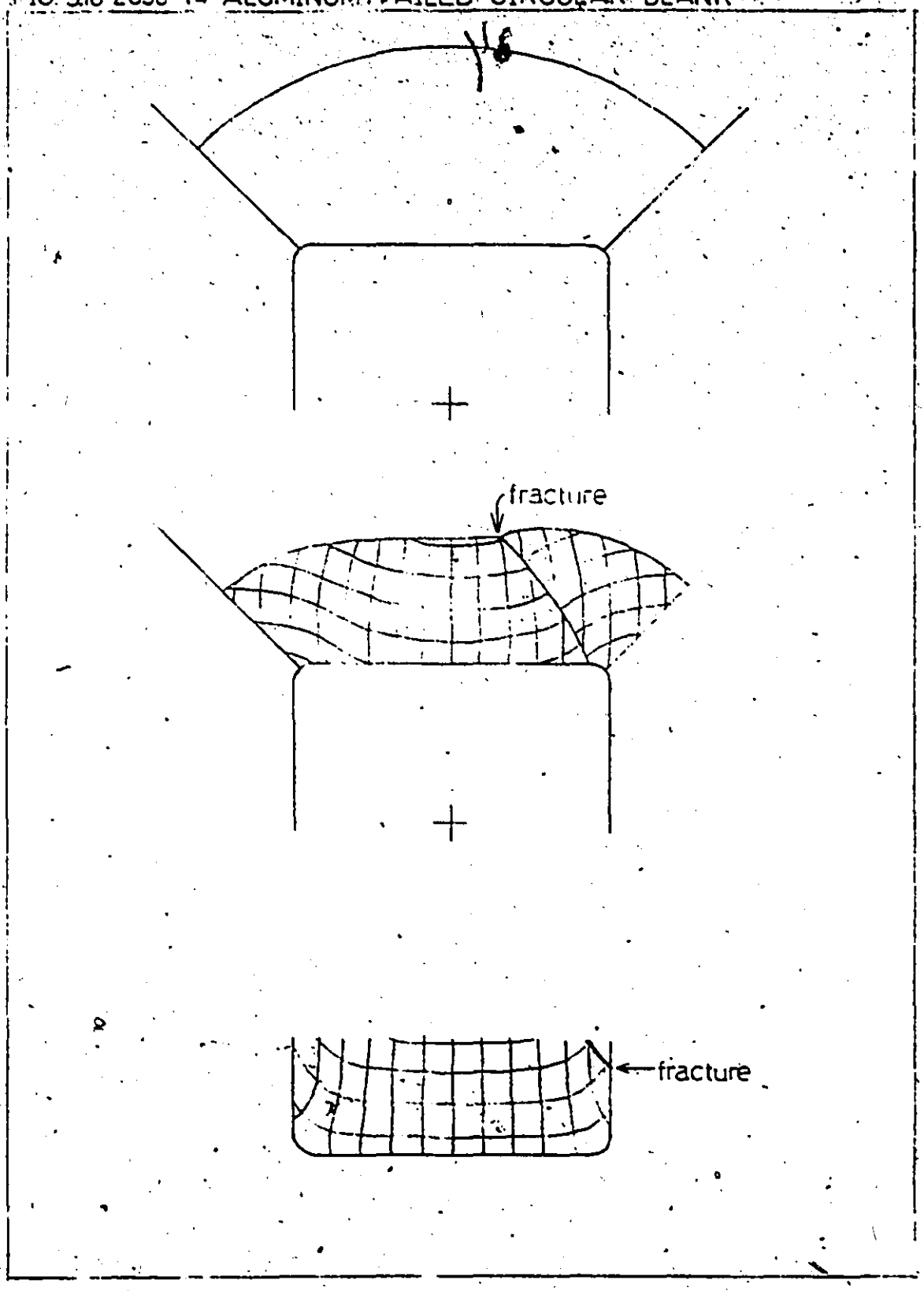

edge of the blank at the corners. In other words, the strain is distributed more, but the same general pattern exists.

In order to get some measure of the distribution of strain, the overall extension of lines at the corner and at the middle of the side wall were calculated (Figure 5.17).

$$e = \frac{\ell_f - \ell_o}{\ell_o} \times 100\%$$

where ℓ_o = length of line in undrawn blank

ℓ_f = length of line in drawn cup

The results are shown in Table 5.2. The extension at the side is significantly greater for the steel and the 3003-0 aluminum than for the other alloys. However the reason for the low side wall extension in the 5182 and 2036 aluminum alloys is that the cups are so shallow. In Figures 5.9-5.16 it may be seen that grid lines at equal height above the bottom, exhibit approximately the same curvature in all materials except the 3003-H14 utility aluminum. This indicates that the shear zone has spread equally well to the centre of the side wall.

5.3 Blank Development

The final step in this investigation was to determine the optimum blank shape. Most of the tests were conducted with steel and 3003-H14 aluminum. As shown in Figures 5.9-5.16, the use of a circular blank results in ears at the corners.

FIG 5.17 CALCULATION OF OVERALL EXTENSION IN THE WALL OF A SQUARE CUP

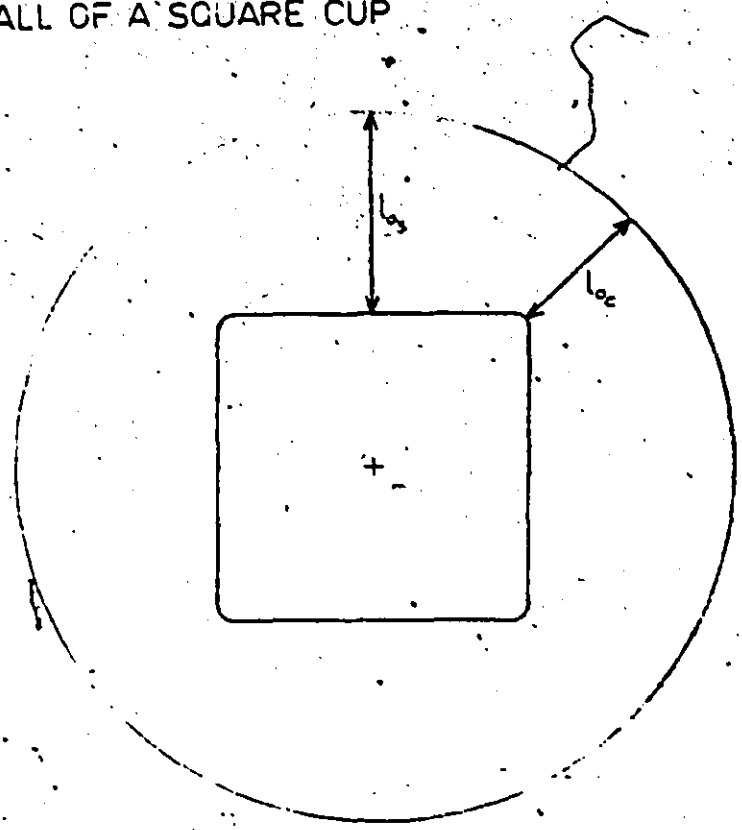

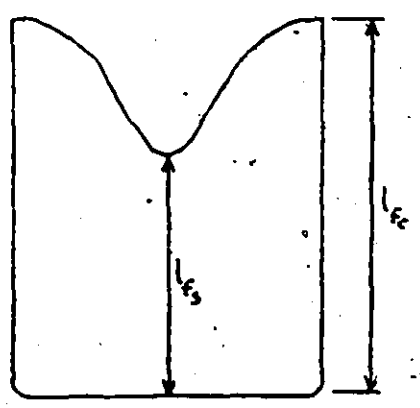

$$e = \frac{l_f - l_o}{l_o} \times 100\%$$

Table 5.2 Total Percentage Extension of Wall Material in Cups Drawn from Circular Blanks

Material	Corner Wall Extension	Side Wall Extension
AKDQ Steel	120	23
3003-H14 Aluminum	110	7
3005-0 Aluminum	118	17
5182-0 Aluminum	100	5
5182-H111 Aluminum	103	5
2036-T4 Aluminum	88	4

Conventional blank development for rectangular parts involves trimming excess material from the corners. Therefore the first step taken here was to use blanks of the shape shown in Figure 5.18.

For the steel the maximum blank size was 6.0" cut at the corners to 4.9" (Figure 5.19)*. This yielded a cup with a maximum useful height of 2.25", i.e., slightly shallower than the circular blank. The failures encountered with this shape were the same type of ductile fracture at the bottom corner as was found in circular blanks.

The largest corner-cut blank of 3003-H14 aluminum (Figure 5.20) measured 6.0" cut at 4.5", and yielded a cup with 1.86" useful depth. This is a marginal improvement over the circular blank. A different failure type was observed in some tests with this material. In blanks with excess material at the sides, ductile splits occurred at the top of the side wall along the die radius (Figure 5.5d).

Recently it has been suggested [10, 24] that leaving excess material at the corners may be advantageous in some drawing operations. Blanks of the shape shown in Figure 5.21 were tried in the hope that the excess corner material would cause more distribution of strain to the side walls and thereby enable deeper cups to be drawn.

---

* Additional material-flow histories for this section are included in Appendix II.

FIG. 518 CORNER-CUT BLANK IN RELATION TO DIE OPENING

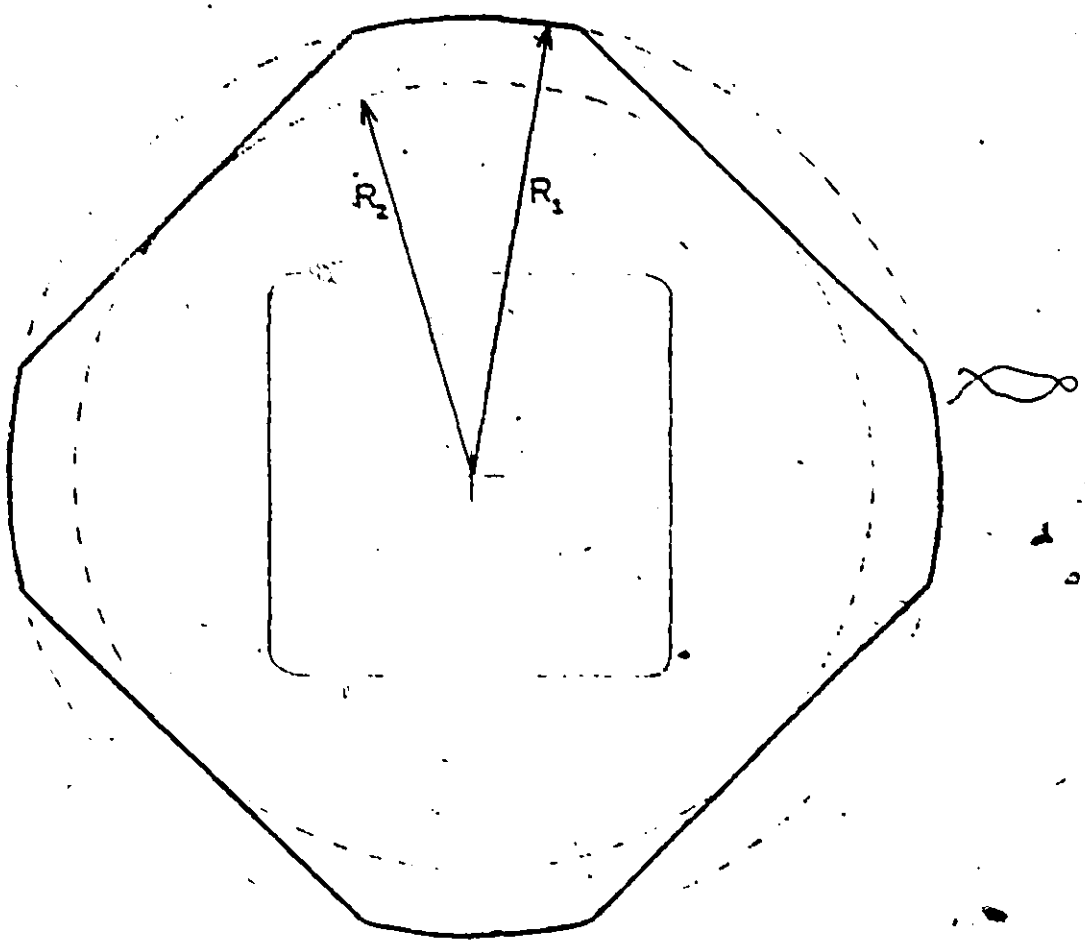

Circular blank of radius R_1 cut at corner to R_2

FIG. 5.19 AKDQ STEEL, CORNER-CUT BLANK

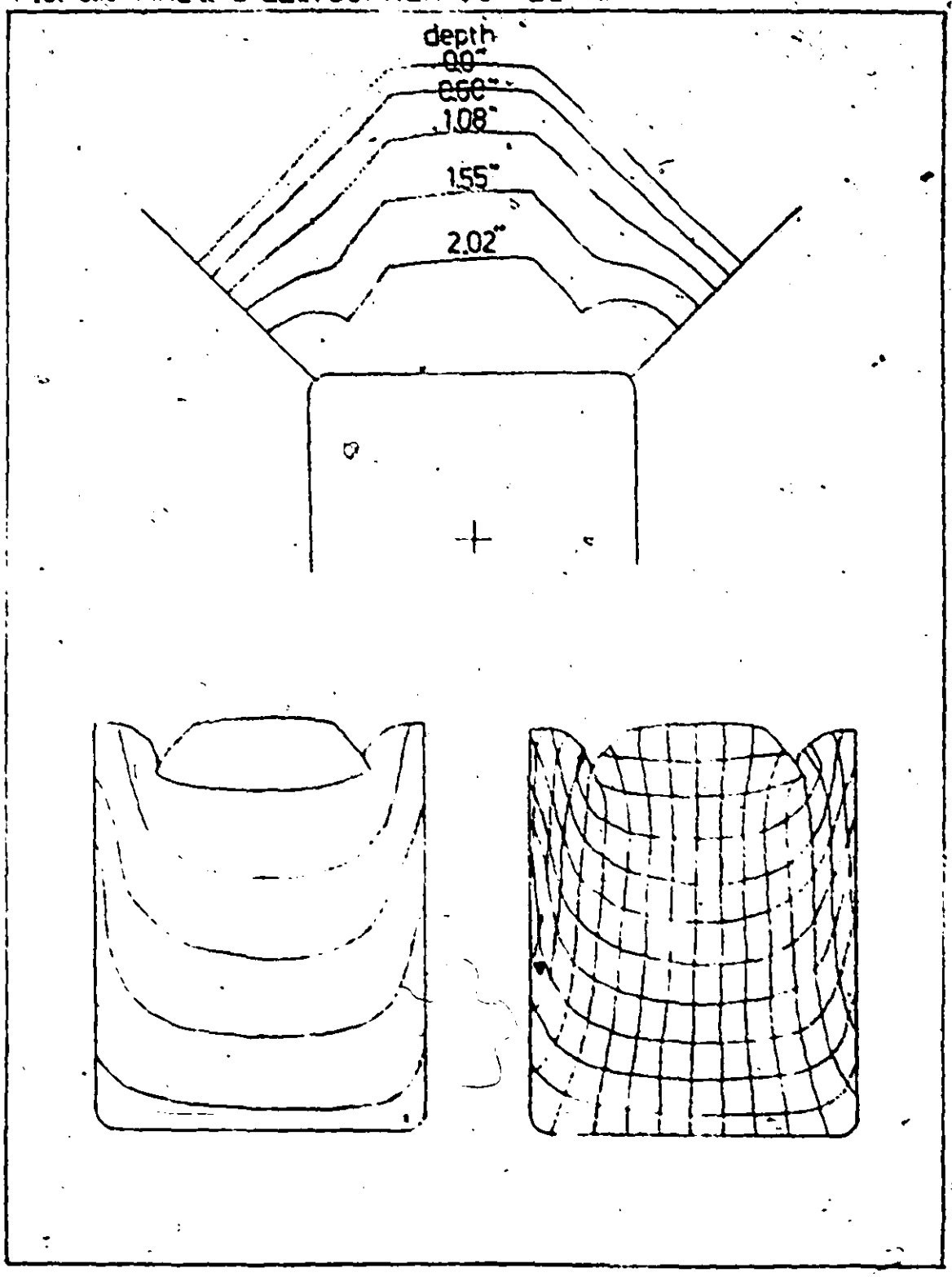

FIG. 5.20 3003-H14 UTILITY ALUMINUM CORNER-CUT BLANK

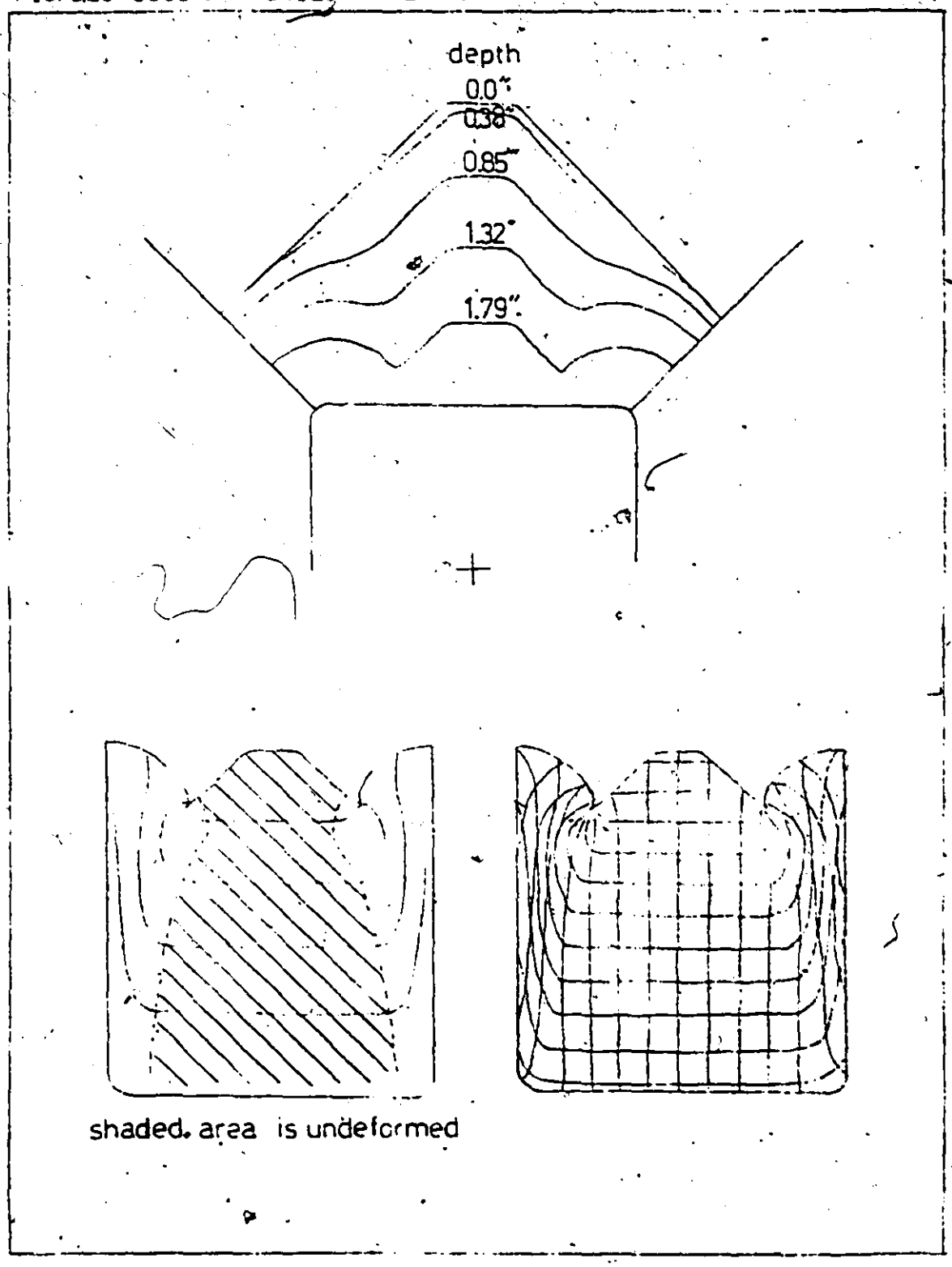

FIG. 521 SIDE-CUT BLANK IN RELATION TO DIE OPENING

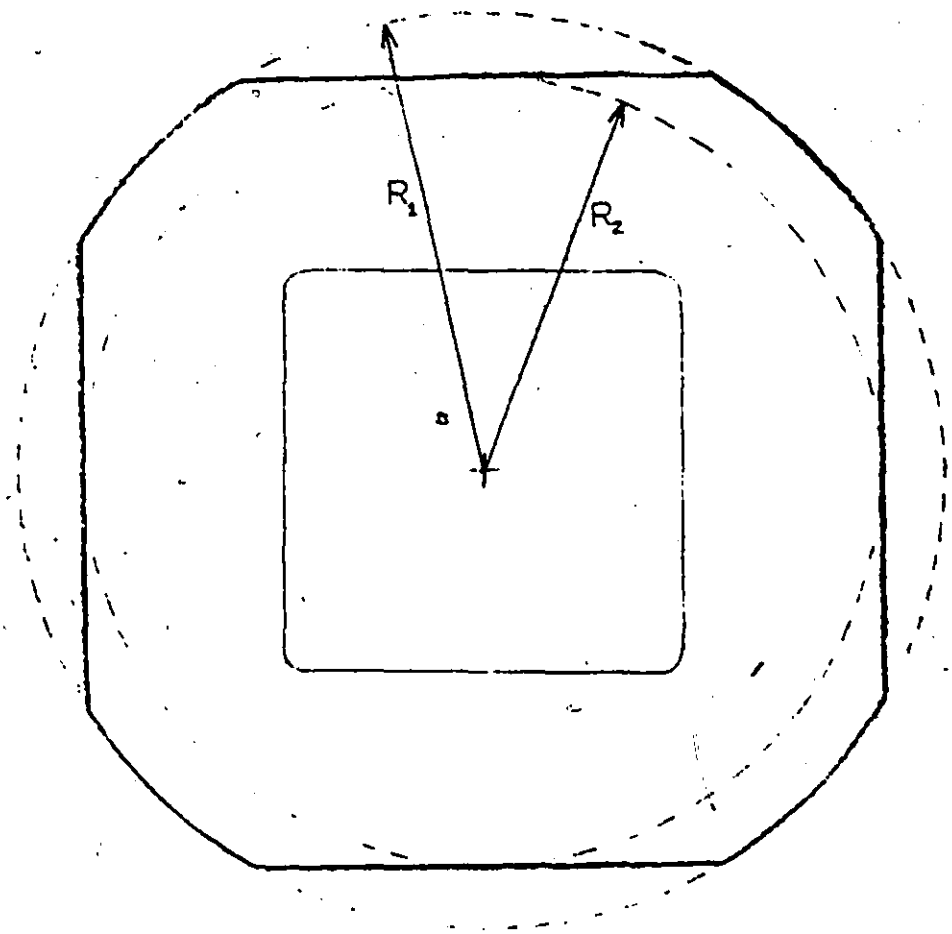

Circular blank of radius R_1 cut at side to R_2

The results are shown in Table 5.3 and Figures 5.22-5.25. Slight improvements in useful depth were obtained for the 3003-H14 and 5182-H111 aluminum, whereas the steel cup was not as deep with this shape as with a circular blank. Failure types were the same as for circular blanks except for the 5182-H111 aluminum, which exhibited a brittle fracture at the bottom corner, at an angle to the cup bottom (Figures 5.5e and 5.4f). It should also be noted that the tendency to buckle (oil can effect) at the centre of the side wall seemed to be greater for this blank shape than for the others.

The side-cut blank may be useful for the 5182 material but since it did not yield an great improvement, it was decided to further develop the corner-cut shape. The useful height with these blanks was limited by two deep cusps on each side of the cup (Figures 5.19 and 5.20). Further development aimed to eliminate these and produce a cup with a straight upper edge. However, it was found necessary to have some increase in height at the corners, otherwise splits occur due to severe strain concentration (Figure 5.5g). The final pattern selected is shown in Figure 5.26.

The results are shown in Tables 5.4 and 5.5 and Figures 5.27-5.30. It is seen that the fully developed blanks result in significantly deeper cups for all materials.

The failure types with fully developed blanks were the same as for circular blanks except that some 3003-H14 aluminum blanks fail at the top of the side wall along the die radius (as with corner-cut blanks), (Figure 5.5d) and

Table 5.5 Maximum Blank Sizes and Useful Depths for Side-Cut Blanks

Material	R_1	R_2	Maximum Useful Depth
AKDQ Steel	6.5"*	5.63"	2.28
3003-H14 Aluminum	6.5"*	5.25"	1.87
5182-H111 Aluminum	4.25"	3.77"	.99

* This is the maximum permitted in the Hille press.

FIG. 522 AKDO STEEL, SIDE-CUT BLANK

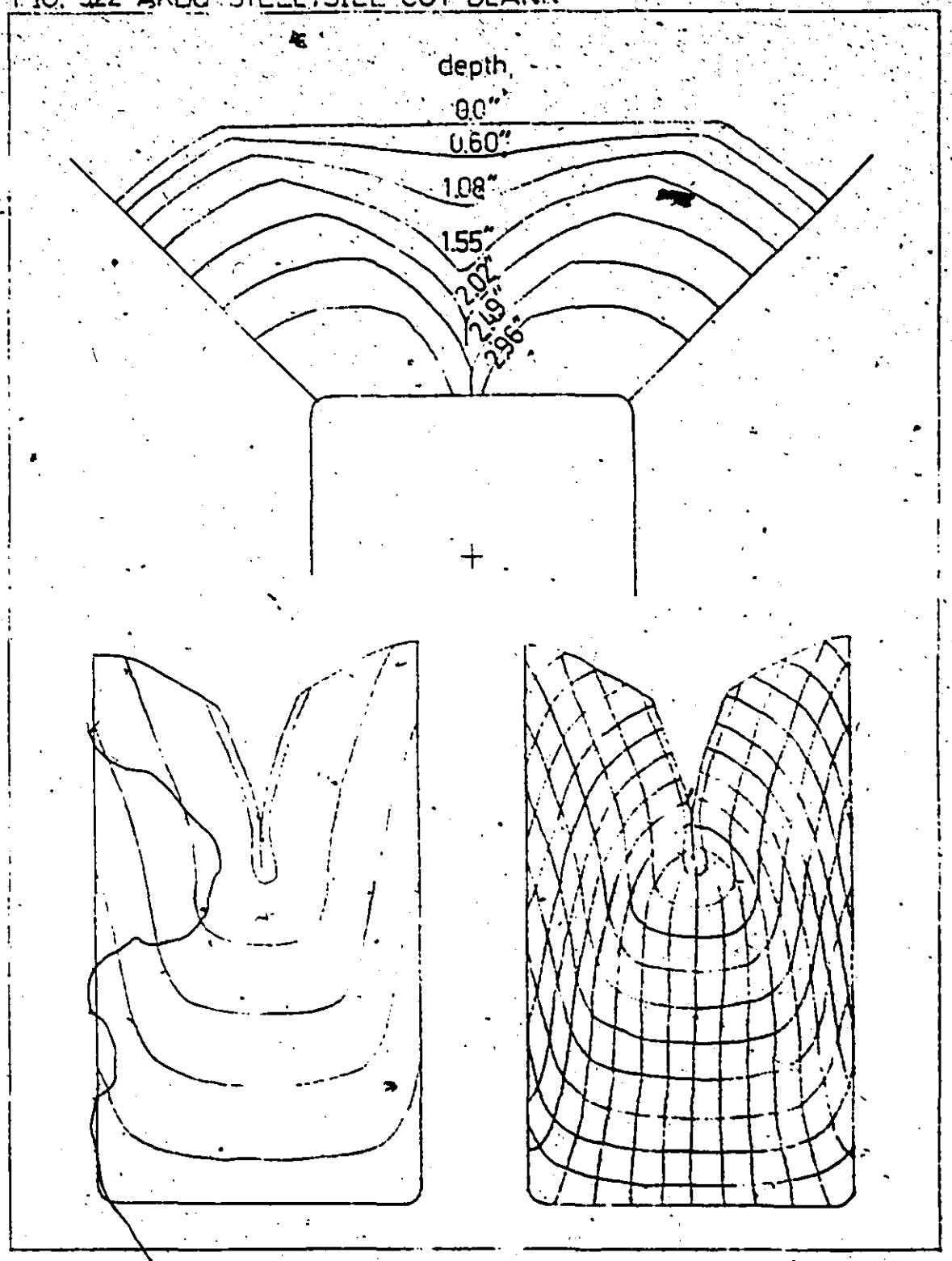

FIG. 5.23, 3003-H14 UTILITY ALUMINUM SIDE-CUT BLANK

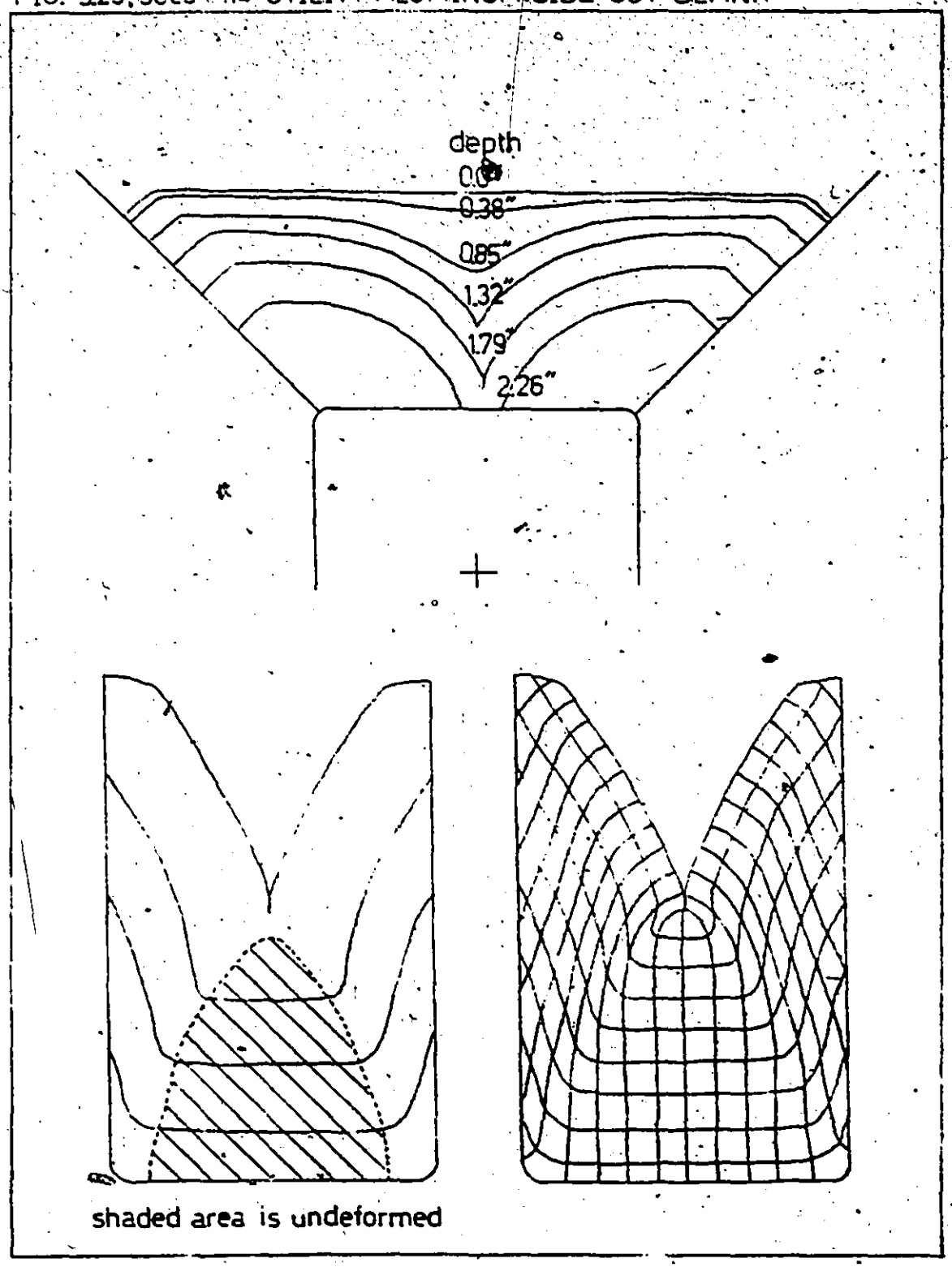

FIG.524 5183-H111 ALUMINUM SIDE-CUT BLANK

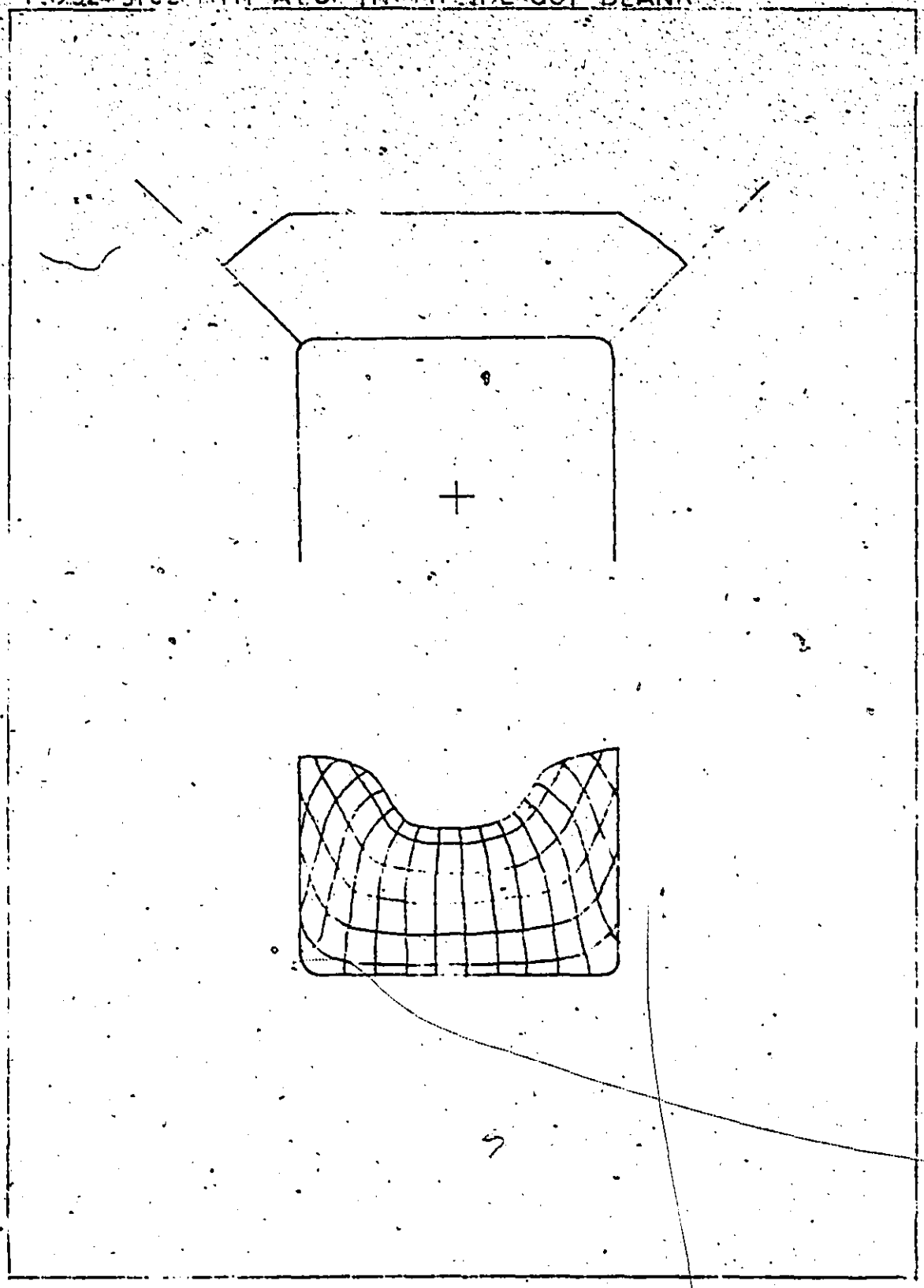

FIG.5.25/5182-H111 ALUMINUM, FAILED SIDE-CUT BLANK

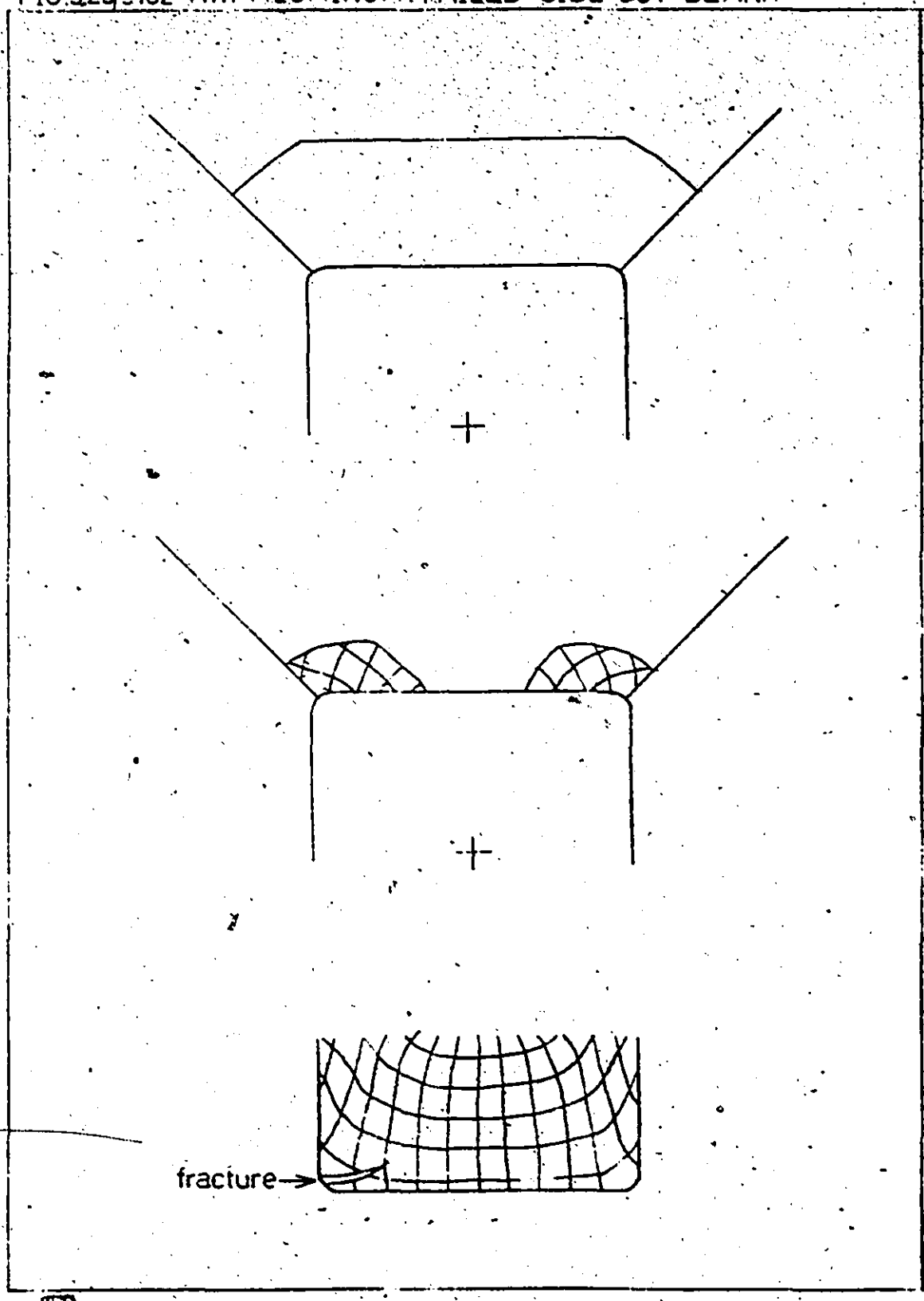

FIG 526 FULLY DEVELOPED BLANK IN RELATION TO DIE OPENING

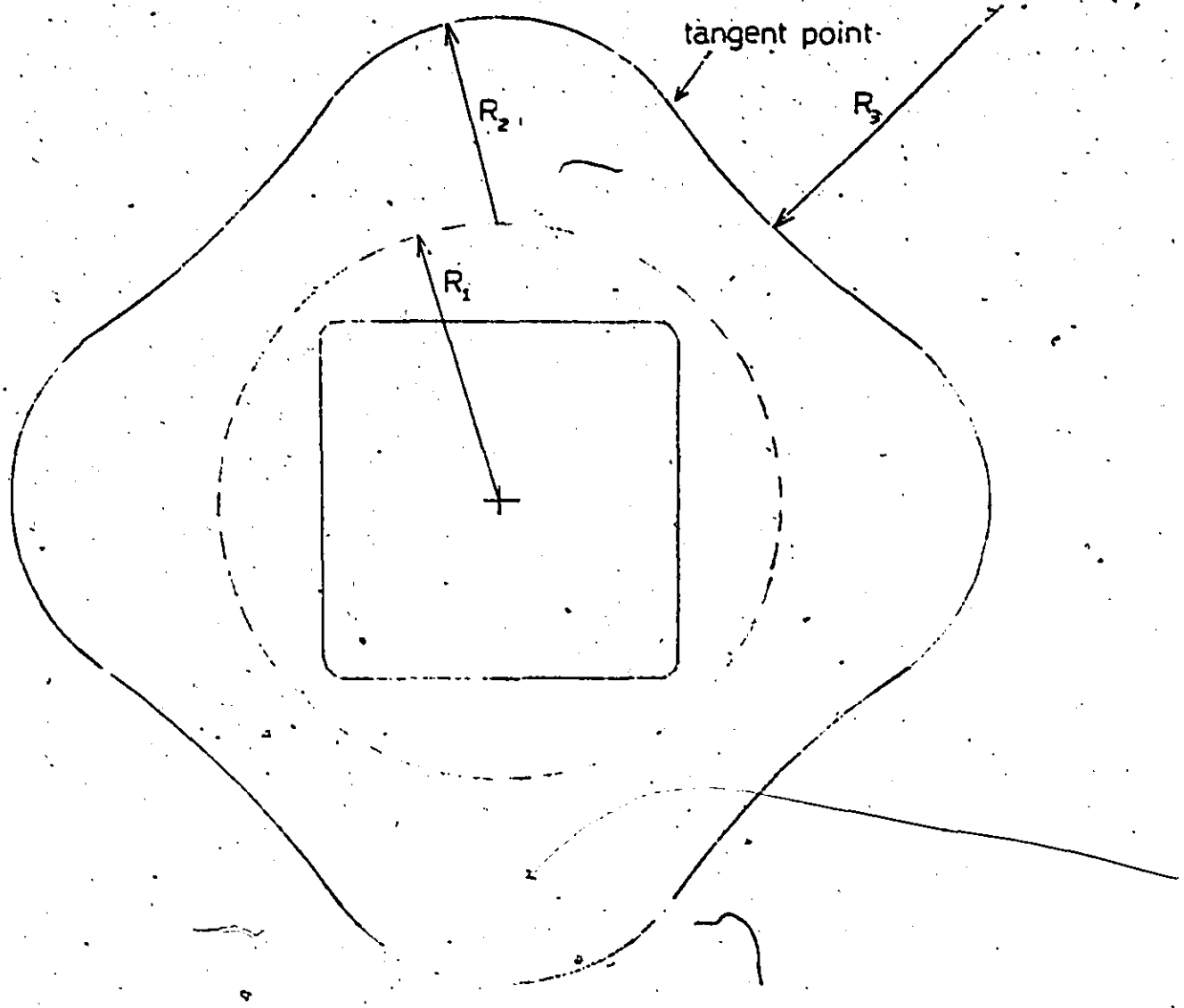

Table 5.4 Dimensions of Fully Developed Blanks.

Material	R_1	R_2	R_3
AKDQ Steel	1.34"	1.57"	∞
3003-H14 Aluminum	1.65"	1.22"	5.91"
5182-0 and 5182-H111 Aluminum	0.43"	1.54"	3.94"

Table 5.5 Maximum Useful Depths of Cups Drawn from Various Materials and Blank Shapes

	AKDQ Steel	3003-H14 Aluminum	5182-0 & 5182-H111 Aluminum
Circular	2.39"	1.82"	0.92"
Side Cut	2.28"	1.87"	0.99"
Corner Cut	2.25"	1.86"	-
Fully Developed	2.52"	2.10"	1.02"

FIG. 527 AKDQ STEEL.FULLY DEVELOPED BLANK

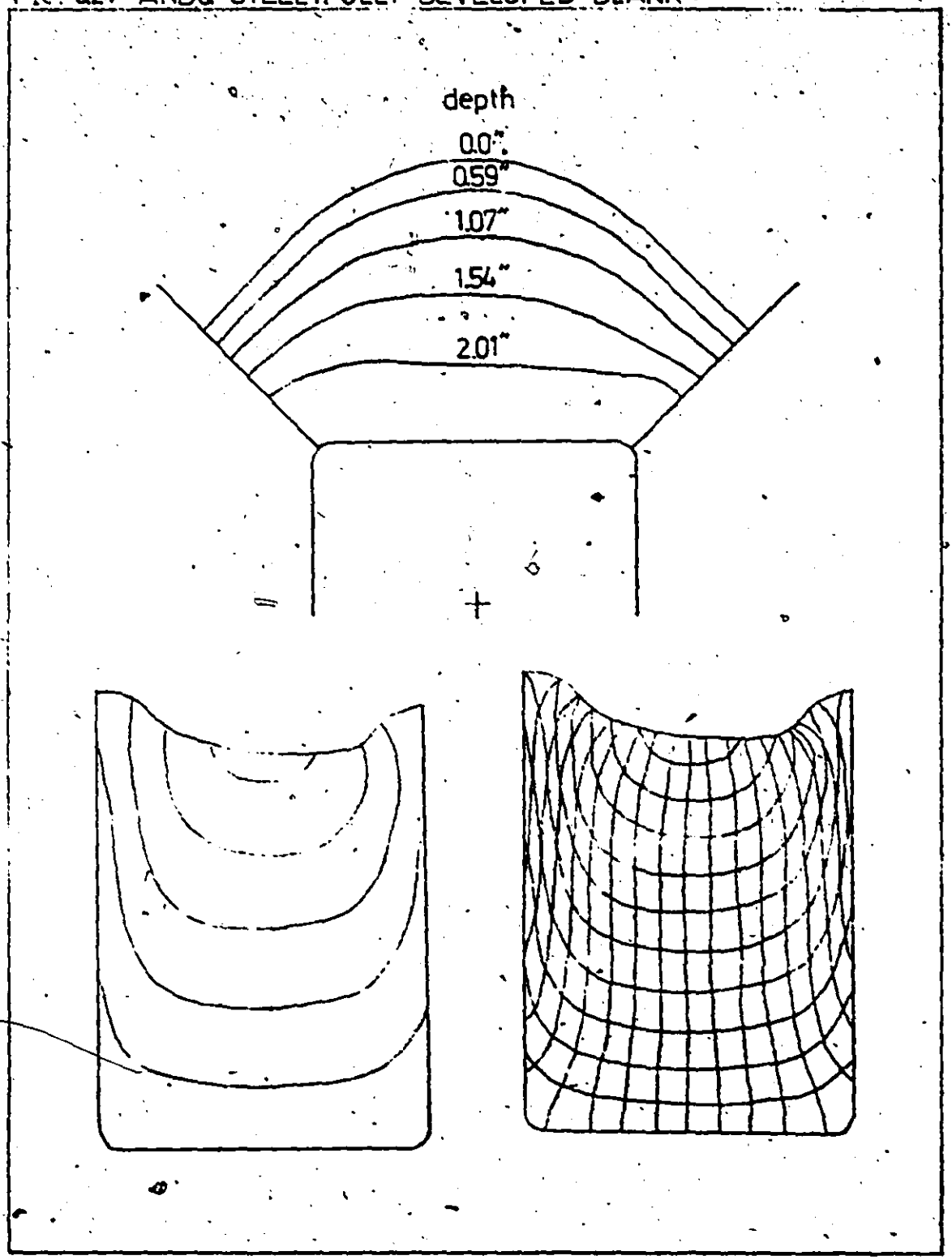

FIG. 52e 3003-H14 UTILITY ALUMINUM FULLY DEVELOPED BLANK

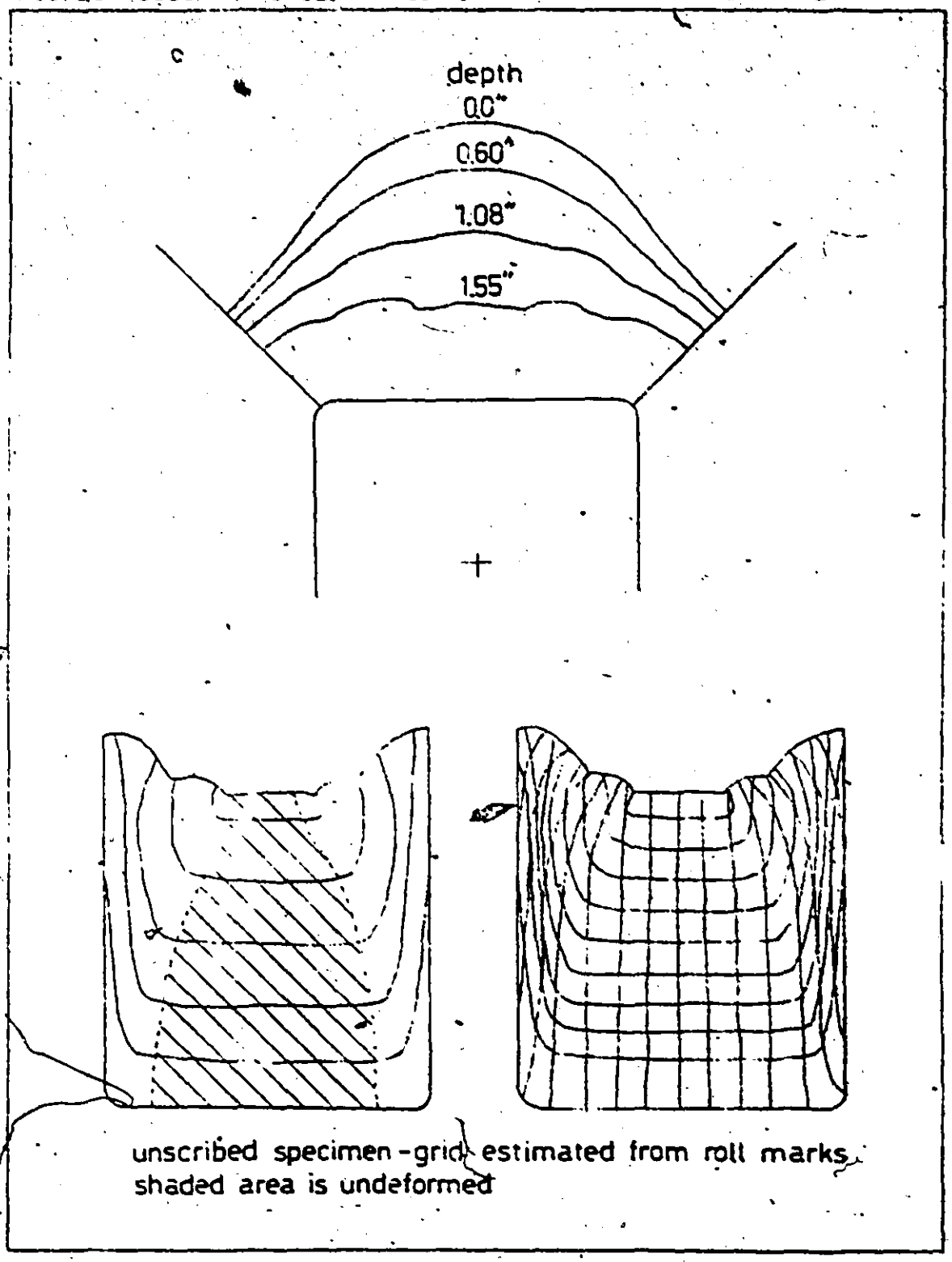

FIG 529 5182-0 ALUMINUM. FULLY DEVELOPED BLANK

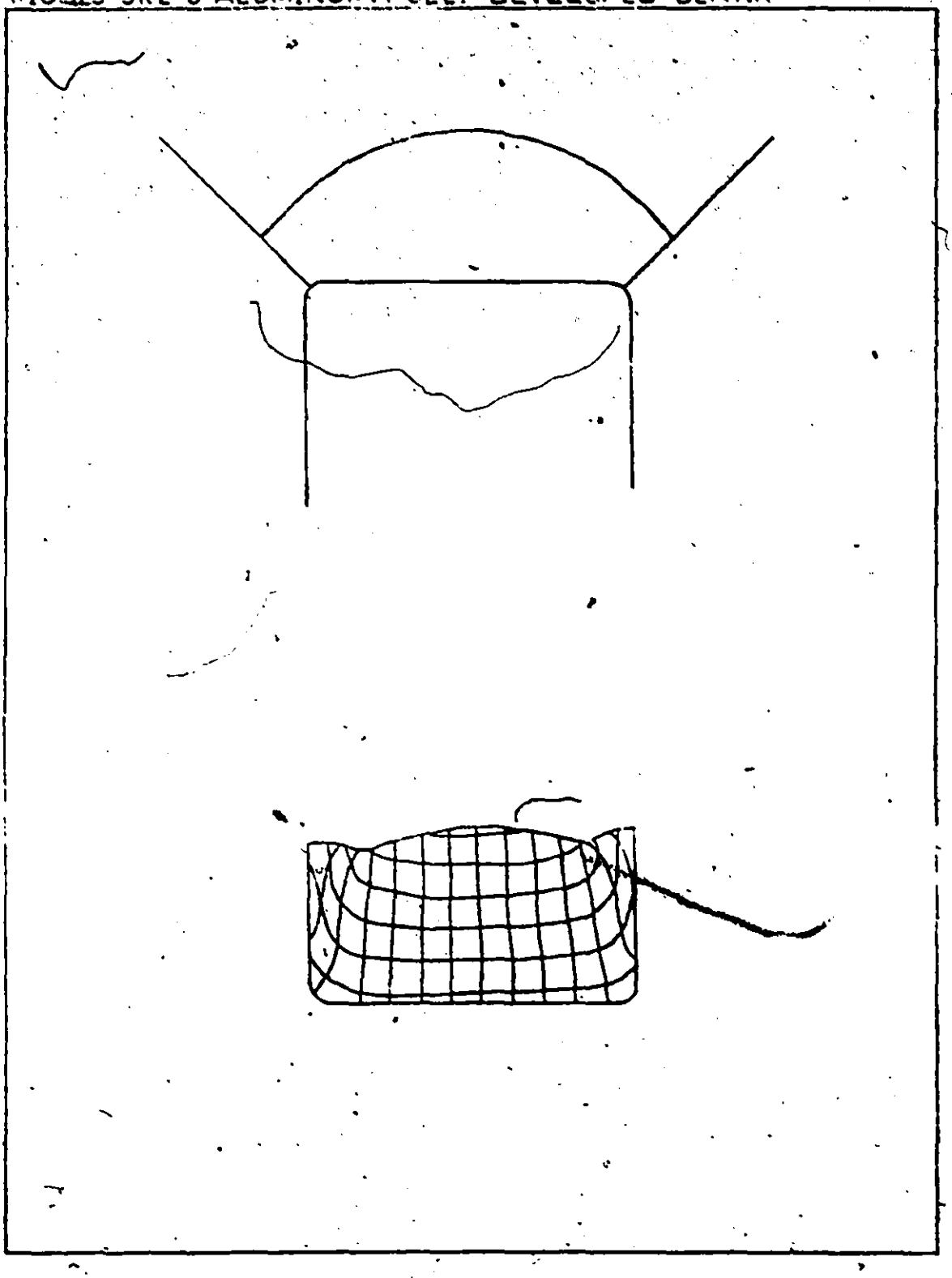

FIG. 5.30 COMPARISON OF CUPS DRAWN FROM DIFFERENT BLANK SHAPES

a) AKDQ Steel

fully developed circular

b) 3003-H14 Utility Aluminum

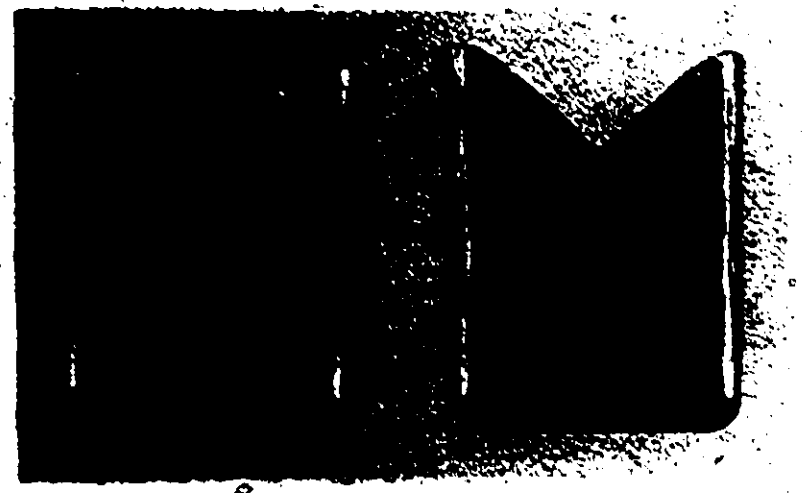

fully developed circular

c) 5182-H111 Aluminum

fully developed side-out circular

FIG. 530 COMPARISON OF CUPS DRAWN FROM DIFFERENT BLANK SHAPES

d) AKDQ Steel

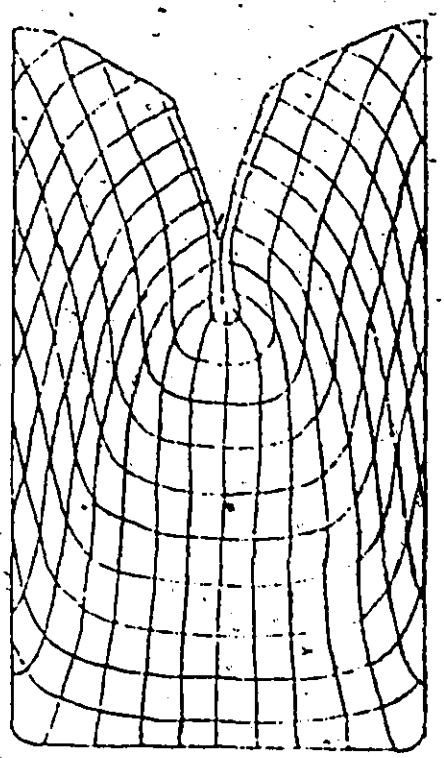

side-cut

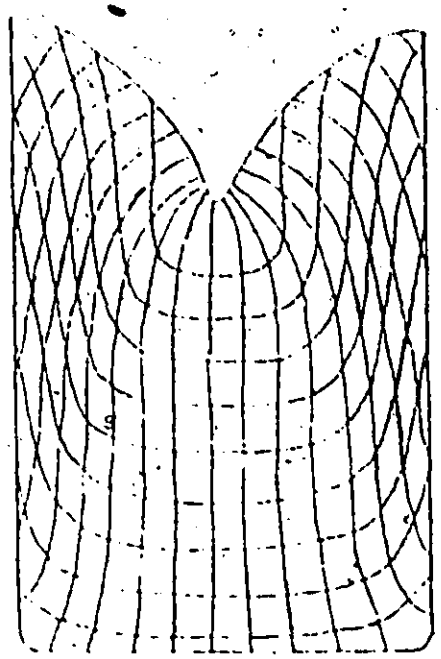

circular

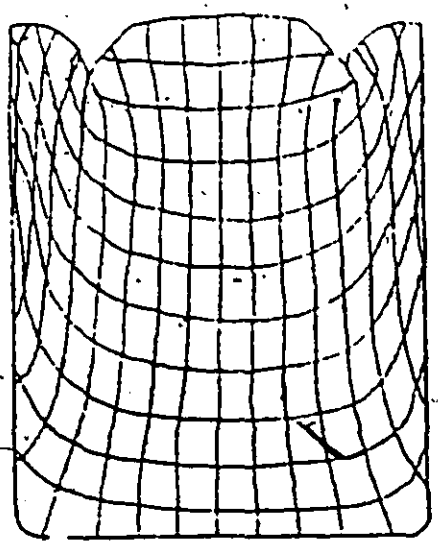

corner-cut

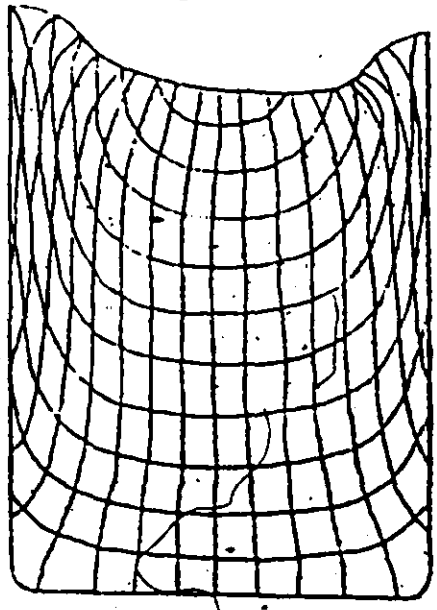

fully developed

some 5182 aluminum blanks fail by an inclined split in the corner wall, (as noted previously in 2036 aluminum) (Figure 5.5f).

In order to assess the effect of blank shape on strain distribution the overall extension of lines at the sides and the corners was calculated. The results are given in Table 5.6. The side extensions are all small but are definitely greater for the steel indicating that it distributes strain better than the 3003-H14 aluminum. As mentioned before the low side strains for the 5182 aluminum are due to the very shallow cup and do not indicate poorer strain distribution.

The change in side strain with different blank shapes is small but the corner strains vary significantly. The trend is to greater strain concentration in the corners as blank shape goes from side cut through circular to corner cut and fully developed.

Figures 5.31 to 5.33 show a comparison of the maximum size blanks of different shapes for three materials. It is interesting that the diameter of all blanks for a given material, measured parallel to the sides of the die opening, is approximately the same while the diameter in the diagonal directions varies greatly.

Figure 5.34 shows a comparison of the fully developed blank for 3003-H14 aluminum with blanks developed using a method suggested by Hobbs [10, 24]. The blank shape resulting from this procedure has more material at the sides and less at the corners. A similar result is found for steel. Trials

Table 5.6 Total Percentage Extension of Wall Material in Square Cups Drawn from Different Blank Shapes and Materials

Blank Shape	AKDQ Steel		3003-H14 Aluminum		5182-H111 Aluminum	
	corner	side	corner	side	corner	side
Side-cut	94	21	83	11	84	5
Circular	120	25	110	7	103	5
Corner-cut	143	29	166	8	-	-
Fully developed	153	28	188	10	119	6

FIG 5.31 COMPARISON OF MAXIMUM SIZE BLANKS OF DIFFERENT SHAPES FOR AKDQ STEEL

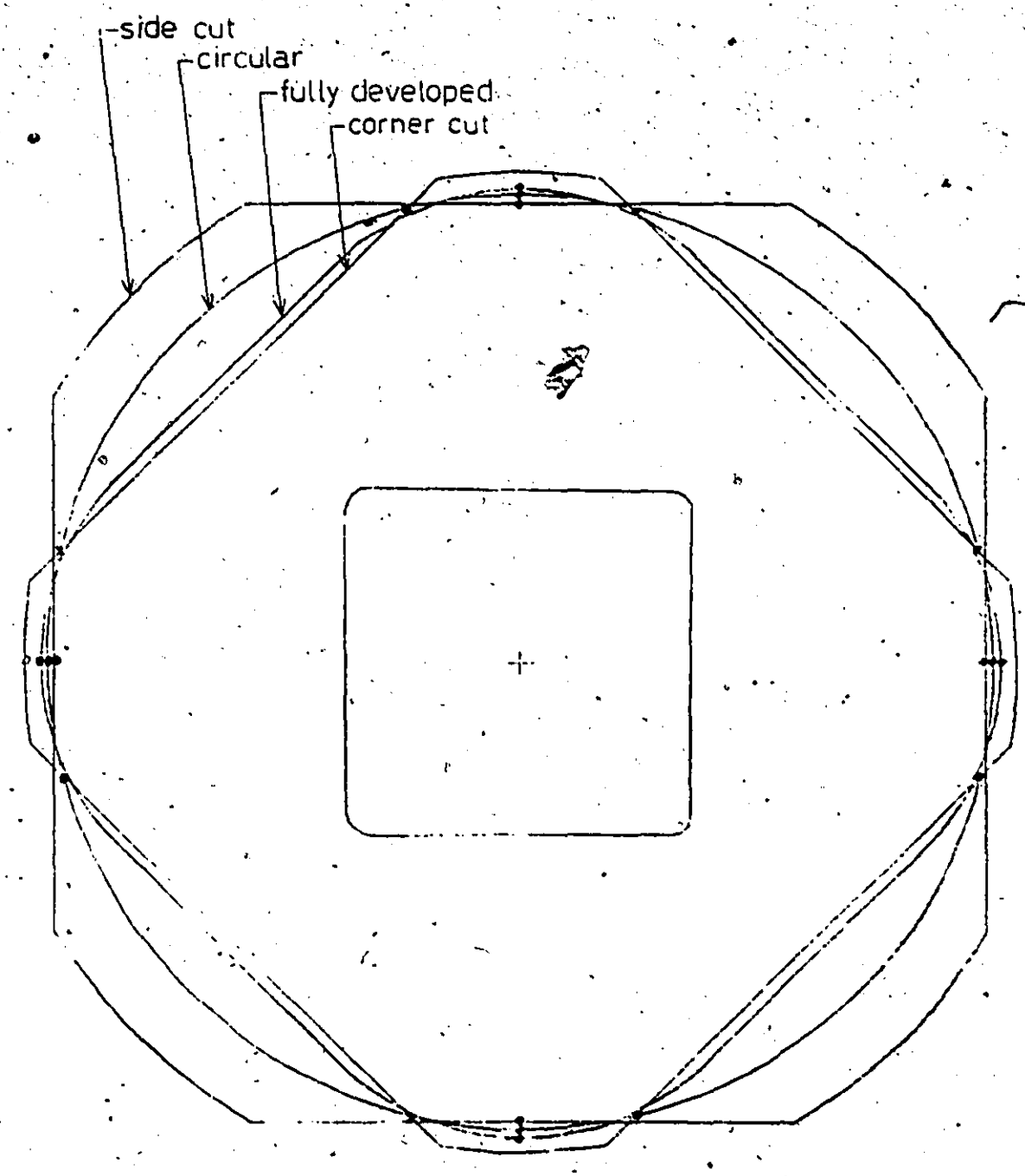

dots indicate locations which become low points on completed cups

FIG. 532 COMPARISON OF MAXIMUM SIZE BLANKS OF DIFFERENT SHAPES FOR 3003-H14 ALUMINUM

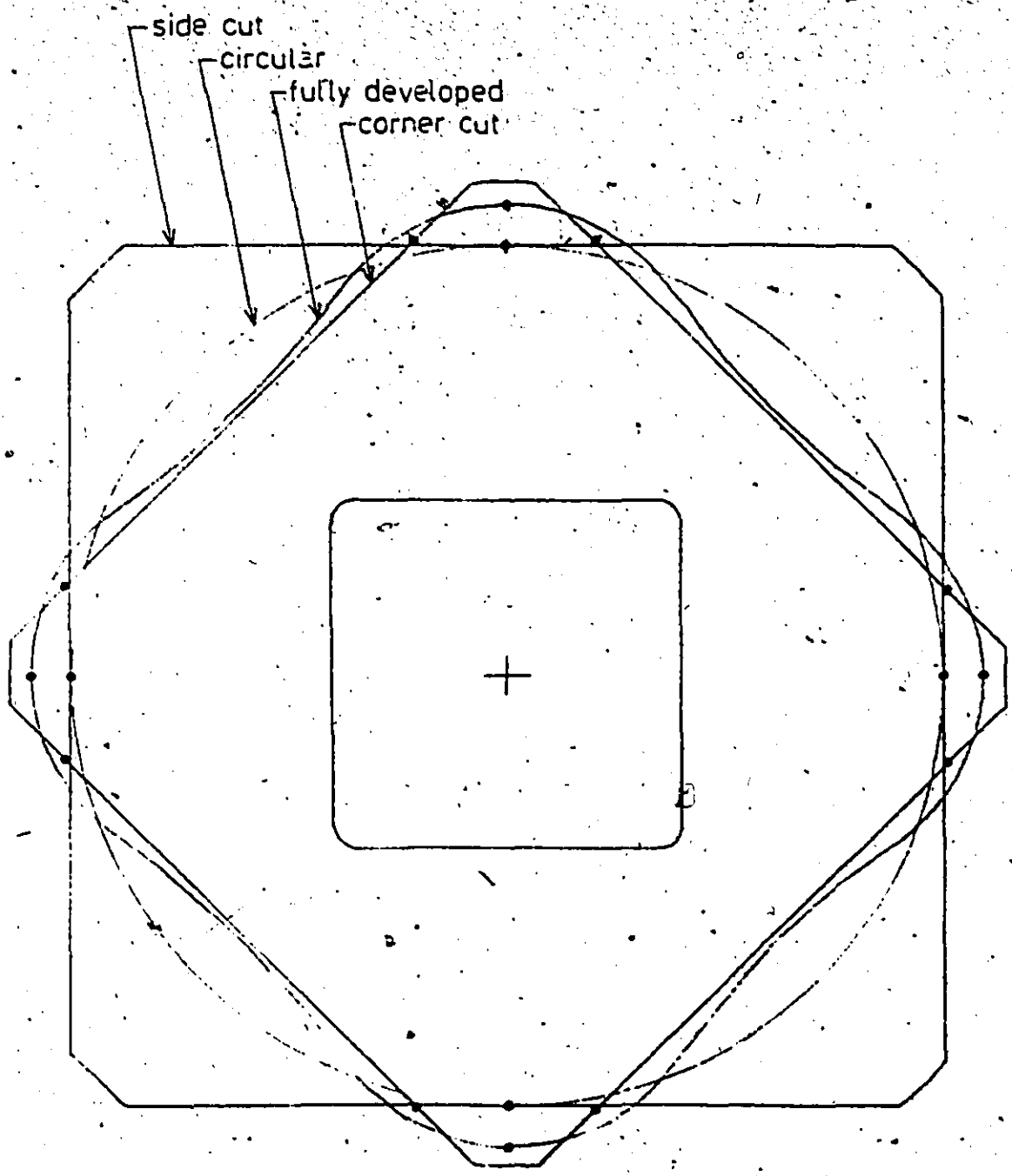

dots indicate locations which become low points on completed cups

FIG. 533 COMPARISON OF MAXIMUM SIZE BLANKS OF DIFFERENT SHAPES FOR 5182 ALUMINUM

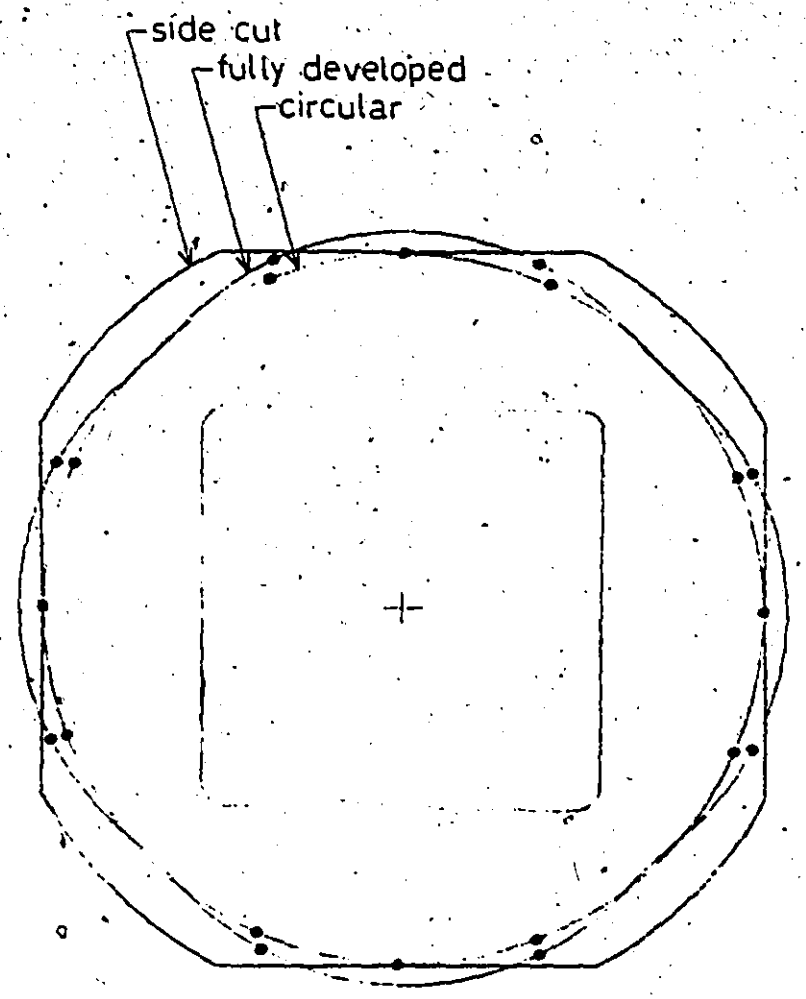

dots indicate locations which become low points on completed cups

FIG 534 COMPARISON OF FULLY DEVELOPED 3003-H14 ALUMINUM BLANK WITH SHAPES PRODUCED BY HOBB'S METHOD

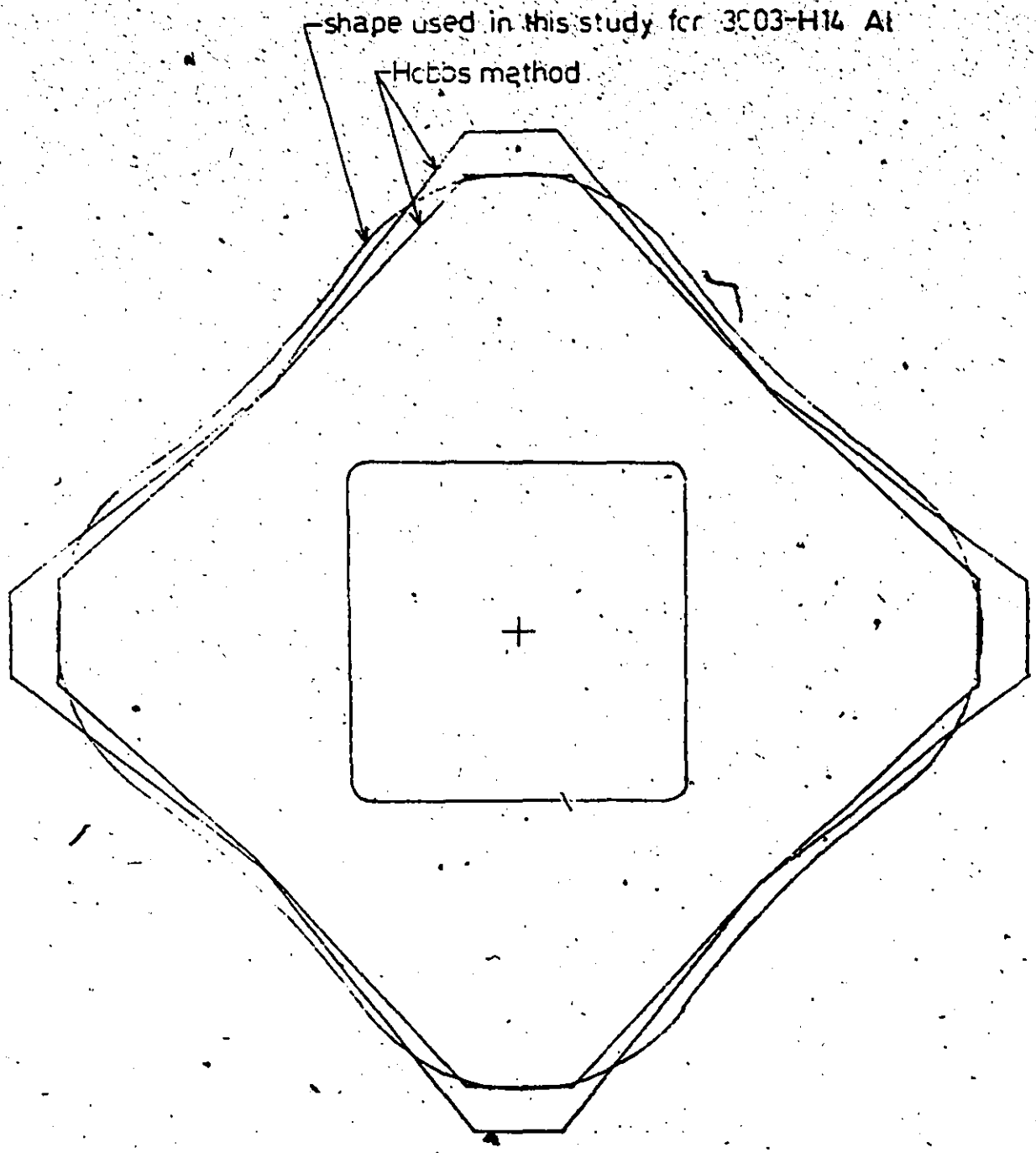

using this shape with the 3003-H14 aluminum resulted in failure at the top of the side wall along the die radius (Figure 5.5d).

5.4 Conclusions

The deepest cups were produced in steel but the 3003 aluminum alloys also drew reasonably well. The 5182 and 2036-T4 aluminum alloys produced only very shallow cups, depth being limited by brittle splitting in the corner wall. The only observable difference between the 5182 tempers (-0 and -H111) was the occurrence of stretcher strains in cups drawn from 5182-0.

Careful blank development increased depth significantly in every case where it was applied. The use of a blank with extra material at the corners may be advantageous for materials like the 5182 and 2036 aluminum which exhibit splitting in the corner wall.

CHAPTER 6

DISCUSSION

6.1 Review of Mechanical Formability Tests

6.1.1 Strain Hardening and Strength

The mechanical formability tests in Chapter 2 indicated that except for the 3003-H14 utility aluminum, the aluminum alloys have a strain hardening ability as great or greater than AKDQ steel. The 5182 aluminum is certainly superior in this respect. The 3003-H14 aluminum, which is a 1/2 hard (strain-hardened) material, exhibits almost no strain hardening.

The 5182 aluminum was almost as strong as the steel over the whole strain range and the 2036-T4 was stronger; the 3003 in both the soft and the 1/2 hard condition was much softer than steel.

6.1.2 Anisotropy

The greatest difference in anisotropy between the materials is in the normal anisotropy as measured by r-value and LDR. The steel is clearly far superior to the aluminum alloys. With an r-value of nearly 2.0, as opposed to r-values less than 1.0 for the aluminum alloys, the steel would be expected to resist thinning and perform better in drawing operations.

The planar anisotropy is also different for steel and aluminum. The steel exhibits its highest r-values and lowest tensile strengths in the 0° and 90° direction whereas the aluminum alloys have higher r-value and lower strength at 45°. The location of ears in the Swift Circular Cup Test is opposite for aluminum and steel.

6.1.3 Fracture Strain

The fracture strain, measured here in the in-plane torsion test, reveals another significant material difference. The steel exhibits the highest fracture strain, the 3003-H14 aluminum somewhat less, the 3003-0 aluminum is another step lower and the 5182 and 2036 aluminum alloys exhibit exceptionally low fracture strains.

It should be noted here that fracture strain is not a commonly used parameter of formability so this difference would not be noticed in most routine testing.

6.1.4 Tensile Elongation

The total elongation in a tensile test is often considered to be a good indication of material ductility. In these tests the steel and the 3003-0 aluminum exhibited large tensile elongation (≈ 35%) while the 5182 and 2036 aluminum alloys had somewhat lower values (≈ 25%). The 3003-H14 utility aluminum exhibited negligible tensile elongation and would therefore be expected to form very poorly.

6.1.5 Summary

Applying conventional thinking to these results one would expect the steel to perform best in forming since it has both good "drawability" (high normal anisotropy) and good "stretchability" (high strain hardening). The 3003-0 aluminum and the 5182 and 2036 aluminum alloys would also be expected to form reasonably well because although they have poor "drawability" they all exhibit high strain hardening, i.e., good "stretchability". The 3003-H14 utility aluminum would be expected to perform very poorly since it lacks both "drawability" and "stretchability".

The results of the square cupping tests indicate however that this assessment is inadequate.

6.2 Square Cup Drawing

6.2.1 Maximum Cup Depth

Figure 6.1 shows the maximum useful heights of cups drawn from circular blanks of the different materials and also shows the principal results of formability testing. The most obvious observation is that the low fracture strain seems to have a drastic effect on the maximum cup height for the 2036 and 5182 alloys. The steel which has high values of all formability parameters, also forms the deepest cups. The 3003 aluminum materials produce cups of intermediate depth.

The decrease in height for the 3003 aluminum materials compared to steel is probably due to the poor normal anisotropy. One might also argue that it was due to the low strain hardening

FIG. 6.1 MECHANICAL FORMABILITY PARAMETERS AND SQUARE CUPPING TEST RESULTS

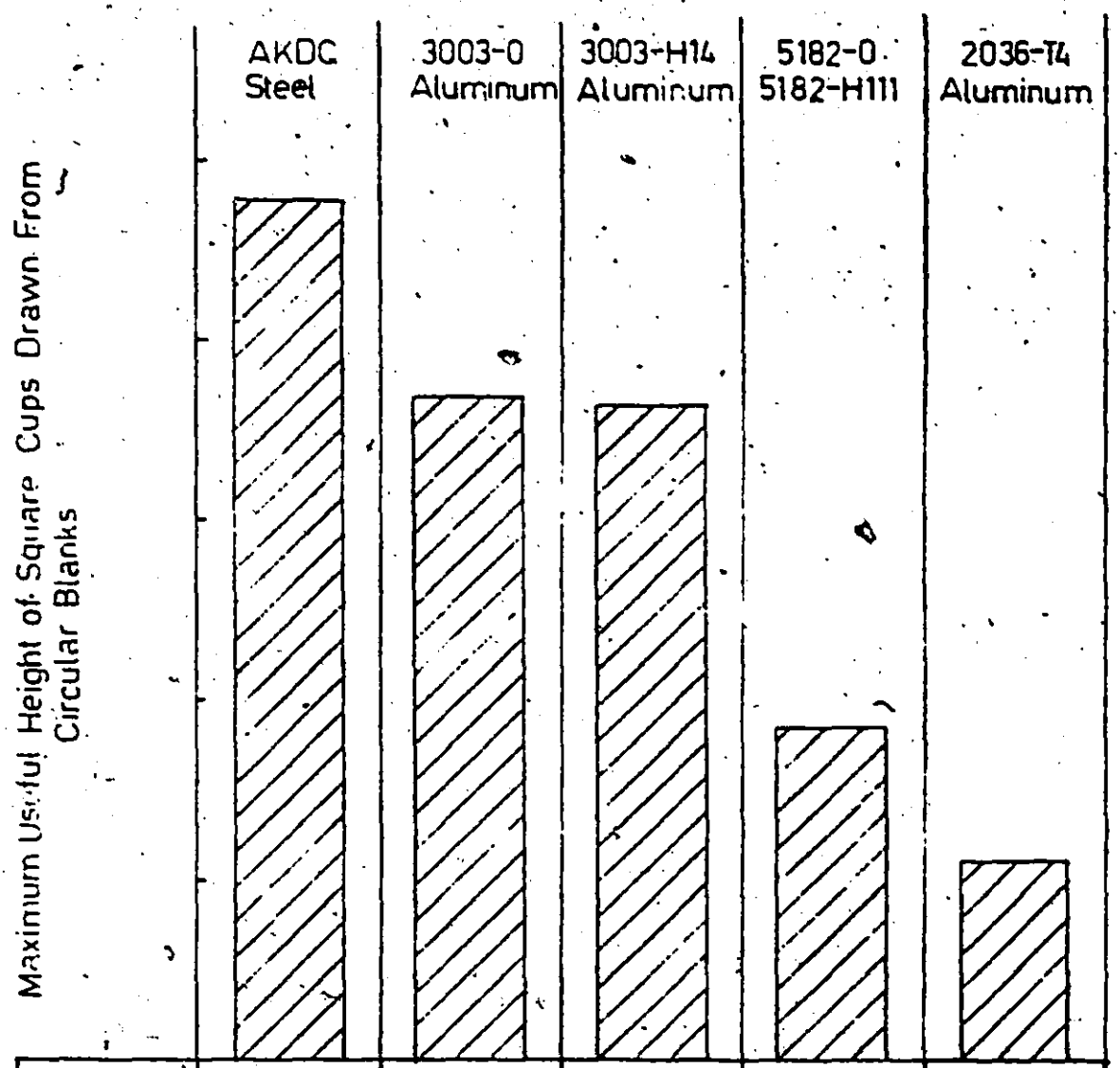

	AKDC Steel	3003-0 Aluminum	3003-H14 Aluminum	5182-0 5182-H111	2036-T4 Aluminum
r-value	high	low	low	low	low
strain hardening	high	high	very low	high	high
fracture strain	highest	medium	high	very low	lowest

of the 3003-H14 material and the lower fracture strain of the 3003-0 material. However the failure in both materials is due to local thinning at the punch radius. In this case fracture strain is not critical since as soon as local thinning occurs, load carrying ability is lost and no further drawing occurs.

The main difference between the two tempers of 3003 aluminum is the strain-hardening ability. The difference is very large and yet the maximum cup height was almost the same for both materials. Thus strain-hardening seems to have little effect on the maximum cup height.

Strain distribution, however is affected by strain hardening. With the 3003-H14 aluminum a large undeformed region exists in the side wall of the cup, whereas with the 3003-0 material, strain is spread from the corners to the centre of the wall.

The fracture strain is a limit to the plastic straining process. In square cup drawing strain is greatest at the corners, but in materials with moderately high fracture strains it does not reach the critical value before local necking occurs over the punch radius. For the 5182 and 2036 alloys the fracture strain is so low that it is reached in the more heavily deformed corner material and failure occurs there.

The optimum orientation of the blank with respect to the die differs for the steel and the aluminum alloys as would be expected. The steel draws best with the rolling direction parallel to a die diagonal whereas the aluminum draws better with the rolling direction parallel to the sides

of the die.

6.2.2 Blank Development.

In every case where it was tried, blank development aimed at producing a flat-topped cup, i.e., no ears or low points, resulted in the deepest possible cup. This shape results in high strain concentration at the cup corners. However it would seem that the higher stress due to work hardening is more than offset by the load reduction due to the reduction in the quantity of material deformed.

For materials such as the 5182 and 2036 aluminum which exhibit brittle fracture high in the corner wall, it may be advantageous to use a blank shape with excess material at the corners. This reduces the strain at the corners and permits deeper cups to be drawn. When this was tried in this study the results were not quite as good as with blanks carefully developed to produce a flat-topped cup, however in some cases a corner-full shape might be a faster way to increase depth than complete blank development.

REFERENCES

1. D. J. Blickwede, "New Knowledge about Sheet Steel", Amer. Soc. Metals, 1970, originally published as a series of articles in Metal Progress, Dec. 1968 to Jan. 1970.

2. S. P. Keeler, "Understanding Sheet Metal Formability", series of 6 articles, Machinery, 1968, Feb.-July.

3. D. M. Finch, S. P. Wilson and J. E. Dorn, "Deep Drawing Aluminum Alloys at Elevated Temperatures", Trans. Amer. Soc. Metals, Vol. 36, 1945, pp. 254-310.

4. S. S. Hecker, "A Simple Forming Limit Curve Technique and Results on Aluminum Alloys", 7th Biennial Congress of the International Deep Drawing Research Group, Amsterdam, Netherlands, Oct. 9-10, 1972.

5. S. S. Hecker, "Formability of Aluminum Alloy Sheets", Trans. A.S.M.E., J. of Eng. Materials and Tech., Jan., 1975, pp. 66-73.

6. A. K. Ghosh, "Strain Localization in the Diffuse Neck in Sheet Metal", General Motors Research Publication GMR-1467, 1973.

7. T. R. Thomson, R. M. Hobbs and I. S. Brammar, "New Forming Grade Steels", 7th Biennial Congress of the International Deep Drawing Research Group, Amsterdam, Netherlands, Oct. 9-10, 1972.

8. D. F. Eary and E. A. Reed, "Techniques of Pressworking Sheet Metal", second edition, Prentice Hall, Englewood Cliffs, N.J., U.S.A., 1974.

9. G. Sachs, "Principles and Methods of Sheet-Metal Fabricating", second edition, Reinhold Publishing Co., New York, 1966.

10. R. M. Hobbs and T. Gibson, "Prediction of Press Performance", Paper 3 from "A Training Course in Sheet Metal Presswork", edited by R. M. Hobbs and T. Gibson, BHP Melbourne Research Laboratories, 1973.

11. R. Hill, "The Mathematical Theory of Plasticity", Clarendon Press, Oxford, 1956.

12. Z. Marciniak, "Aspects of Material Formability", Metalworking Research Group, Dept. of Mech. Eng., McMaster University, 1974.

13. Z. Marciniak, "Assessment of Sheet Metal Fracture Sensitivity by Method of Torsioning the Rings", International Deep Drawing Research Group, Amsterdam, May, 1972.

14. R. L. Whitely, "The Importance of Directionality in Drawing Quality Sheet Steel", Trans. Amer. Soc. Metals, Vol. 52, 1960, pp. 154-169.

15. T. Ikeshima, T. Okamoto and M. Fukuda, "The Theoretical Analysis of r Value Effects on L.D.R. with the Application of Width Reduction", Colloquium on "Anisotropy and Tensile Test Properties and Their Relationship to Sheet Metal Forming", International Deep Drawing Research Group, London, England, June 3, 1964.

16. T. Thomson, "The Relationship of Laboratory Testing to Press Performance of Cold Rolled and Annealed Steels", Paper 4 from "A Training Course on Sheet Metal Presswork", edited by R. M. Hobbs and T. Gibson, BHP Melbourne Research Laboratories, 1973.

17. J. L. Duncan, Int. J. Mech. Sci., Vol. 9, 1967, pp. 157-158.

18. R. Sowerby and J. L. Duncan, "Failure in Sheet Metal in Biaxial Tension", Int. J. Mech. Sci., Vol. 13, 1971, pp. 217-229.

19. P. G. McCormick, "Serrated Yielding and the Occurrence of Strain Gradients in an Al-Cu Alloy", Scripta Metallurgica, Vol. 6, 1972, pp. 1133-1138.

20. A.S.M. Metals Handbook, Vol. 4, 1961, pp. 169-170.

21. K. Lange and R. Dalheimer, "Investigation of the Influence of Various Parameters on the Deep Drawing Quality of Sheet Metals", 8th International M.T.D.R. Conference, University of Manchester, (Pergamon Press), Sept. 12-15, 1967.

22. A. Ovreset and J. L. Duncan, "Polyethylene Film as a Lubricant for Metal-Working at High Contact Pressures", J. Inst. Metals, Vol. 93, 1964-65, pp. 403-405.

23. M. G. El-Sebaie and P. B. Mellor, "Plastic Instability Conditions in the Deep Drawing of a Circular Blank of Sheet Metal", Int. J. Mech. Sci., Vol. 14, 1972, pp. 535-556.

24. R. M. Hobbs, "Die Design Rules and Prediction of Press Performance", Australian Institute of Metals, First National A.S.F.G. Conference, Marysville, Australia, August 15-16, 1973.

APPENDIX L

PROGRAM FOR N-VALUE FITTING

```
C   LEAST SQUARES FIT OF STRESS=XK*STRAIN**DM
C   TO STRESS-STRAIN DATA
C    B(I)=TRUE STRESS
C    A(I)=TRUE STRAIN
C     A(I) AND B(I) ARE THE RAW DATA.A LINEAR FIT
C   IS MADE TO THE LOGARITHMS OF STRAIN AND STRESS I.E.X(I),
C   Y(I).N IS THE NUMBER OF PAIRS OF POINTS.C IS THE
C   INTERCEPT IN LOG SPACE.DM IS THE SLOPE IN LOG SPACE I.E.
C   THE N-VALUE.DLM,DLC ARE THE STANDARD DEVIATIONS.DLMS,
C   DLMC ARE THE VARIANCES.SEE IS THE STANDARD ERROR OF
C   ESTIMATE.D(I) IS THE DEVIATION OF A MEASURED VALUE FROM
C   THE FITTED LINE IN LOG SPACE.DD(I) IS THE DEVIATION OF A
C   MEASURED POINT FROM THE FITTED CURVE IN REAL SPACE.W(I)
C   IS THE WEIGHT ASSIGNED TO A PAIR OF VALUES TO
C   COUNTERACT THE INHERENT WEIGHTING OF THE LOGARITHMS.
      DIMENSION A(60),B(60),W(60),X(60),Y(60),D(60),DD(60)
      DIMENSION BT(60),AT(60)
C    NTHRO IS THE NUMBER OF POINTS TO BE THROWN OUT FROM THE
C   BEGINNING OF THE LIST BEFORE THE FIT.AT(I),BT(I) ARE THE
C   THROWN VALUES
      READ (5,1) NTHRO
C    READ NTRI=NO. OF SETS OF DATA
      READ (5,1) NTRI
      DO 500 J=1,NTRI
C   READ AND CONVERT DATA
      READ(5,1) N
      N=N-NTHRO
      IF(NTHRO.EQ.0)GO TO 21
      READ (5,2) (BT(I),AT(I),I=1,NTHRO)
21    READ (5,2) (B(I),A(I),I=1,N)
      DO 20 I=1,N
      W(I)=B(I)*B(I)
      X(I)=ALOG(A(I))
      Y(I)=ALOG(B(I))
20    CONTINUE
C   LEAST SQUARES FIT OF Y(I) VS. X(I) GENERAL LINE
      SUMW=0.0
      SUMX=0.0
      SUMY=0.0
      R=FLOAT(N)
      DO 10 I=1,N
      SUMX=SUMX+W(I)*X(I)
      SUMY=SUMY+W(I)*Y(I)
10    SUMW=SUMW+W(I)
      XAV=SUMX/SUMW
      YAV=SUMY/SUMW
```

```
      DW=0.0
      SUMM=0.0
      DO 11 I=1,N
      DW=DW+W(I)*(X(I)-XAV)*(X(I)-XAV)
11    SUMM=SUMM+W(I)*(X(I)-XAV)*Y(I)
      DM=SUMM/DW
      C=YAV-DM*XAV
      SUMD=0.0
      DO 12 I=1,N
      D(I)=Y(I)-DM*X(I)-C
12    SUMD=SUMD+W(I)*D(I)*D(I)
      DLMS=SUMD/(DW*(R-2.0))
      DLM=SQRT(DLMS)
      DLCS=(1.0/SUMW+(XAV*XAV)/DW)*SUMD/(R-2.0)
      DLC=SQRT(DLCS)
      XK=EXP(C)
      WRITE (6,3) XK,DM,DLM
      WRITE (6,4)
      SUMDS=0.0
      DO 13 I=1,N
      DD(I)=B(I)-XK*A(I)**DM
C  PLOTPT AND OUTPLT ARE MCMASTER LIBRARY SUBROUTINES
C      PRODUCING A PLOT
      CALL PLOTPT(A(I),DD(I),4)
      WRITE (6,5) A(I),B(I),DD(I)
13    SUMDS=SUMDS+DD(I)**2
      SEE=SQRT(SUMDS/(R-2.0))
      WRITE (6,6) SEE
      WRITE (6,7)
      IF(NTHRO.EQ.0)GO TO 499
      WRITE (6,8) (BT(I),AT(I),I=1,NTHRO)
499   CALL OUTPLT
500   CONTINUE
1     FORMAT(I3)
2      FORMAT(F6.0,4X,F6.4)
3     FORMAT(1H1,*     K=*,F8.0,//,*     N-VALUE=*,F6.4,//,
     1*     STD. DEV. OF N=*,F6.4,///)
4     FORMAT(*     STRAIN-     STRESS     DEVIATION*,/)
5     FORMAT(4X,F6.4,2(5X,F6.0))
6     FORMAT(//,* MODIFIED STD. ERROR OF ESTIMATE=*,F8.0,//)
7     FORMAT(* POINTS DISCARDED BEFORE THE FIT*)
8     FORMAT(4X,F6.0,5X,F6.4)
      STOP
      END
```

APPENDIX II

MATERIAL FLOW PICTURES FOR DEVELOPED STEEL AND UTILITY ALUMINUM BLANKS IN SQUARE CUP DRAWING

FIG. II.1 AKDQ STEEL, SIDE-CUT BLANK

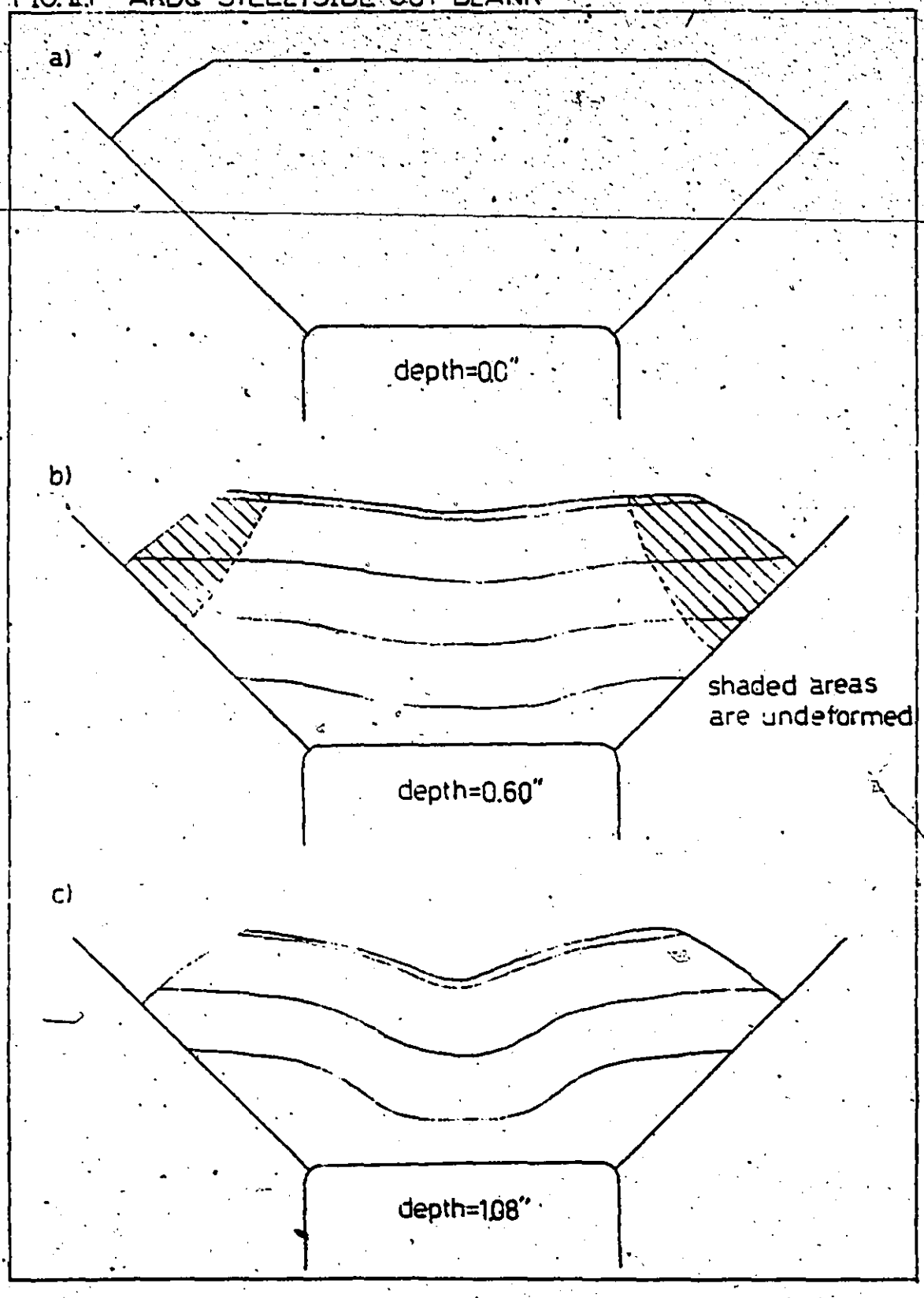

FIG. II.1 AKDQ STEEL SIDE-CUT BLANK

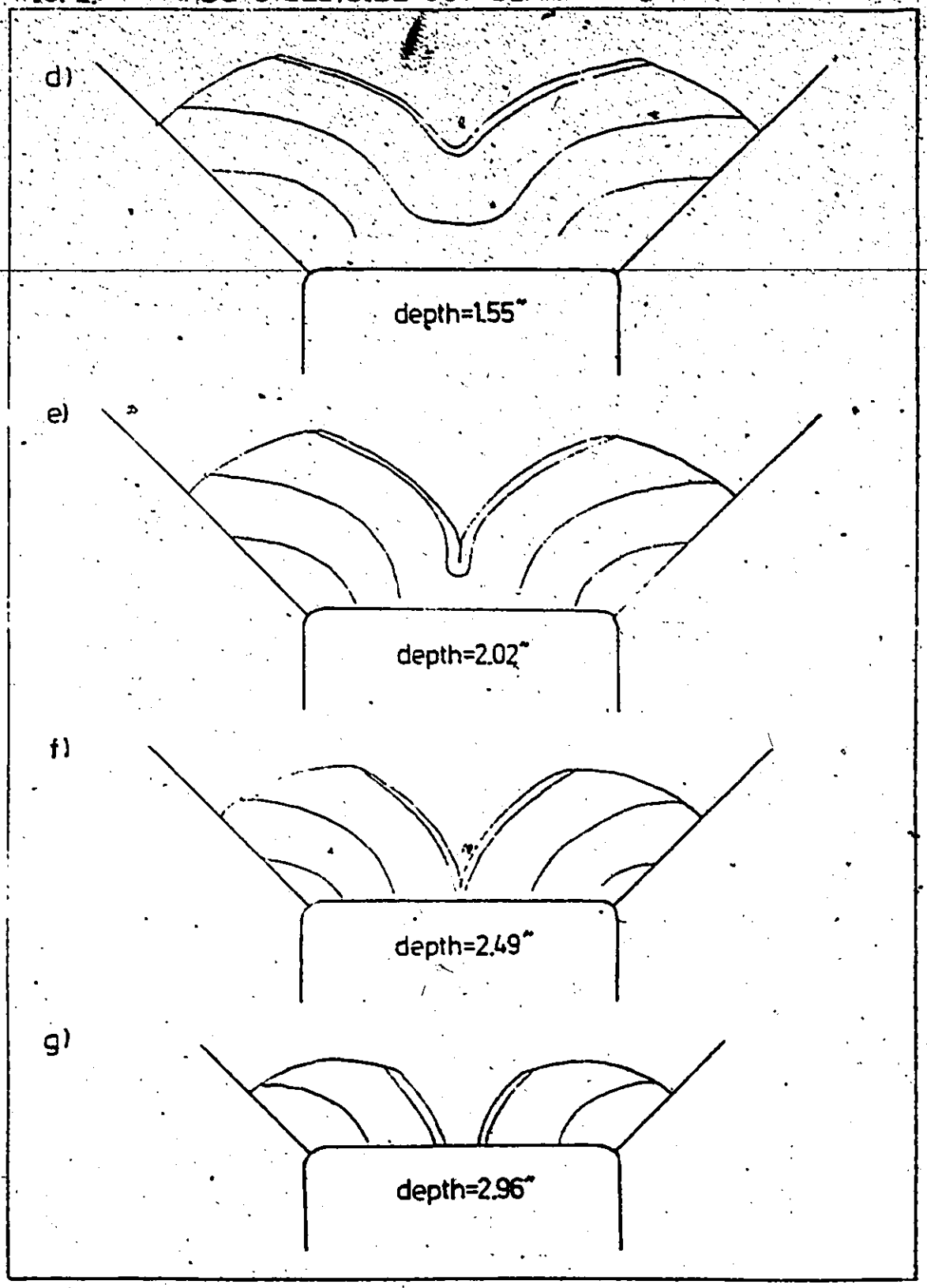

FIG. II.2 AKDO. STEEL, CORNER-CUT BLANK

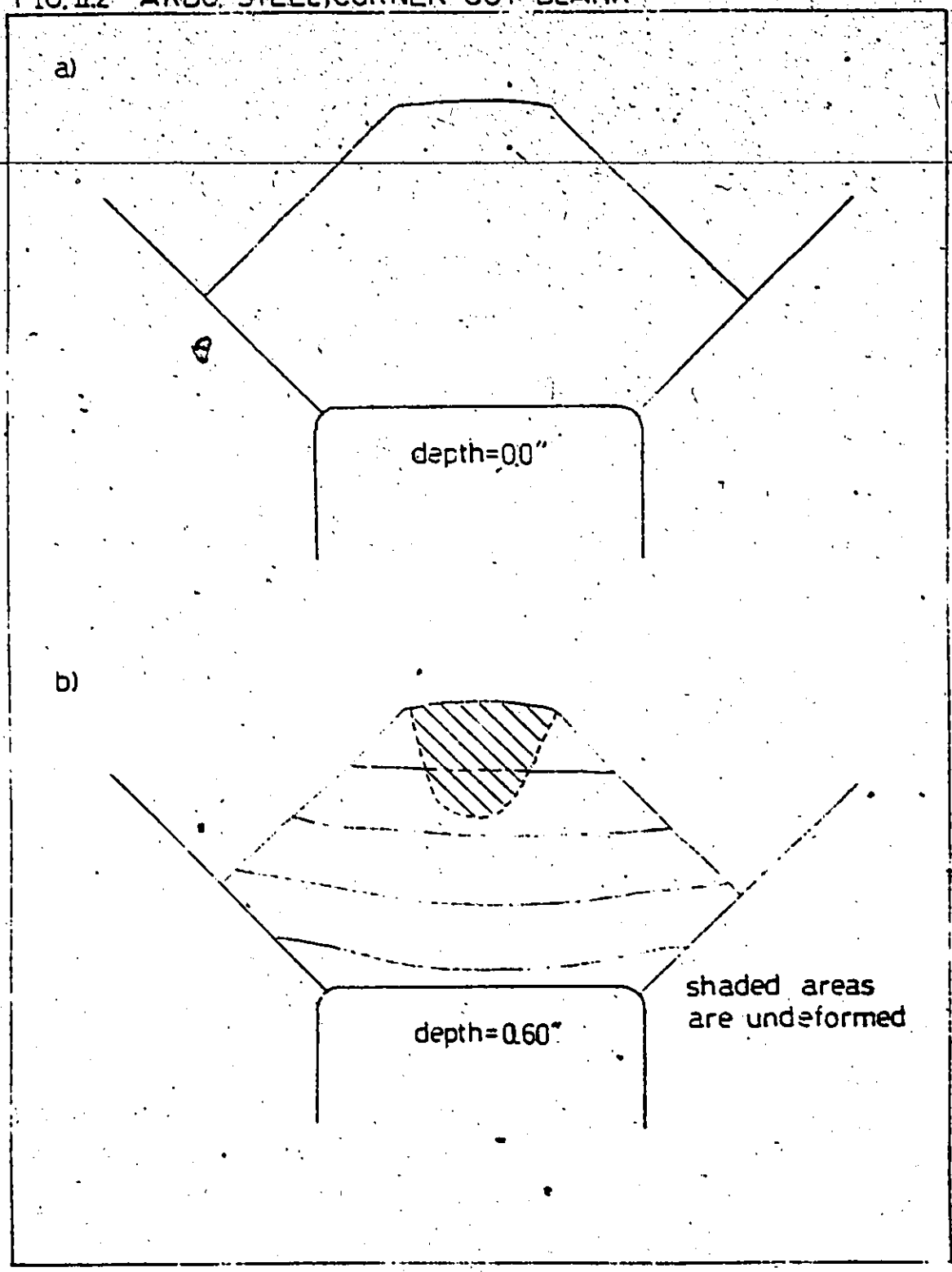

FIG. II.2 AKDQ STEEL CORNER-CUT BLANK

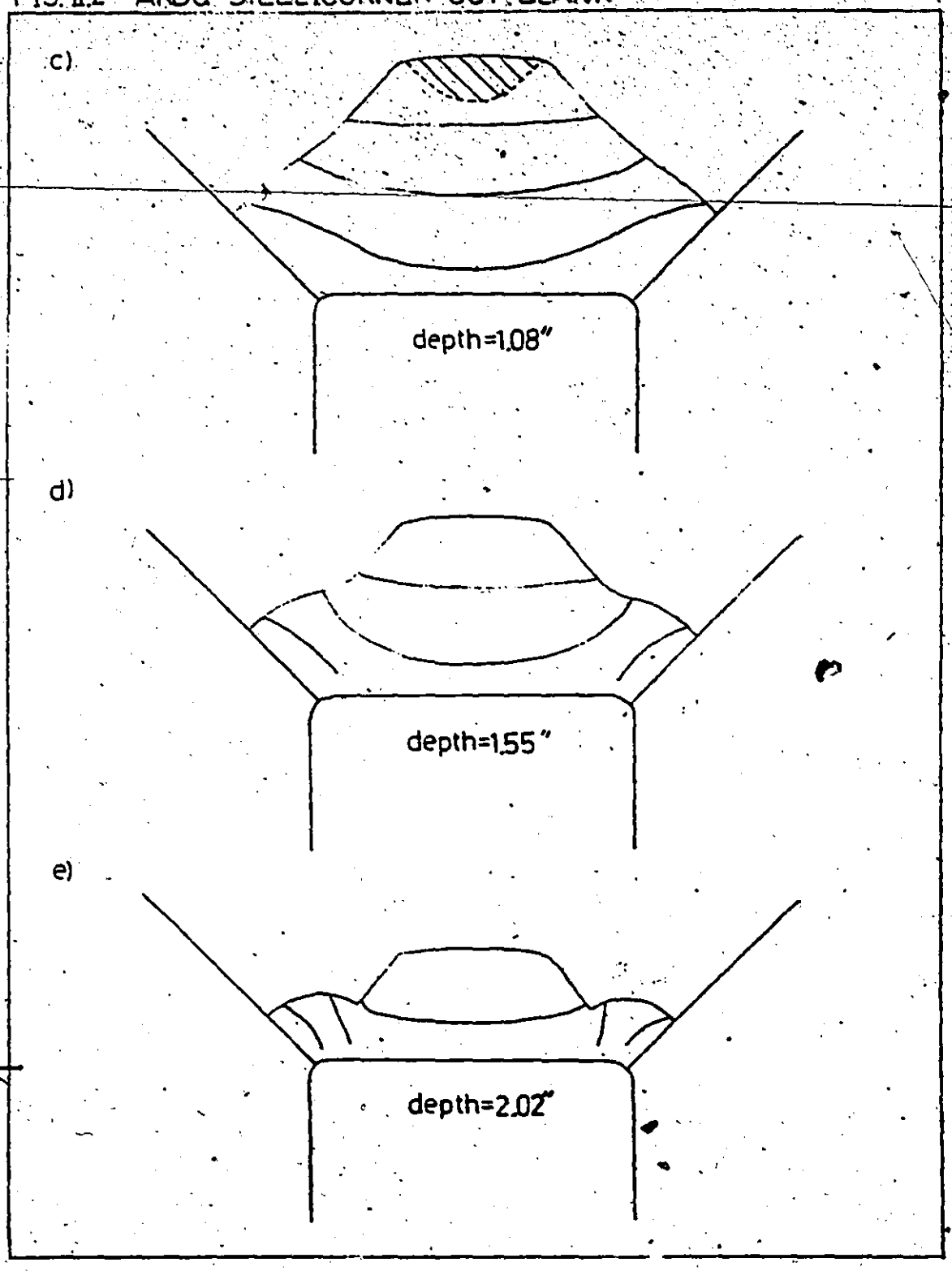

FIG. II.3 AKDQ STEEL, FULLY DEVELOPED BLANK

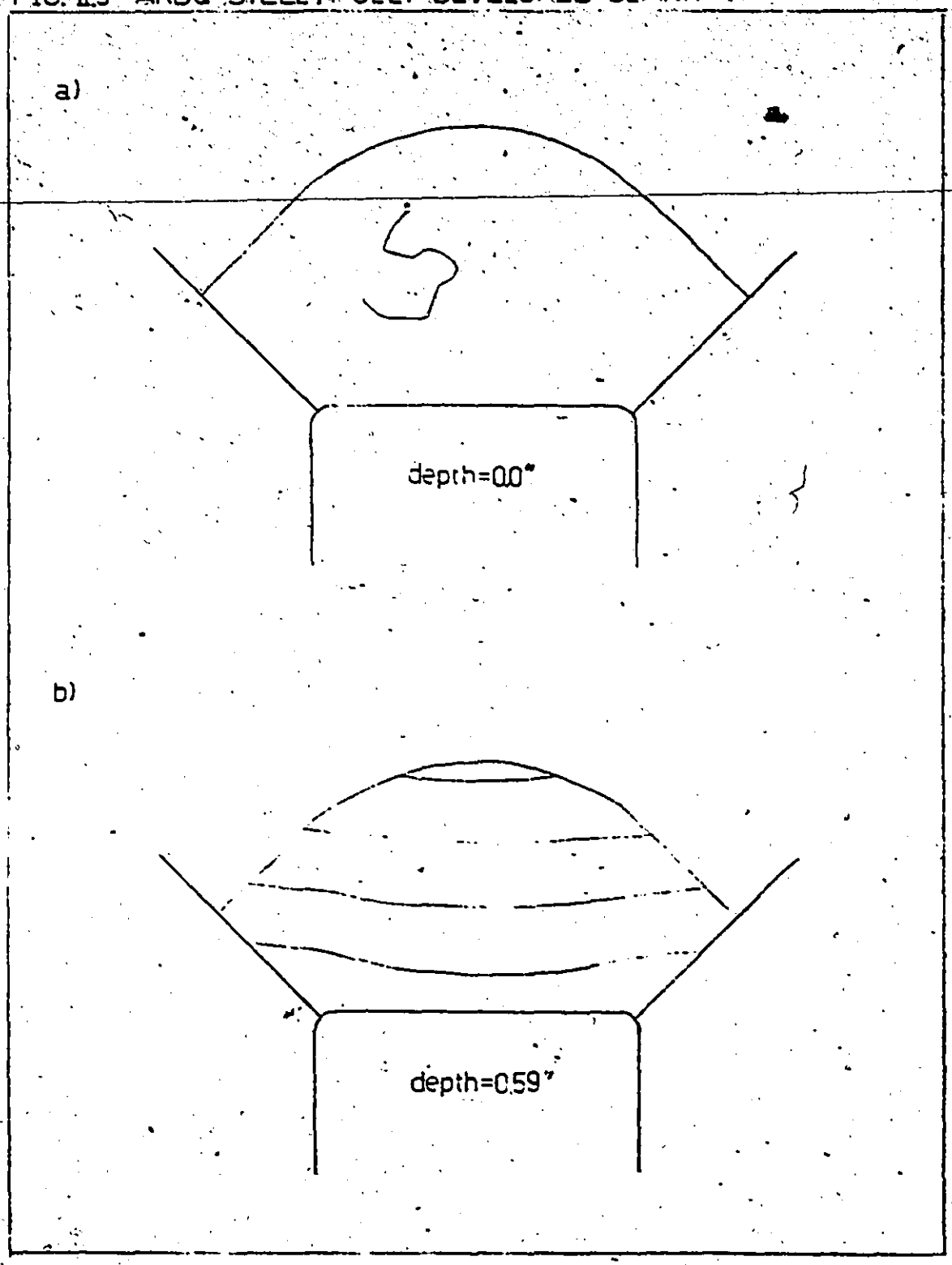

FIG. II.3 AKDQ STEEL, FULLY DEVELOPED BLANK

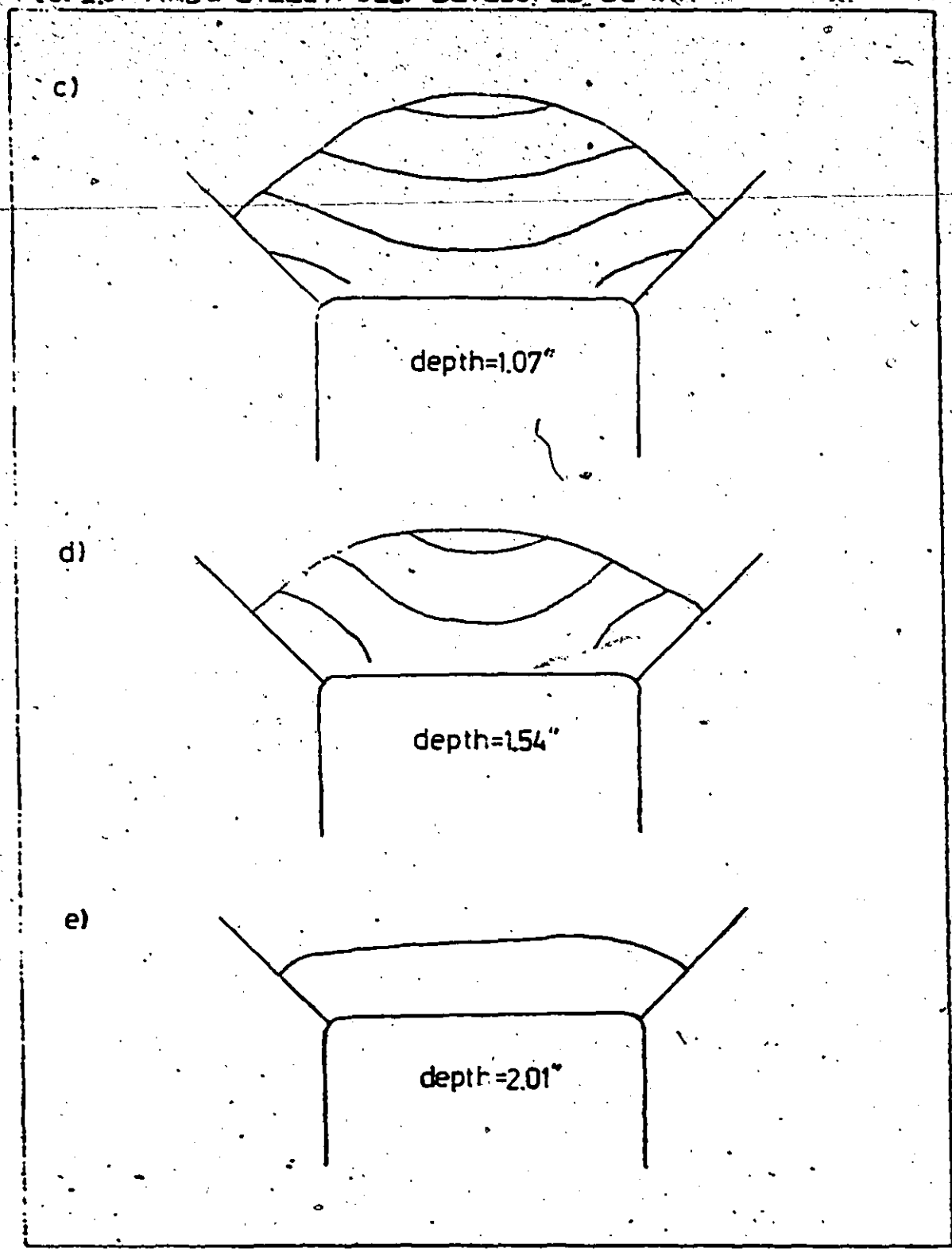

FIG. II.4 3003-H14 UTILITY ALUMINUM SIDE-CUT BLANK, ½ SIZE

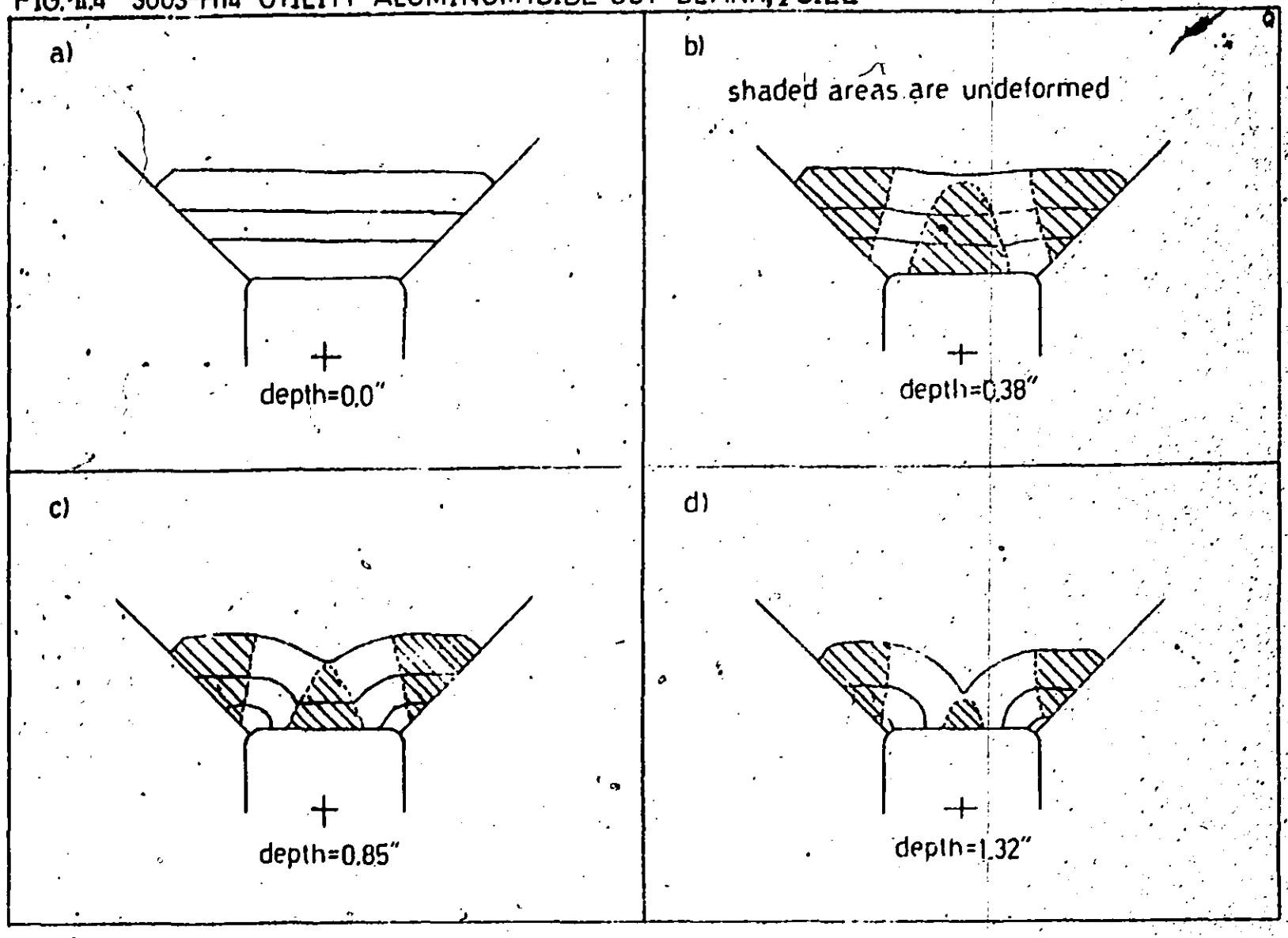

FIG. II.4 3003-H14 UTILITY ALUMINUM, SIDE-CUT BLANK, ½ SIZE

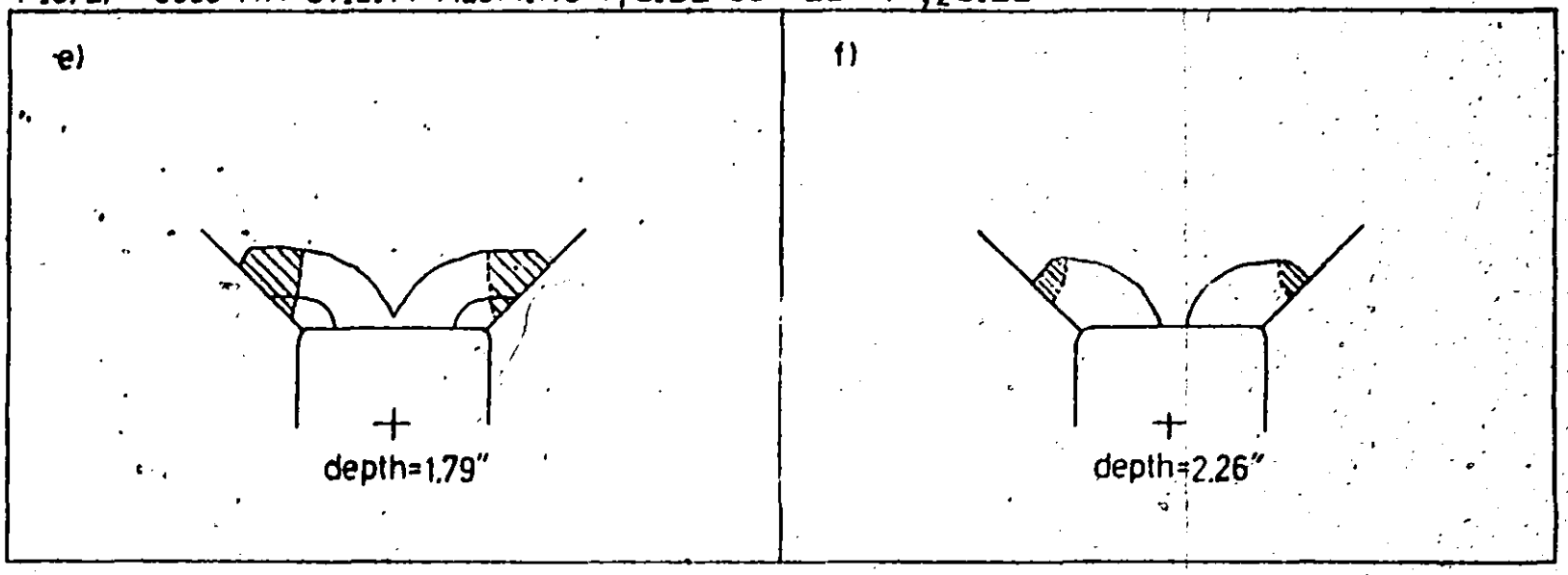

FIG. II.5 3003-H14 UTILITY ALUMINUM, CORNER-CUT BLANK, $\frac{1}{2}$ SIZE